EVALUATION OF AGE HARDENING ON THE CHARACTERISTICS OF ASPHALTS AND MIXTURES

By

COMMANDUR T. CHARI

A DISSERTATION PRESENTED TO THE GRADUATE SCHOOL
OF THE UNIVERSITY OF FLORIDA IN
PARTIAL FULFILLMENT OF THE REQUIREMENTS
FOR THE DEGREE OF DOCTOR OF PHILOSOPHY

UNIVERSITY OF FLORIDA

1988

DEDICATED TO MY FAMILY

AND THE

MADRAS SAPPERS AND MINERS

(their engineering skills are only next to their gallantry in the field)

ACKNOWLEDGMENTS

Dr. Byron E. Ruth's reputation came to me through one of my colleagues, an erstwhile graduate student of his. Since then and all through my work here, as also in the capacity of chairman of my supervisory committee, his teaching, guidance and generosity of spirit have made this study possible. My sincere gratitude is extended to him. Dr. Mang Tia, cochairman of my supervisory committee, has provided many, many hours of active support and intimate guidance right through the various stages of this project. Special thanks are given to him. I am grateful to Dr. P. V. Rao, Dr. J. W. Williams and Mr. G. C. Page for having given of their expertise and time in liberal measure and also serving on my supervisory committee. Indeed, I consider it a privilege to have had all these distinguished professionals on my committee.

Dr. S. K. Khanna, Secretary, University Grants Commission of the Union of India, formerly of the University of Roorkee, developed through his teaching and inspiration, my interest in pavements and materials. I would like to express my gratitude to him.

I would like to express my appreciation to the Florida Department of Transportation (FDOT) for providing the financial support, testing facilities, materials and personnel that have made this research possible. To the many individuals at the Bureau of Materials and Research at FDOT, who contributed significantly to the completion of this work, I offer my thanks. In particular, I am indebted to Messrs. Gale C. Page, Kenneth H. Murphy, G. P. Eunice and Edward Leitner for giving so generously of their time.

Assistance of Mr. Daniel Richardson in setting up the experimental facilities is greatly appreciated. The ever-changing manuscripts were typed with care and skill by Ms. Pat Cribbs and a special word of thanks is offered to her.

I thank all these people again. Finally, my gratitude is extended to the Indian Corps of Engineers for having provided me the necessary leave arrangements and my near and dear, for seeing me through this adventure.

TABLE OF CONTENTS

PAGE

ACKNOWLEDGMENTS.......iii

LIST OF TABLES.......viii

LIST OF FIGURES.......xi

ABSTRACT.......xiv

CHAPTERS

1 INTRODUCTION.......1

- 1.1 Background.......1
- 1.2 Study Objectives.......2
- 1.3 Scope of Study.......3

2 LITERATURE REVIEW.......5

- 2.1 Background.......5
- 2.2 Asphalt Cement Variability by Refinery Source.......6
- 2.3 Mechanisms of Asphalt Hardening.......7
- 2.4 Spectrochemical Methods of Analysis.......11
- 2.5 Infrared Absorption Spectroscopy.......22
- 2.6 Ultraviolet Stress in Sunlight.......29

3 EQUIPMENT AND FACILITIES.......33

- 3.1 Ultraviolet Chamber.......33
- 3.2 Forced Draft Oven.......43
- 3.3 Conventional Ovens.......43
- 3.4 Strength Tests.......43
- 3.5 Constant Stress Rheometer Test.......47
- 3.6 Infrared Spectroscopic Test.......47

4 MATERIALS AND LABORATORY PROCEDURES.......60

- 4.1 Materials.......60
- 4.2 Laboratory Procedures.......64

5 THIN FILM AND ROLLING THIN FILM OVEN TESTS.......86

5.1 Introduction 86
5.2 Results 87
5.3 Analysis of Results 87
5.4 Summary of Findings 112

6 INFRARED ABSORPTION SPECTROSCOPY ON RESIDUES FROM TFO AND RTFO TESTS 116

6.1 Introduction 116
6.2 Examination of IR Absorption Spectra 117
6.3 Analysis of Results 141
6.4 Summary of Findings 149

7 RESULTS OF MIXTURE STRENGTH TESTS 151

7.1 Introduction 151
7.2 Results 152
7.3 Analysis of Results 152

8 RESULTS OF CONSISTENCY AND RHEOLOGY TESTS ON RECOVERED ASPHALT RESIDUES 178

8.1 Introduction 178
8.2 Results 179
8.3 Analysis of Results 185

9 RESULTS OF INFRARED ABSORPTION SPECTROSCOPY ON RECOVERED ASPHALT RESIDUES 210

9.1 Introduction 210
9.2 Results 211
9.3 Analysis of Results 212
9.4 General Observations and Findings 218

10 INTERPRETATION OF FIELD DATA 223

10.1 Introduction 223
10.2 Field Sampling and Testing 223
10.3 Hardening Trends 228
10.4 Comparisons of Field and Laboratory Aging 239

11 ANALYSIS AND DISCUSSION OF RESULTS 242

11.1 Introduction 242
11.2 TFOT and RTFOT Procedures 242
11.3 Relationships Between Mixture Properties and Asphalt Viscosity 244
11.4 Comparison of Laboratory Exposure Types 247
11.5 Effect of Natural Weathering 251
11.6 Assessment of Ketone Factor 254
11.7 IR Spectral Evaluation of Hardening 256
11.8 A Framework for Better Specifications 264

12 CONCLUSIONS AND RECOMMENDATIONS 267

12.1 Conclusions..267
12.2 Recommendations....................................270

APPENDIX

A PROPERTIES OF MARSHALL SPECIMENS........................272
B RESULTS OF MIXTURE STRENGTH TESTS.......................291
C RESULTS OF CONSISTENCY AND RHEOLOGY TESTS ON RECOVERED RESIDUES...310
D RESULTS OF IR SPECTRAL TEST ON RECOVERED RESIDUES..........324
E RATIOS USED FOR MULTIPLE REGRESSION ANALYSIS................345
REFERENCES..349
BIOGRAPHICAL SKETCH...354

LIST OF TABLES

TABLE		PAGE
4. 1	Source of Materials and Job Mix Formula for Asphalt Concrete Mix	62
4. 2	Washed Sieve Analysis of Aggregate Blend	63
4. 3	Maximum Specific Gravities of Mixtures	65
4. 4	Unit Weights and Air Void Contents of Marshall Specimens	66
5. 1	TFOT and RTFOT Effects on Penetration	88
5. 2	TFOT and RTFOT Effects on Absolute Viscosity	89
5. 3	TFOT and RTFOT Effects on Kinematic Viscosity	90
5. 4	TFOT and RTFOT Effects on Penetration Retained	91
5. 5	TFOT and RTFOT Effects on Absolute Ratio	92
5. 6	Result of ANOVA on Penetration Data	94
5. 7	Result of ANOVA on Percent Penetration Retained	96
5. 8	Grouping of Asphalts on the Basis of Percent Penetration Retained from Duncan's Test	97
5. 9	Grouping of Temperature by Oven Type on the Basis of Percent Penetration Retained from Duncan's Test	98
5.10	Grouping of Oven Type by Temperature on the Basis of Percent Penetration Retained from Duncan's Test	100
5.11	Results of ANOVA on Absolute Viscosity	101
5.12	Results of ANOVA on Absolute Viscosity Ratio	107
5.13	Grouping of Asphalts by Temperature on the Basis of Absolute Viscosity Ratio from Duncan Test	108
5.14	Results of ANOVA on Kinematic Viscosity	113
5.15	Relationship Between RTFOT and TFOT Effects	114
6. 1	Measured Absorbances at 1600 and 1700 cm^{-1}	130

6. 2 Ratio of Absorbances Expressed as Carbonyl Ratio at $1700\ cm^{-1}$..........131

6. 3 Ketone Anhydride Development Factors..........136

6. 4 Results of ANOVA on Ketone Anhydride Development Factor....142

6. 5 Grouping of Asphalts by Temperature on the Basis of Ketone Anhydride Development Factor..........144

6. 6 Results of Flash and Smoke Point Tests..........146

6. 7 Comparative Rating of Asphalt Based on Penetration, Absolute Viscosity and Spectral Measurement..........148

7. 1 Result of ANOVA on Indirect Tensile Strength..........155

7. 2 Grouping of Type of Exposure by Asphalt for 90 Day Duration on the Basis of Indirect Tensile Test..........156

7. 3 Grouping of Asphalts by Type of Exposure for 90 Day Duration on the Basis of Indirect Tensile Strength......157

7. 4 Regression Coefficients for Relation Between Indirect Tensile Strength and Duration of Exposure..........162

7. 5 Regression Coefficients for Relation Between Resilient Modulus and Duration of Exposure..........173

7. 6 Regression Coefficients for Relation Between Fracture Energy and Duration of Exposure..........176

8. 1 Result of ANOVA on Absolute Viscosity..........187

8. 2 Grouping of Asphalts on the Basis of Absolute Viscosity....189

8. 3 Grouping of Exposure Type on the Basis of Absolute Viscosity..........190

8. 4 Regression Coefficients for Relation Between Absolute Viscosity and Duration of Exposure..........194

8. 5 Grouping of Asphalts for 90 Day Duration on the Basis of Penetration..........198

8. 7 Grouping of Exposure Type on the Basis of Penetration......199

8. 8 Regression Coefficients for Relation Between Penetration and Duration of Exposure..........202

8. 9 Results of ANOVA on Constant Power Viscosity (η_j) at 77° F (25° C)..........204

8.10 Grouping of Asphalts on the Basis of Constant Power Viscosity (n_j) at 77° F (25° C)....206

8.11 Grouping of Exposure Type on the Basis of Constant Power Viscosity (n_j) at 77° F (25° C)....207

8.12 Regression Coefficients for Relation Between Constant Power Viscosity (n_j) at 77° F (25° C) and Duration of Exposure....208

9. 1 Result of ANOVA on Ketone Factors....213

9. 2 Grouping of Asphalts by Type of Exposure for 90 Day Duration on the Basis of Ketone Factors....215

9. 3 Grouping of Type of Exposure by Asphalt for 90 Day Duration on the Basis of Ketone Factors....216

9. 4 Grouping of Types of Measure by Asphalt for 90 Day Duration on the Basis of Ketone Factors....217

9. 5 Regression Coefficients for Relation Between Ketone Factors (reference measurements at 1600 cm^{-1}) and Duration of Exposure....222

10. 1 Characteristics of Test Pavements in Hernando County....226

10. 2 Viscosity and Penetration Tests on Asphalts and Residues from I-75 Project....229

10. 3 Viscosity and Penetration Tests on Asphalts and Residues from US-301 Project....230

10. 4 Results of Tests on Samples from Interstate-75....231

10. 5 Results of Tests on Samples from US-301 (Section No. 2)....232

10. 6 Comparison of Hardening Effects Due to Laboratory Aging....240

11. 1 Results of Tests After Six Months of Natural Weathering....252

11. 2 Equivalence Between Six Months Natural Weathering and Aging in Laboratory....253

11. 3 Constant Power Viscosities (n_j) at 59° F (15° C) of Original Asphalts....258

11. 4 Results of Regression with Three Independent Variables....259

11. 5 Results of Regression with Two Independent Variables....260

11. 6 Correlation Matrix with Four Variables....261

11. 7 Results of Regression Excluding 90 Day Data....263

LIST OF FIGURES

FIGURE PAGE

2.1 Range of Frequencies Used in Spectrochemistry..............14

2.2 Portrayal of an Electromagnetic Wave..............15

2.3 Relationship Between the Incident and Transmitted Radiant Power..............17

2.4 Generalized Spectrochemical Instrument..............19

2.5 Typical Relative Spectral Energy Distribution of UV-B Lamp..............32

3.1 Ultraviolet Chamber..............35

3.2 Picture of the Ultraviolet Chamber..............36

3.3 Rotation of Lamps in UV Chamber..............38

3.4 Plan of Ultraviolet Chamber Showing Locations of Samples of Different Exposure Durations..............40

3.5 Positions of Specimens in Ultraviolet Chamber..............42

3.6 Picture of the Forced Draft Oven..............44

3.7 Picture of MTS Machine..............45

3.8 Picture of Loading Arrangement..............46

3.9 Picture of Cannon Schweyer Rheometer..............48

3.10 Schematic of Cannon Schweyer Rheometer..............49

3.11 Picture of IBM 9000 Mini Computer..............50

3.12 Typical BD SX Fourier Transform Infrared Spectrophotometer System..............52

3.13 Picture of FTIR System Used..............53

3.14 Essential Components of a Single-Beam Grating Spectrometer..55

3.15 Essential Components of a Rapid Scanning Fourier Transform Spectrometer....................56

3.16 Picture of Sealed Cells, Vial and Syringe....................59

4.1 Stress Components in a Circular Disk....................72

4.2 Typical Load-Pulse Deformation Trace....................75

5.1 Relation Between Percent Penetration Retained and Oven Temperature for TFOT....................102

5.2 Relation Between Percent Penetration Retained and Oven Temperature for RTFOT....................104

5.3 Relation Between Mean Absolute Viscosity Ratio and Oven Temperature....................110

6.1 IR Spectrum of Original Asphalt Chevron AC-30....................118

6.2 IR Spectrum of Original Asphalt Belcher AC-30....................119

6.3 IR Spectrum of Original Asphalt Amoco AC-30....................120

6.4 IR Spectrum of Original Asphalt Mariani AC-30....................121

6.5 IR Spectrum of Original Asphalt Marathon AC-30....................122

6.6 IR Spectrum of Original Asphalt Texaco 85-100....................123

6.7 IR Spectrum of Original Asphalt Texaco Airblown 85-100....................124

6.8 IR Spectrum of Original Asphalt Esso 25-35....................125

6.9 IR Spectrum of Original Asphalt Boscan 85-100....................126

6.10 IR Spectrum of Original Asphalt Chevron AC-20....................127

6.11 IR Spectrum of Original Asphalt Chevron AC-20 Modified....................128

6.12 Carbonyl Ratio of Asphalt Residue After TFOT v.s. Oven Temperature....................132

6.13 Carbonyl Ratio of Asphalt Residue After RTFOT v.s. Oven Temperature....................134

6.14 Ketone Anhydride Development Factor of Asphalt Residue After TFOT v.s. Oven Temperature....................137

6.15 Ketone Anhydride Development Factor of Asphalt Residue After RTFOT v.s. Oven Temperature....................139

7.1 Relation Between Indirect Tensile Strength And Duration of Exposure....................159

7.2 Relation Between Horizontal Deformation and Duration of Exposure..164

7.3 Relation Between Resilient Modulus and Duration of Exposure..169

7.4 Relation Between Fracture Energy and Duration of Exposure..175

8.1 Effect of Type and Duration of Exposure on Absolute Viscosity..180

8.2 Effect of Type and Duration of Exposure on Penetration.....183

8.3 Relation Between Viscosity and Duration of Exposure for Different Levels of Temperature........................191

8.4 Relation Between Penetration and Duration of Exposure......200

9.1 Relation Between Ketone Factors and Duration of Exposure...219

10.1 Location Plan of Interstate-75 Test Sections...............224

10.2 Location Plan of US-301 Test Sections.......................225

10.3 Relation Between Absolute Viscosity and Duration of Field Aging on I-75..233

10.4 Relation Between Absolute Viscosity and Duration of Field Aging on US-301.......................................234

10.5 Relation Between Penetration and Duration of Field Aging on I-75..235

10.6 Relation Between Penetration and Duration of Field Aging on US-301...236

10.7 Relation Between Ketone Factor and Duration of Field Aging on I-75..237

10.8 Relation Between Ketone Factor and Duration of Field Aging on US-301...238

11.1 Relation Between Indirect Tensile Strength and Asphalt Viscosity..245

11.2 Relation Between Resilient Modulus and Asphalt Viscosity...248

11.3 Relation Between Fracture Energy and Asphalt Viscosity.....249

Abstract of Dissertation Presented to the Graduate School
of the University of Florida in Partial Fulfillment of the
Requirements for the Degree of Doctor of Philosophy

EVALUATION OF AGE HARDENING ON THE CHARACTERISTICS OF ASPHALTS AND MIXTURES

BY

Commandur T. Chari

April 1988

Chairman: Byron E. Ruth
Cochairman: Mang Tia
Major Department: Civil Engineering

A research study was conducted to evaluate the effects of age hardening on the characteristics of asphalts and mixtures. Eleven asphalts, covering a spectrum of sources and types, were subjected to exposure in the Thin Film and Rolling Thin Film Oven Tests at three different temperatures. Consistency measurements were made before and after the tests.

Ten of the eleven asphalts were used to make Florida Type S-1 asphalt concrete mixtures. A total of 540 Marshall specimens were fabricated at an asphalt content of 6.5 percent. The compacted specimens had an average air void content of 5 percent. Equipment for aging the specimens at 140° F included conventional oven, ultraviolet chamber and forced draft oven. The specimens were exposed for 1, 7, 28 and 90 days using the three different aging treatments. Also, one set of specimens was exposed to natural weather conditions for assessment of age hardening at time periods of 6 months, 1 year, 2 years and 3 years.

Resilient modulus and fracture energy values were determined for unaged and aged Marshall specimens that had been prepared with four of the ten asphalts. Indirect tensile tests were performed on all test specimens. Asphalt residues were recovered from the broken samples and subjected to consistency tests. Rheometer tests were conducted at two temperatures for evaluation of aging effects. Also, asphalts recovered from two paving projects at various ages were evaluated for consistency and infrared spectral characteristics.

Infrared spectroscopic techniques were used to identify and quantify changes brought about by oxidation and age hardening. A value termed Ketone Factor was developed as a function of absorbances.

Analyses of variance and regression analyses were performed on the results to determine the significance of test parameters and to establish relationships. The results of the study identified those testing techniques which characterized asphalts and their susceptibility to oxidative and age hardening. Comparisons are made between hardening in the field and by laboratory procedures. A framework for future specifications is presented.

CHAPTER 1
INTRODUCTION

1.1 Background

Asphalt and asphalt-based materials are used extensively as binders, sealants and waterproof coatings in a wide variety of applications because of their desirable cohesive and thermomechanical properties, resistance to weathering, ease of processing and comparatively low cost. However, it is well known that changes in the original properties of all conventional asphalts do take place during construction and field aging. While a certain amount of change can be tolerated, it is important to ensure in the process of selection of an asphalt, that the materials not only have the necessary properties at the time of placement, such as proper viscosity and temperature susceptibility, but also have good long term performance [1]. In recent years, it has been the experience that at times, asphalts may meet current test specifications and yet show poor long term performance. One of the problems encountered is excessive rate of hardening of the binder.

Confining the discussion to the use of asphalts in pavement engineering, it is noted that the excessive rate of hardening would cause the asphalt mixture to become brittle and the pavement to crack prematurely. This problem is compounded by variations in temperature of the pavement layer which, in certain climatic zones, could reach 140° F (60° C) on a hot summer's day and drop to well below 32° F (0° C) in winter. The thermoplastic nature of asphalt now becomes a liability, suffering various changes in its properties depending on the prevailing temperature regime.

To add to the uncertainties of performance, a wide variety of asphalts are available commercially, their physical and chemical properties dependent upon crude sources and refining techniques. Since the 1973 oil embargo, there has been some dissatisfaction about the quality and variability of the properties of available asphalts.

It therefore becomes necessary to clearly identify the potential of asphalts with regard to some of their important properties, both short and long term, and take that into consideration so that a better and more durable facility is engineered. This study concerns itself with the evaluation of age hardening of asphalts and mixtures, with particular reference to a paving application.

1.2 Study Objectives

The primary objectives of this study are as follows:

1. Determine trends in age hardening or extent of variability in age hardening of some typical asphalt cements by using different measurement techniques.
2. Study the effects of asphalt type, heat, ultraviolet light, forced draft and natural weathering on the hardening rate of asphalts.
3. Acquire pertinent field and laboratory data from paving projects, on the properties of in-service asphalts and asphalt mixtures up to a service age of 18 months, and make a comparative study between field and laboratory aging.

4. Develop and assess procedures for studying aging of asphalt using infrared spectroscopic techniques.

Stated study objectives lead on to the following

1. Identifying measurements which can sensitively assess age hardening.
2. Identifying procedures which can recognize asphalt quality with greater confidence.
3. Providing a basis for a framework for future specifications.

1.3 Scope of Study

Eleven different asphalts covering a broad spectrum of types were selected and used in the testing program. For each of the asphalts, Thin Film and Rolling Thin Film Oven Tests were performed at three temperatures and physical and spectral parameters measured before and after the Oven Tests. Thereafter, 10 of the 11 asphalts were subjected to a detailed study. Each of these asphalts was used to make Florida Type S-1 asphalt concrete mixes and 540 Marshall specimens were fabricated from these mixes. The specimens were compacted with an average air void content of 5 percent and with an asphalt content of 6.5 percent. Aggregate source, specifications and proportions were kept constant.

The compacted mix specimens were subjected to the following aging conditions:

1. Conventional oven at 140° F (60° C) for durations of 1, 7, 28 and 90 days.
2. Ultraviolet chamber at 140° F (60° C) for durations of 1, 7, 28 and 90 days.

3. Forced draft oven at 140° F (60° C) for durations of 1, 7, 28 and 90 days.
4. Aging in natural weather conditions on the roof for durations of 6 months, 1 year, 2 years and 3 years.

Of the aged Marshall specimens, tests were run on those pertaining to four asphalts, to determine resilient moduli and fracture energy. Indirect tensile tests were run on all the aged Marshall specimens. After the strength tests, asphalt residues were recovered from the broken samples and the following tests were performed:

1. Absolute Viscosity at 140° F (60° C).
2. Penetration at 77° F (25° C).
3. Schweyer Rheometer at 77° F (25° C) and 59° F (15° C).
4. Infrared spectral analysis.

Samples in the form of recovered asphalts were obtained from two paving projects at various ages, both from wheel path and between wheel path of traffic lane. The following tests were conducted on the recovered samples:

1. Absolute Viscosity at 140° F (60° C).
2. Penetration at 77° F (25° C).
3. Infrared spectral analysis.

Statistical analyses were used to evaluate all the collected and generated data. Regression trends were plotted and patterns of hardening established. Correlations between variables of interest were attempted.

CHAPTER 2
LITERATURE REVIEW

2.1 Background

During the last fifty years or so there has been a steady increase in the scope and complexity of research on the nature and properties of highway asphalts. Nevertheless, the state of art in asphalt technology is still such that universal agreement does not exist among asphalt producers and consumers as to the requirements needed in specifications for highway asphalts to ensure satisfactory product performance.

This is not surprising, for an analysis of the data and information available reveals that most of the reported research has been on asphalts that were

1. not well defined in terms of fundamental physical and chemical properties,
2. insufficiently characterized by simulated laboratory performance tests under accelerated aging conditions, and
3. rarely documented as to their actual performance characteristics under various construction, traffic and environmental conditions.

Are present asphalt specification tests able to identify the important properties that control field construction and pavement performance? That indeed is the big question.

This chapter presents a literature review on the variability of paving asphalts by refinery source, the mechanism of asphalt hardening, the principle and application of spectrometry in general, infrared absorption spectroscopy in particular and the fundamentals of ultraviolet light in the context of age hardening.

2.2 Asphalt Cement Variability by Refinery Source

Is asphalt as good as it used to be? This statement is often repeated. There is a general belief that the oil companies are taking out the "goodies" from the asphalt and using them as feedstock. Are the oil companies using less-than-desirable crudes to manufacture asphalt?

Published literature contains limited information to indicate asphalt cement property variation by refinery source. Button, Epps, Little and Gallaway [2] have quoted Puzinauskas [3] that physical properties (including temperature susceptibility) of asphalt cements produced in 1979 have the same range of values as those produced in 1964. Studies at Pennsylvania State University [4] done on a statistical basis from data collected by them from specific refining sources indicated that the physical properties of asphalt cements from certain refineries have changed with time, whereas asphalts from other refineries show no significant change. Button et al, [2] are not certain whether these changes are significant from the standpoint of pavement construction and performance. They also observed that asphalt cements produced in the post-1976 period have a greater resistance to TFOT hardening than do those asphalt cements produced prior to 1977. Anderson and Dukatz [4] studied changes in the physical and chemical properties of asphalt produced before and after the 1973 oil embargo and concluded that temperature susceptibility of the sampled asphalts increased over the time period 1950-1980. Increases in shear susceptibility were noted over the sampling period, however, because of the limited data base, the authors advise caution while viewing this conclusion. The most significant conclusion made by them was that asphalt properties vary with region and the changes in asphalt properties over the time period 1950-1980 also varied with region. Burati et al. [6] studied variation of asphalt properties between refinery sources in South Carolina and noted that there is a variability between sources and that properties of asphalts from the same source, varied from month-to-month.

It therefore seems apparent, that the need of the hour, as it has been throughout the past 50 years or so, may not be for an improved asphalt quality, whatever that may mean, but for a better understanding of the engineering properties (especially with time) of a particular asphalt, and applying that information to the design of the paving mixture.

2.3 Mechanisms of Asphalt Hardening

Asphalt durability can be defined as resistance to change in original properties, for the worse, during construction and in-service aging. The aging of asphalt can be caused by a number of factors such as oxidation, loss of volatile oils, and changes in structure and chemical composition.

2.3.1 Oxidation

Early literature all indicated that oxidation was a prime cause of asphalt deterioration. Data indicating that oxygen contributes to an increase in hardness was first reported nearly 50 years ago in a study where layers of asphalt cements, liquid asphalts and tars were exposed to light, air and solar heat for one year [6].

It is now well known that the most important factor associated with hardening is the oxidation of the asphalt throughout the entire thickness of the asphalt concrete pavement. Hardening of the surface is generally greater due to greater availability of oxygen and higher temperature and ultraviolet light [7]. This is confirmed by the results of other investigators where the top quarter inch of the pavement was found to have a viscosity 50 percent greater than at depths of one half inch [8].

2.3.2 Air Voids Content

Both surface and at depth hardening are probably most influenced by the voids content. Pavements with lateral cracking and high air voids had a greater degree of hardening and oxidation than uncracked pavements with low voids [9]. Tests on samples taken periodically after construction indicated increased hardening with age. In a classic study by Goode and Lufsey [10], it was found that air void content or permeability, per se, did not appear to be the only factor affecting the rate of hardening. Air void content, combined with film thickness, appeared to have the greatest effect on hardening rate.

Page, Murphy, Ruth and Roque [11] concluded that by considering air void content at some selected age, the recovered asphalt viscosity or penetration usually indicates harder asphalts for high air void content samples. They also observed that certain asphalts when used in a properly designed mix and compacted to achieve a 6 percent or less air void content, appear to exhibit very low or no age hardening over the 3- to 5-year period of the investigation.

2.3.3 Asphalt Content and Aggregate Gradation

It is interesting to note that higher asphalt contents did not reduce the amount of hardening [7]. It appears that the film thickness has a lesser effect for graded mixtures. This is partially verified by the results of another study where it was found that hardening during the first few months of service was due to the laying and compaction operation [12]. Also, the different designs using both a coarse graded and dense graded mixture with the same asphalt content did not influence hardening during mixing and after 20 months.

2.3.4 Climatic Effects

Climatic effects as observed in Australia, appear to have a significant effect on hardening. The rate of thermal oxidation was approximately doubled for every 10° C (18° F) rise in temperature [13]. Reaction with oxygen, both in absence and presence of light, was concluded to be the primary cause of hardening.

2.3.5 Crude Source

Corbett and Schweyer [14] conclude that crude source is a variable affecting both the composition and the corresponding flow properties of the original asphalt used in paving. They estimate that there are as many as 600 different compositions being used today in North America. Investigations in Saskatchewan showed that there was a relationship between asphalt source or refinery and the amount of transverse cracking [15]. It was observed that the largest changes in properties of the binder occurred in the pugmill and during the first twelve months of service. However, some asphalts were affected more by mixing than in situ aging and vice-versa.

2.3.6 Predicting Asphalt Durability

Green, Tolonen and Peters [16] investigated several laboratory techniques for predicting asphalt durability. Their studies included rolling thin film oven, weatherometer exposure, chemical composition and vanadium analysis, which were related to environmentally exposed specimens to produce predictable responses. Kemp and Predoehl [17] studied the weathering of four briquettes in four distinctly different field environments for four years. The controlled variables included three different asphalts, three void ranges and two aggregate sources. They found that thermal oxidation is the most significant factor affecting the rate and amount of asphalt hardening in hot climates. Voids and aggregate porosity are also contributing factors but are dependent upon the susceptibility of the asphalt to these factors.

Santucci, Goodrich and Sundberg [18] reported that viscosity is a more sensitive measure of asphalt changes during oven durability tests than penetration. Asphalt binders always increase in viscosity starting with the hot-mix cycle. A two to four-fold increase in viscosity and a 30 percent decrease in penetration generally occurs by the time the pavement is a year old [14]. Thereafter, the viscosity level increases more slowly and typically reaching about 20,000 poises at 60° C (140° F) in about 25 years, based on an original AC-20 asphalt.

To Page et al. [11], it appeared feasible to predict or simulate in-service hardening by using the asphalt in mixtures compacted to different air void contents and then subjected to heating in an oven at 60° C (140° F). Also, they observed that the effect of plant mix temperature on hardening was proportional to the TFOT temperature.

2.4 Spectrochemical Methods of Analysis

2.4.1 Theoretical Background

Some of the earliest means used for the characterization of objects and substances were based upon the observation of color. Even today, the description of any object usually includes a statement regarding color. Color arises from the absorption and emission of light by matter, each form of matter displaying its own absorption or emission behavior. In fact, this behavior is so important that an entire subdiscipline of chemistry called spectrochemical analysis has been developed around it. In this portion of the review, the fundamental principles of spectrochemistry will be examined and a few specific techniques which employ these principles for purposes of qualitative and quantitative chemical analysis will be considered.

In spectrochemical analysis, the spectrum of electromagnetic radiation is employed to determine chemical species and to characterize their interactions with electromagnetic radiation [18]. A spectrum is a plot of some measurable property of the radiation, $f(\nu)$, as a function of the frequency of the radiation, ν. From a spectrum, two important pieces of information can be obtained. First, from the shape of the spectrum, a chemical species can often be identified qualitatively. Second, from the magnitude of $f(\nu)$ at chosen frequencies, the amount of a chemical species present can be determined quantitatively.

To amplify on these statements, it is necessary to recall the fact that, for a photon (quantum of electromagnetic radiation), frequency is related to energy through the Planck equation,

$$E = h\nu \qquad (2.1)$$

where E is the energy of the photon, ν is the frequency and h is Planck's constant (6.624 x 10^{-27} erg sec). Therefore, a photon of electromagnetic radiation has a definite energy and can cause transitions between the energy states in atoms, molecules and other chemical species. To cause such a transition, the energy of the photon must be equal to the difference between the energy states involved in the transition. Thus, we can examine chemical species by using electromagnetic radiation as a probe, the frequency of the radiation being related to the energy change associated with the observed transition.

Because energy states differ among chemical species, it is to be expected that the energy changes involved in the transitions will also differ. This implies that a spectrum will be a highly individual property of each substance, and that observation of the spectrum can be employed to advantage for identification of the substance. In effect, the spectrum is a map of the transitions which occur between energy states of the chemical species. Furthermore, the number of times each transition occurs during a fixed interval is related to the total number of chemical species which can undergo that transition. Therefore, if the measured parameter, f(ν), in a spectrum can be related to the total number of transitions, the spectrum can be used to determine the concentration of species present.

There is no restriction on the frequency of electromagnetic radiation employed in spectrochemistry. In fact, spectrochemical analysis can utilize frequencies ranging from those of audio waves (10 to 10,000 Hz)* to those of gamma rays (10^{22} Hz). Over this enormous range of frequencies, the principles of spectrochemical analysis remain unchanged, the only difference being the magnitude of the energy changes which are probed. Figure 2.1 shows the range of frequencies commonly used in spectrochemistry.

---

* 1 Hz = 1 cycle per second

2.4.2 Some Relevant Characteristics of Electromagnetic Radiation

Because the interaction of radiation with chemical species is the foundation upon which spectrochemical analysis is based, several important characteristics of electromagnetic radiation need emphasis.

Figure 2.2 portrays a sinusoidally oscillating electromagnetic wave, traveling through space in an arbitrary direction n. As its name implies, the wave consists of oscillating electric (E) and magnetic (M) fields, which are orthogonal to each other and which travel at a constant velocity (c). Assuming the wave has a constant frequency of oscillation (ν), the wavelength will be a constant and equal to the distance the wave travels during one period $\frac{1}{\nu}$ of its oscillation. Therefore the wavelength (λ) can be calculated from the well-known formula:

$$\text{distance} = \text{velocity} \times \text{time}$$

$$\lambda = c \times \frac{1}{\nu} = \frac{c}{\nu} \tag{2.2}$$

Because of this relationship to frequency (ν), wavelength (λ) is often used as the horizontal axis for a spectrum.

It should be noted that wavelength is inversely proportional to frequency and, therefore, to energy as well. Because it is sometimes desirable to refer to the energy of a spectrochemical transition, a quantity proportional to energy is often used instead of wavelength or frequency. This quantity, called a wave number has units of cm^{-1}

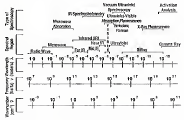

Figure 2.1 Range of Frequencies Used in Spectrochemistry

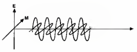

Figure 2.2 Portrayal of an Electromagnetic Wave

(reciprocal centimetres), is given the symbol $\overline{\nu}$ and is defined by the expression

$$\overline{\nu} = \frac{1}{\lambda} = \frac{\nu}{c} \tag{2.3}$$

Several other characteristics of electromagnetic waves are important to spectrochemical analysis. One such characteristic, monochromaticity, refers to the spectral purity of the wave. For an idealized wave such as that depicted in Figure 2.2, only a single frequency exists. Such a wave is said to be monochromatic. Actually, few truly monochromatic waves are ever employed in spectrochemistry. More often, the radiation used contains a range of frequencies spread over a certain spectral interval. This bandwidth is often of considerable importance in spectrochemical measurements and can affect both the qualitative and quantitative validity of an analysis.

2.4.3 Absorption of Radiation

If a beam of electromagnetic radiation is sent into a chemical sample, it is possible for the sample to absorb a portion of the radiation. This phenomenon is depicted in Figure 2.3 which shows a beam of radiation having a radiant power P_0 being directed into a sample. Each specific frequency, ν_1, ν_2 and so on, which comprises the beam of radiation will, of course, have its own energy, $h\nu_1$, $h\nu_2$ and so on. If the chemical sample contains a species whose energy states differ by any of these exact energies, the sample will absorb radiation at those frequencies. This behavior is illustrated in Figure 2.3, in which a chemical species having energy level G and E is portrayed. If the species (atom, molecule or ion) exists in the lower (ground) energy state G before its encounter with the beam of radiation, it can be excited to the upper state E. In this excitation, the species must absorb

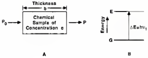

Figure 2.3 Relationship Between the Incident and Transmitted Radiant Power

a quantity of energy $h\nu_1$, which is exactly equal to the difference in energy between states G and E.

Energy required to excite the species to the upper energy state E is drawn from the beam of radiation, so that the total radiant power of the beam is diminished at the frequency of absorption, ν_1. Therefore, after encountering a number of absorbing species in the sample, the beam will exit from the sample with a reduced radiant power P. It should be recognized that only those frequencies capable of being absorbed by the sample will be attenuated in a purely absorbing sample, all other frequencies will pass through the sample with no power loss. This result suggests the possibility that components in the sample can be identified from the absorption spectrum, that is, from the frequency components of the radiation which are absorbed. Understandably, the diminution in the radiant power of the beam at each frequency should be related to the number of absorbing chemical species present in the sample. This information provides the basis for quantitative analysis.

2.4.4 Spectrochemical Measurements

Figure 2.4 depicts a generalized spectrochemical instrument, arrows indicating the flow of information through the instrument. In this arrangement, an input device is used to convert information on chemical composition and structure into information in the form of electromagnetic radiation. Therefore, this device is a transducer which encodes the chemical information into another form, namely electromagnetic information.

To decode or extract the chemical information encoded in the radiation, a second transducer, commonly called the detector, is required. In the spectrochemical instrument, the function of a detector is to

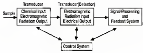

Figure 2.4 Generalized Spectrochemical Instrument

provide a measurable electrical signal which is proportional to the radiant power of the radiation incident upon the detector. The final output can take many forms, from a simple meter deflection to columns of numbers or graphical displays from a computer.

A final but indispensable component of the generalized spectrochemical instrument is the control system. This device is responsible for coordinating all the events and operations that take place in the instrument, from selection and introduction of the sample to interpretation of the readout signal.

2.4.5 Quantitative Laws of Absorption

Quantitative methods of analysis based upon the absorption of radiant energy by matter require the measurement of radiant power and a quantitative understanding of the laws which govern the extent of absorption.

Consider the transmission of electromagnetic radiation through a container of absorbing species. It can be stated quite simply that the extent of absorption depends upon the number of encounters between photons and species capable of absorbing them. As the photons pass through the medium, the rate at which they are absorbed depends upon the number of photon-absorber collisions, which in turn depends on the power of the electromagnetic radiation and on the concentration of the sample species. For example, if the rate of photon absorption is to be doubled, the number of photon-absorber collisions can be doubled by doubling the number of photons or by doubling the number of absorbers. In either case, collisions will occur twice as often, and the rate of absorption will go up by a factor of two. If the population densities of both photons and absorbers were doubled, they would bump into each other four times as often, and the rate of absorption would increase by a factor of four.

The relationship between radiant power, concentration, and rate of absorption are embodied in two laws: Lambert's law, which expresses the dependence of the rate of absorption on the power of the photon beam, and Beer's law, which relates the absorption rate to the concentration of absorbing species in the sample. The most familiar expression of the combined Lambert-Beer law is usually written as

$$\log \left(\frac{P_o}{P}\right) = abc \tag{2.4}$$

where P_o = power of incident radiation, any units

P = power of transmitted radiation, any units

a = absorptivity, liter gm^{-1} cm^{-1}

b = sample path length, cms

c = concentration factor, gms/liter

The quantity $\log \left(\frac{P_o}{P}\right)$ is defined as absorbance and is given the symbol A. Because A is directly proportional to the concentration of the absorbing species, some instruments for absorption measurements are calibrated to read directly in absorbance units.

2.4.6 Deviations from the Lambert-Beer law

Deviations from the law are of three types--real chemical and instrumental. Real deviations arise from changes in the refractive index of a medium which occur because of variations in the concentrations of its components. A rigorous derivation assumes a constant refractive index for the absorbing medium; any error in this assumption produces a consequent uncertainty in the experimental results. Generally, errors caused by changes in refractive index are minimal, so that real deviations from Lambert-Beer's law are neglected in most absorption spectrochemical analyses.

Chemical deviations from Lambert-Beer's law are caused by shifts in the position of a chemical or physical equilibrium involving the absorbing species. Consider, for example, the following reaction between an absorbing species A and another secies B to form species C and D

$$A + B \rightleftharpoons C + D$$

Any change affecting the position of this equilibrium will alter the concentration of A.

The use of non-monochromatic radiation is the most common instrumental cause of deviations from Lambert-Beer's law. In most spectral regions, it is difficult or impossible to obtain truly monochromatic radiation.

2.5 Infrared Absorption Spectroscopy

A rapid development of infrared absorption spectroscopy began at the end of World War II when the first commercial instrument became available in the United States. At the present time, infrared spectroscopy is used extensively for the investigation of molecular structure and the analysis of functional groups.

2.5.1 Basic Principle

The basic principle of this method is that interaction of infrared electromagnetic radiation with mass results in absorption of certain wavelengths of radiation, the energy of which is, in some way, related to the energy states of the molecules or groups of atoms within the molecules. In the spectrum produced, the absorption intensity is recorded as a function of wave number or wavelength, specific groups of atoms in the molecules give rise to characteristic absorption bands whose wave numbers fall within a definite range regardless of the composition of the remainder of the molecules. This constancy of absorption wave numbers makes possible the determination of functional groups present in the substance being analyzed. From the exact value of the wave numbers at which absorption is observed, conclusions may be drawn about the influence of adjacent groups in the molecule or in neighboring molecules on the vibration of the group in question. It is then possible to create a picture of the molecular configuration and to determine details of the probable structure. Because of the great variety of possible vibrations in most molecules, it is practically impossible to find two compounds which would have identical spectra. For this reason, the infrared spectrum is often referred to as a 'fingerprint' of a molecule [19]. If a large enough library of spectra is available, it is possible to identify compounds, and in favorable instances, even mixtures of compounds, by comparison with such reference spectra.

2.5.2 Spectroscopic Analysis of Asphalts

The analysis of asphalts is no simple matter because of the variety of molecular types and structures present as well as their relatively high molecular weights. Because the number of molecules in asphalt with different chemical structures and reactivities is extremely large, the determination of asphalt composition by separation of asphalt into its molecular components is generally considered impractical [20].

Beitchman [21] described a method for the preparation, irradiation and infrared analysis of thin films of air blown asphalts. He observed that increases in absorption at wavelengths of 2.91 microns (wave number of 3430 cm^{-1}), 5.88 microns (1700 cm^{-1}) and 9.71 microns (1030 cm^{-1})

were produced by exposure of unsupported films of asphalt to the radiant energy of a carbon arc. Wright and Campbell [6] reported on the work done by Greenfield and Wright who modified this method and used it to show the relationship between the change in absorption of the carbonyl band due to carbon arc exposure, and the time to failure of the same asphalts in accelerated weathering machines. The change in absorption of the carbonyl band was called the "carbonyl index". Twenty-four asphalts were evaluated in this study and with the exception of certain modified asphalts, an inverse relationship was shown for cycles to failure versus increase in carbonyl index. In discussing the relationship between carbonyl index and durability, Greenfield and Wright concluded that when very high oxidation results are obtained for a fixed irradiation period, the carbonyl index is limited as an indicator of durability. Unusually high values of change in absorbance may or may not indicate poor durability. Low values, however, are excellent indicators of good durability.

Using methods similar to that of Beitchman [21], Wright and Campbell [6] studied the oxidation rate of eight air blown asphalts by measuring the change in infrared absorption at 5.88 microns (1700 cm^{-1}) with time of exposure to the radiant energy of a carbon arc. While all the asphalts oxidized at different rates, those from the same geographical areas had similar rates, those from different areas differed considerably. An inverse relationship was found between the rate of oxidation and the accelerated weathering durability of each asphalt. The results of this study indicated that by the use of infrared spectra of asphalt films, oxidation-rate results can be obtained rapidly and accurately. The authors summed up by stating that "oxidation rate data offer a potential basis for predicting natural weathering durability, as well as development of a product quality specification" (p. 264).

Smith, Schuetz and Hodgson [22], in their study of roofing asphalts, noted the sensitivity of infrared spectra for making quantitative comparisons of the functional groups in asphalts. Reporting the relationship between carbonyl absorption and weatherability, the authors found no correlation between the initial carbonyl content and weatherability. For a given type of hydrocarbon composition, an asphalt that has undergone considerable oxidative aging from blowing may not withstand additional oxidation from weathering so well as one which has not been blown so much. In the few instances that they encountered in which asphalts have closely similar hydrocarbon structures but differ in carbonyl concentration, the ones with the greatest amount of carbonyl weather least well. Another possibility emphasized by them is that a greater amount of carbonyl can be tolerated in an asphalt high in methylene chain content than in one with lower methylene chain content.

Commenting on the changes induced in asphalts by heat and ultraviolet irradiation, Smith et al. made the following three important observations.

1. The absolute infrared absorption band changes from oxidation of asphalts by weathering are large as compared to most of the hydrocarbon absorption band differences in asphalts. The stronger absorptivities of oxygen bands make the differences among them more easily measured than in hydro-carbon structures, and for routine testing, this comparative ease of measurement has merit.

2. There are cases where the poorer weathering asphalts showed just slightly higher changes in carbonyl content than the more durable asphalts.

3. Ultraviolet irradiation produces changes corresponding to those at the surface of weathered asphalts, while heating in the dark or under infrared radiation produces changes corresponding to those which occur below the surface of the weathered asphalt.

From the foregoing, it will be seen that early researchers who used infrared spectroscopy for characterization of asphalts found the technique useful in determining the general chemical structural types present. However, the strongly associating polar functionalities present were never adequately identified or characterized because of several inherent problems such as overlapping and ill-defined absorption bands, and the shifting of absorption bands from hydrogen bonding.

2.5.3 Functional Groups

The hydrocarbon components of asphalt exhibit both polar and nonpolar intermolecular forces. The nonpolar hydrocarbon components are usually predominant in the saturated paraffins and less condensed naphthenes. These have weak intermolecular forces. Stronger intermolecular forces are associated with the highly polar hydrocarbon components. These are the highly condensed naphthenic and aromatic ring structures with attached functional groups. The chemical functional groups which are associated with the heteroatom of sulfur, oxygen and nitrogen impart polarity and functionality to the asphalt molecules [23]. Functionality determines how the molecules will interact with one another and with molecules of other materials while polarity induces strong molecular interactions. Thus the heteroatoms combined in the functional groups have a great effect on the physical properties and the differences in the performance of asphalts from different sources [24]. Examples of some of the more important functional groups which are an integral part of large asphalt molecules are

Naturally Occurring	Formed on Oxidative Aging
Polynuclear Aromatic	Sulfoxide
Phenolic	Anhydride
2 - Quinolone Type	Carboxylic Acid
Pyrrolic	Ketone
Pyridinic	
Sulfide	
Carboxylic Acid	

The chemical functionality method of identifying the molecular action within the asphalt molecule itself and with molecules of other materials is a relatively new and potentially productive tool in the investigation of asphalt chemistry and composition. It differs from the more traditional method of separating an asphalt into its generic constituents and has an advantage by looking at an asphalt as a whole. Moreover, if one considers the different chemical functionalities that comprise and dominate the properties of the various asphalt molecules, the number of types of functionalities that need to be taken into account narrows down to a manageable number [23]. This will be seen from the listing above.

2.5.4 Age Hardening and Functional Group Analysis

The principal cause of age hardening and embrittlement of asphalt used in pavements, is the atmospheric oxidation of certain asphalt molecules with the formation of highly polar and strongly interacting chemical functional groups containing oxygen [20]. Thus, the ability to identify and quantify asphalt chemical functionality provides an important tool for assessing the effects of composition on asphalt properties and, thus, the performance of asphalts in service.

From a study of available literature on the subject [22, 23, 25, 26, 27, 28], the following facts are apparent:

1. Net changes in the IR absorption spectra can be a useful technique for following relative changes in the level of asphalt oxidation.

2. Strong absorption at 1700 cm^{-1} results primarily from the development of ketones and anhydrides, the major functional groups formed from hydrocarbon oxidation in asphalts.

3. The carbonyl absorption region between 1600 cm^{-1} and 1800 cm^{-1} would be of particular interest since it contains the absorption bands for carboxylic acids, ketones and anhydrides. Ketones and anhydrides are formed on oxidative aging and carboxylic acids occur naturally in the asphalt but increase on oxidative aging. Together, these three functional groups are the most significant chemical functionalities which are an integral part of large asphalt molecules and which can be related to oxidative aging.

From the literature, it was seen that spectra obtained from 5 wt/vol percent solutions in THF exhibit the following major characteristics:

1. Free carbonyl absorption of acid types occurs at about 1730 cm^{-1}.

2. Free carbonyl absorption of 2-quinolone types occurs at about 1685 cm^{-1}.

3. A broad band centering at about 1600 cm^{-1} results primarily from aromatic carbon-carbon double bonds.

4. An increase in the level of oxidation causes an increase in carbonyl absorption of carboxylic acid at about 1730 cm^{-1}.

5. An increase in the level of oxidation causes a significant increase in carbonyl absorption in the 1700 cm^{-1} region, which is due to the formation of ketones and anhydrides.

It is also noted that an intense band at 1030 cm^{-1} results from sulfoxides, the functional group most easily formed in asphalt on oxidation [29]. However, it is possible that greater sulfoxide absorption intensity may be observed for specimens recovered from the pavement than laboratory oxidized specimens, probably because of infrared absorption by traces of finely suspended mineral matter present in the asphalt after recovery from the pavement [29].

2.6 Ultraviolet Stress in Sunlight

2.6.1 Ultraviolet Spectrum

European weathering literature and the medical profession divide the solar UV spectrum into three ranges [30]. UV-A is the radiation with wavelengths between 400 nm and 315 nm. UV-B has wavelengths in the 315 nm to 290 nm range. UV-C includes the solar radiation with wavelengths below 290 nm, which never reaches the earth's surface.

The 400 nm upper limit for UV-A is the generally accepted boundary between visible light and ultraviolet light. The 315 nm boundary between the UV-A and UV-B ranges defines the point at which UV energy begins to cause adverse effects and pigmentation changes in the human skin. Sunburn begins to occur at wavelengths below 315 nm and reaches a peak at 297 nm. The UV-C boundary of 290 nm is a sharp cutoff of solar radiation at the earth's surface caused by ozone absorption.

2.5.2 Effects of Ultraviolet Light

The quantum theory explains the different effects of UV-A, UV-B and UV-C. Light energy is transmitted in discrete units called photons. Photons behave much like tiny projectiles traveling at the speed of light. The size of a photon or the energy in a photon is inversely proportional to its wavelength-the shorter the wavelength, the bigger the photon. Photochemical reactions are caused by a single photon colliding with a single electron. If the photon is "big" enough (i.e., contains more energy than the organic bond strength) the electron is knocked out of its orbit and a reaction occurs. If the photon is not big enough, the energy of collision is harmlessly dissipated and no reaction occurs. For each type of chemical bond, there is a critical threshold size of photon (and hence a threshold wavelength) with enough energy to cause a reaction. Light of any wavelength shorter than the threshold wavelength can break the bond, but light of wavelengths longer than the threshold can never break the bond, regardless of the intensity (brightness) of the light [31].

The sun emits radiation with wavelengths well below 242 nm. The energy of photons with wavelengths below 242 nm is high enough to dissociate oxygen and create ozone. Ozone, in turn, is a highly effective UV absorber, absorbing all solar radiation below 290 nm, so that energy of such wavelengths never reaches the earth's surface at sea level. Ozone partially absorbs UV-B so that the amount of UV-B in sunlight varies with solar altitude. At solar altitudes between 60 and 90 degrees, the maximum amounts of UV-B reach the earth's surface and the sunlight cutoff wavelength is approximately 295 nm.

2.6.3 Spectral Energy Distribution

This is a general term for the characterization of the amount of radiation present at each wavelength. Spectral Energy Distribution (SED) can be expressed in terms of power in watts, irradiance in watts/sq.m. or energy in joules. The shape of the SED would be identical in all of these units. Fluorescent lamps are frequently described by relative SEDs which show the amount of radiation at each wavelength as a percentage of the amount of radiation of the peak wavelength. Figure 2.5 illustrates a typical relative SED of a UV-B lamp [32].

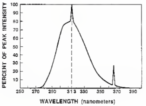

Figure 2.5 Typical Relative Spectral Energy Distribution of UV-B Lamp

CHAPTER 3
EQUIPMENT AND FACILITIES

This chapter describes the ultraviolet chamber, forced-draft oven and non-forced-draft oven which were used to provide various types of aging conditions for asphalt specimens in this study. Thereafter, the testing equipment, apparatus and facilities utilized for the strength, rheology and spectral tests are described.

3.1 Ultraviolet Chamber

3.1.1 Ultraviolet Fluorescent Sun Lamps

These lamps are such that radiation at 254 nm from a low-pressure mercury arc is transformed to light of lower wavelengths (predominatly UV light) by a phosphor. The spectral energy distribution of a fluorescent UV lamp is determined by the emission spectrum of the phosphor and the UV transmission of the glass tube.

Electrically, these lamps are the same as ordinary 48 inch fluorescent lamps, but their output is quite different. The UV lamps produce largely UV, with little energy spent in the production of visible light. Since the photo-chemical effectiveness of light increases with decreasing wavelengths, ultra-violet light is the controlling factor in sunlight deterioration. Because the special lamps produce only UV, they can give rapid deterioration despite their low wattage. Furthermore, the lamps suppress UV of shorter wavelengths that are not found in natural sunlight, because such unnatural energy can cause abnormal deterioration.

The UV stress obtained with the fluorescent sunlamp emitting UV-B is comparable to noon midsummer sunlight on a clear day and such lamps are most widely used for simulating the damage caused by outdoor sunlight.

In the UV chamber fabricated for the experimentation, 40-watt fluorescent UV-B lamps (UVB-313) manufactured by the Q-Panel Company were used. The lamps were 48 inches in length and identical to the ordinary 40-watt fluorescent lamps. The peak emission of the lamps is at a wavelength of 313 nm. Most of the output is in the UV-B region, with some output in the UV-A region.

3.1.2 Design of the UV Chamber

The chamber was fabricated from 3/8 inch plywood in the shape of a trapezoidal box with a 4'2" x 3'8" rectangular base and a height of 1' 10", external dimensions. The two sides of the chamber were hinged to permit access into the chamber and the interiors of these two hinged sides were used to mount four lamp assemblies, each assembly carrying two lamps. The roof of the chamber was used to mount one more lamp assembly carrying two lamps. Aluminum sheeting was fixed to the base of the chamber in order to prevent staining of the woodwork and to increase reflectance. This base was designed to receive 48 specimens at any one time. Insulation stripping, hooks, chains and handles were provided. The chamber was painted white on both the exterior and interior. Figure 3.1 illustrates the chamber. A picture of the chamber with one of the sides open is shown in Figure 3.2.

3.1.3 Lamp Mounting and Rotation

Lamps are arranged in two sets of four lamps each on the interior sides of the chamber, with two more lamps on the top interior. The ten

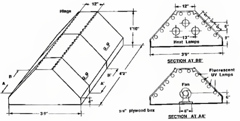

Figure 3.1 Ultraviolet Chamber

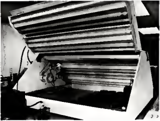

Figure 3.2 Picture of the Ultraviolet Chamber

UV-B lamps are installed in standard fixtures complete with electrical fittings and reflectors, which had been mounted permanently in the interior of the chamber. Since fluorescent lamps are diffuse light sources, this arrangement provides uniform irradiation of the test surface, without the complications of a revolving specimen holder.

Considering that the manufacturer recommended lamp life is 1600 hours, at which time the UV lamps supposedly still retain 60 percent of the original output, it is necessary to replace and rotate the tubes periodically, so that at any time, the output inside the chamber as a whole is an average of lamps at five different points on the age/output curve. This is done by replacing two of the tubes at intervals of 360 hours and rotating the position of the rest as illustrated in Figure 3.3. This results in an 1800 hour life for each lamp. Such periodic fractional relamping ensured stable UV output as the lamps aged.

3.1.4 Temperature Control

The destructive effects of UV exposure are accelerated when temperature is increased. Although temperature does not affect primary photochemical reactions, it does affect secondary reactions involving the by-products of the primary photon/electron collision.

It is therefore necessary to provide accurate control of UV exposure temperature. A typical temperature condition of 60° C (140° F) was considered appropriate. To maintain this level of temperature, a thermostat was installed with the sensor located at midpoint of the sample area. Heating arrangement consisted of three lamps mounted on one vertical endside of the chamber. One of the lamps was an infrared heatlamp (Warm Up), manufactured by General Electric Company. The other

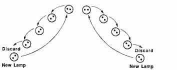

Figure 3.3 Rotation of Lamps in UV Chamber

two lamps were plant lights (Gro and Sho 150 watt bulbs), also manufactured by General Electric Company. Circulation of heat was improved by a fan installed at the opposite end of the chamber. A dummy specimen instrumented with thermisters was used to monitor specimen temperature.

It is seen that once a steady state temperature condition is reached, the heating arrangement is seldom activated, the chamber temperature remaining steady at 60° C (140° F) with all UV-B lamps lighted and the fan constantly running.

3.1.5 Positions of Specimens

The exposure area at the base of the chamber can be divided into three exposure zones, one corresponding to the area directly beneath the two top tubes and the other two corresponding to the two adjacent sides which lie beneath the two sides of the chamber carrying the remaining lamps. It is probable that the intensity of radiance may be different in the middle zone as compared to that in the outer zones. It is also probable that the irradiance inside the chamber may be affected by the heating lamps positioned to one side of the chamber, thereby creating a bias towards one side of the chamber.

In order to ensure a certain uniformity in exposure conditions, the utilizable base area of the chamber is gridded as shown by Figure 3.4. Two columns of the grid are used to accommodate specimens for one duration of exposure and thus the eight columns cater for four exposure durations. The space for 90 day duration is located nearest the fan and the 1 day duration nearest the heating lamps. Intermediate locations, in that order, are alloted to 28 day and 7 day durations.

FAN

90*	90	28	28	7	7	1	1
90	90	28	18	7	7	1	1
90	90	28	28	7	7	1	1
90	90	28	28	7	7	1	1
90	90	28	28	7	7	1	1
90	90	28	28	7	7	1	2

HEATING LAMP

NOTE: *The numbers represent the different exposure durations in days.

Figure 3.4 Plan of Ultraviolet Chamber Showing Locations of Samples of Different Exposure Durations

Within the location for a particular duration of exposure, twelve grid positions are available. With three replicate specimens for each asphalt type, it is possible to simultaneously expose specimens fabricated from four different asphalt types. The distribution of specimens by asphalt types is done in a deliberate manner such that one replicate specimen is positioned in each zone (one in the middle zone and one each in the two outer zones). The positioning arrangement is further refined by ensuring that (a) in the two outer zones, one replicate specimen is placed nearer to the middle in one zone while another replicate is placed farthest from the middle in the other zone, (b) the two positions within one zone are crossed over, (c) in the middle zone, specimens are moved around in a counterclockwise manner.

Serial (a) neutralizes the bias created by proximity of the UV lamps. Serials (b) and (c) attempt to neutralize the bias created by the heating lamps on one side of the chamber.

Figure 3.5 illustrates the actual positions of the Marshall specimens for all the asphalts tested.

In order to cut time of running of the chamber, 90 day specimens were exposed for 60 days at the locations indicated and, thereafter, moved to the 29 day location where the specimen remained for 15 days and then moved to the 7 day location for the final 15 days of exposure. This movement enabled vacation of the 90 day location at an earlier instant, so that the next batch of specimens could be inducted sooner.

FAN

CH 35	AM 09	CH 33	AM 14	CH 45	AM 20	CH 49	AM 39
BE 51	MA 03	BE 19	MA 27	BE 46	MA 54	BE 30	MA 14
AM 34	MA 45	MA 49	BE 05	BE 03	CH 09	CH 16	AM 57
CH 55	BE 01	AM 21	CH 07	MA 43	AM 56	BE 20	MA 42
AM 51	CH 19	AM 42	CH 27	AM 01	CH 32	AM 27	CH 25
MA 39	BE 58	MA 09	BE 37	MA 16	BE 54	MA 57	BE 45

HEATING LAMPS

NOTE: CH - Chevron, BE - Belcher, AM - Amoco, MA - Mariani

FAN

TX 09	SO 01	TS 42	SO 09	TX 59	SO 52	TX 33	SO 34
TA 38	BO 34	TA 33	BO 19	TA 58	BO 21	TA 34	BO 35
SO 20	BO 55	BO 53	TA 12	TA 07	TX 20	TX 60	SO 19
TX 32	TA 03	SO 45	TX 21	BO 46	SO 57	TA 21	BO 62
SO 10	TX 54	SO 06	TX 34	SO 30	TX 52	SO 33	TX 51
BO 60	TA 49	BO 25	TA 44	BO 33	TA 08	BO 03	TA 48

HEATING LAMPS

NOTE: TX - Texaco, SO - Esso, TA - Texaco Airblown, BO - Boscan

FAN

DM 20		DM 05		DM 02		DM 24	
DI 05		DI 20		DI 9		DI 21	
			DI 22	DI 17	DM 19	DM 23	
DM 18	DI 24		DM 11			DI 15	
	DM 22		DM 08		DM 01		DM 15
	DI 11		DI 06		DI 14		DI 16

HEATING LAMPS

NOTE: DI - Chevron AC 20, DM - Chevron AC-20 Modified

Figure 3.5 Positions of Specimens in Ultraviolet Chamber

3.2 Forced Draft Oven

A standard laboratory oven of approximately 2 cubic feet capacity was modified to enable air flow through the oven. This was done by providing a large inlet port on one side of the oven and a small exit port on the top of the oven. These two ports were connected externally by flexible aluminium ducting. A 375 cfm air booster was placed external to the oven, in the duct line, adjacent to the inlet port. Some air vents were provided on the duct so as to include a small amount of fresh air in the recycled flow. The oven temperature was maintained at 60° C (140° F) with the help of a thermostat switch and sensor. Figure 3.6 depicts the oven.

3.3 Conventional Ovens

Standard laboratory ovens with over-temperature protection were used to age the specimens at a stable temperature of 60° (140° F). Thermometers were installed and the temperature was monitored regularly.

3.4 Strength Tests

The MTS electro-hydraulic closed loop testing machine was used for the resilient modulus, indirect tensile and fracture energy testing. See Figure 3.7. The machine consisted mainly of a control unit, load frame, load cell, servovalve and hydraulic power supply. Two stainless steel loading strips 12.7 mm (1/2 in.) wide were used to apply the load to the specimen as shown in Figure 3.8. The loading strips were curved at the interface with the specimen with a radius of 51 mm (2 in.). Two guide rods were used to prevent any eccentricity in loading. The horizontal deformations of the specimen were measured by two identical

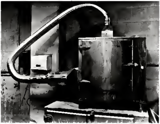

Figure 3.6 Picture of the Forced Draft Oven

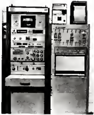

Figure 3.7 Picture of MTS Machine

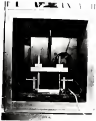

Figure 3.8 Picture of Loading Arrangement

Linear Variable Differential Transformers (LVDTs) mounted on opposite sides of the specimen. The output voltages of the two LVDTs were connected in series to obtain one output representing the sum of the two voltages. The output voltages of the LVDTs and the load cell were calibrated and connected to a multi-channel drum chart recorder.

3.5 Constant Stress Rheometer Test

A Cannon Schweyer Constant Stress Rheometer was used in this study (see Figure 3.9). A schematic of the test set-up is shown in Figure 3.10.

The apparatus consists of a nitrogen gas operated pnuematic cylinder which applied a specific force to the plunger in the sample tube. A LVDT measured the movement of the plunger and the output voltage was digitized and acquired by a data analysis system developed by Tia and Ruth (unpublished). The data system was operated on a IBM 9000 Mini series computing device (see Figure 3.11).

The plunger force is set by adjusting the pressure of the nitrogen gas entering the cylinder, which is read by one of the two pressure gages. The sample tube is inserted into an insulated aluminium block which is maintained at the test temperature using coolant from a refrigeration unit in combination with an electrical wire heater.

3.6 Infrared Spectroscopic Test

3.6.1 The Testing System

The infrared spectroscopy tests were run on a Nicolet 60 SX research-grade Fourier Transform Infrared Spectrophotometer System in the Materials Science and Engineering Laboratory of the University of

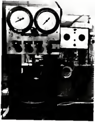

Figure 3.8 Picture of Cannon Schweyer Rheometer

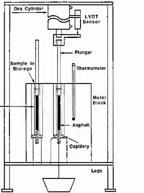

Figure 3.10 Schematic of Cannon Schweyer Rheometer

Figure 3.11 Picture of IBM 9000 Mini Computer

Floride. The system offers a resolution of 0.25 cm^{-1} throughout the standard range of 5,000 - 400 cm^{-1}. The components are arranged into two main groups, the data acquisition system including the computer, disk drives, and terminal, and the spectrometer including the optical bench and washer control. Figure 3.12 depicts a typical 60 SX system configuration. Figure 3.13 illustrates the system which was used.

3.6.2 Fourier Transform Infrared Spectroscopy [33]

The Fourier Transform Infrared (FTIR) spectrometer essentially comprises of two parts:

1. an optical system which uses an interferometer.
2. a dedicated computer.

The computer controls the optical components, collects and stores data, performs computations on data and displays the needed spectra. The use of a dedicated computer with a spectrometer has certain advantages. However, the major advantages of an FTIR spectrometer result from the use of an interferometer rather than a grating or prism of a conventional IR spectrometer.

Major distinctions between FTIR spectrometers are based on the design of the interferometer and the manner in which the interferometer is operated. It may be operated by scanning in a discontinuous, step-wise manner (step scan interferometer), a slow continuous manner with chopping of the infrared beam (slow scanning), or rapidly without chopping of the infrared beam. The rapid scanning Fourier transform spectrometer with a Michelson interferometer seems to have emerged as the most practical form of FTIR spectrometer for commercial development and widespread application to chemical problems in all regions of the infrared spectrum.

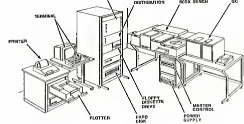

Figure 3.12 Typical 60 SX Fourier Transform Infrared Spectrophotometer System

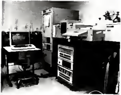

Figure 3.13 Picture of FTIR System Used

3.6.3 Grating Spectrometer Optical System

Figure 3.14 shows the essential components of one configuration of a single-beam grating spectrometer for comparison with the FTIR instrument. Light from the infrared source is focussed through the sample and onto the entry slit, which is at the focus of a collimating mirror. The collimated beam is dispersed by the grating, and light of a selected narrow frequency band is directed through the exit slit and chopper to the detector. A calibrated mechanical linkage to the grating provides a readout of frequency or wavelength and a direct plot of detector response versus wavelength is obtained.

3.6.4 Fourier Transform Infrared Spectrometer Optical System

A schematic diagram of the essential components of a rapid scanning Fourier transform spectrometer is given in Figure 3.15. The light from an infrared source is collimated and sent to the beam splitter of a Michelson interferometer. The beam is divided, part going to the moving mirror and part to the fixed mirror. The return beams recombine at the beam splitter undergoing interference. The reconstructed beam is then directed through the sample and focussed onto the detector. The motion of the mirror results in a signal at the detector which, for a given wavelength λ, varies sinusoidally with a frequency f. A laser beam, undergoing the same change of optical path as the infrared beam, serves to reference that position of the mirror during the scan and initiates the collection of data points from the signal of the infrared detector at uniform levels of mirror travel. The data points are digitized by an analog-to-digital converter and stored in a computer memory. The result is an interferogram, i.e., a record of the signal of the infrared detector as a function of the difference in path (retardation) for the

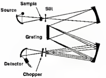

Figure 3.14 Essential Components of a Single-Beam Grating Spectrometer

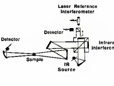

Figure 3.15 Essential Components of a Rapid Scanning Fourier Transform Spectrometer

two beams in the interferometer. The interferometer scans are generally taken quite rapidly (a few seconds each) to avoid extensive signal averaging before digitization. Data from additional scans can be co-added to the data stored in computer memory to improve the signal-to-noise ratio of the interferogram.

The averaged interferogram is prepared for computation and a Fourier transformation is performed on the interferogram using a fast Fourier transform algorithm. The Fourier transform converts the signal as a function of retardation to a signal as a function of frequency.

3.6.5 Advantages of Fourier Transform Infrared Spectroscopy

FTIR spectroscopy offers significant advantages as compared to conventional dispersion infrared spectroscopy, namely;

1. Higher signal-to-noise ratios for spectra obtained under conditions of equal measurement time.
2. Higher accuracy in frequency for spectra taken over a wide range of frequencies. The signal-to-noise advantage is a consequence both of the concurrent measurement of the detector signal for all resolution elements of the spectrum and of the high optical throughput of the FTIR spectrometer. The improvement in frequency accuracy of the FTIR spectrometer is a consequence of the use of a laser which references the measurements made by the interferometer.
3. Convenient data handling and plotting of data.
4. Simplicity of the optical system.

3.6.6 Sealed Cells

Liquids are examined for their spectral characteristics in sealed cells. These cells for handling solutions vary in thickness from 0.1mm to 1mm, the thickness representing the path length through the film of solution held between two crystal windows. The crystal windows are generally constructed of optical grade Sodium Chloride (NaCl) or Potassium Bromide (KBr).

In the initial stages of this study, Perkin-Elmer 0.1mm NaCl cells were used. It was found that the absorbance values and the signal-to-noise ratio were low. To improve the quality of the spectra, a Spectra Tech 1.0mm NaCl cell was procured and adopted for use. The tenfold increase in path length resulted in higher absorbance values and a high signal-to-noise ratio. Figure 3.16 shows the two types of sealed cells.

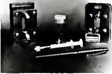

Figure 3.16 Picture of Sealed Cells, Vial and Syringe

CHAPTER 4
MATERIALS AND LABORATORY PROCEDURES

This chapter describes the materials and laboratory procedures used in the testing program on laboratory-controlled samples in this study. It includes a description of the properties of asphalts and aggregates used, the fabrication of Marshall specimens, the various laboratory aging conditions, the tests on Marshall specimens and the tests on the aged asphalt residues. The randomization process in assignment of treatments to the laboratory-controlled samples is also presented.

4.1 Materials

4.1.1 Asphalts

Eleven different asphalts covering a broad spectrum of sources and types were selected and used in the testing program. The asphalts chosen are

1.	Amoco	AC-30
2.	Chevron	AC-30
3.	Marathon	AC-30
4.	Mariani	AC-30
5.	Belcher	AC-30
6.	Texaco Airblown	85-100 pen.
7.	Texaco	85-100 pen.
8.	Boscan	85-100 pen.
9.	Esso Nolan	25-35 pen.

10. Chevron AC-20

11. Chevron AC-20 with 10% Modifier

4.1.2 Aggregates

The aggregates used were obtained from V.E. Whitehurst and Sons, Inc. in Gainesville. Table 4.1 lists the aggregate types and blends used, as well as the job mix formula and the specification range for the S-1 mix.

4.1.3 Marshall Specimens

Of the 11 asphalts chosen, 10 were identified as being of sufficient interest to warrant closer study and consequently each of these asphalts was used to make Florida Type S-1 asphalt concrete mixes and Marshall specimens were fabricated from these mixes. A total of 540 Marshall specimens were fabricated, 60 specimens of each asphalt type for the asphalts at serials (1) to (9) above (with the exception of Marathon AC-30) and 30 specimens each of serials (10) and (11).

Corresponding to each asphalt type, the blended aggregate was checked for gradation. This was done by randomly selecting a pan of the aggregate blend and carrying out a washed sieve analysis, results of which are shown in Table 4.2.

Maximum specific gravity by the Rice Method was determined on randomly selected mixes. One determination was done per asphalt type. For the four AC-30 asphalts, the average of four Rice tests was used as the maximum specific gravity. For the three 85-100 asphalts, the average of three Rice tests was taken, and for the two AC-20 asphalts, the average of two tests was taken. For the Esso Nolen 25-35 pen asphalt, the result specific to this hard asphalt was taken, in view of

Table 4.1 Source of Materials and Job Mix Formula for Asphalt Concrete Mix

Material Number	Material Type	Producer	Pit No.
1	#67 Stone	Florida Rock Industries	34-106
2	#89 Stone	Florida Rock Industries	34-106
3	#140 Screenings	Florida Rock Industries	34-106
4	Local Sand	Whitehurst Construction Co.	Alachua, Fl

Percentage by Weight of Total Aggregate Passing Sieves
(Dry Sieve)

Blend	25.5%	24.5%	25%	25%	Job Mix	Specification
No.	1	2	3	4	Formula	Range for S-1 Mix
3/4	100	100	100	100	100	100
1/2	73.70	100	100	100	92.79	88-100
3/8	36.50	99.43	100	100	83.67	75-93
#4	2.30	45.50	94.64	99.50	60.28	47-75
#10	1.37	10.82	63.37	99.10	43.56	31-53
#40	1.31	4.75	25.44	77.50	27.23	19-35
#80	1.23	4.03	10.18	15.00	7.60	7-21
#200	1.05	3.41	4.93	1.97	2.83	2-7
SpGr	2.42	2.40	2.54	2.57	2.483	

Table 4.2 Washed Sieve Analysis of Aggregate Blend

Seive Size	Percent Passing 1	2	3	4	5	6	7	8	9	Job Mix Formula
3/4	100	100	100	100	100	100	100	100	100	100
1/2	87.72	93.01	95.15	92.55	95.34	90.84	92.80	92.66	96.52	92.79
3/8	79.32	81.13	84.38	83.69	85.99	79.83	83.83	82.90	87.04	83.67
#4	58.90	61.29	62.46	57.15	63.05	56.54	57.02	62.92	59.51	60.28
#10	43.95	44.98	44.73	41.56	45.36	40.81	42.03	47.00	44.34	43.58
#40	27.94	28.76	29.08	26.37	27.82	25.04	26.42	30.60	29.17	27.23
#80	8.07	9.47	9.12	7.85	8.03	7.56	8.08	10.21	10.59	7.60
#200	3.09	3.6	3.80	3.52	3.08	2.81	3.15	4.92	5.68	2.83

its uniqueness. Table 4.3 summarizes the maximum Specific Gravities determined and those adopted.

Mixtures were prepared using the aggregate gradation above with an asphalt content of 6.5 percent and compacted by the 50-blow Marshall compaction method. Table 4.4 gives average values and standard deviations of unit weight and air void content for the different mixtures. Table A-1 in the Appendix presents the test values for all specimens.

4.2 Laboratory Procedures

4.2.1 Laboratory Aging Conditions

The compacted asphalt mix specimens were subjected to the following aging conditions:

1. Aging in normal oven at 140° F for duration of 1, 7, 28 and 90 days.

2. Aging in forced-draft oven at 140° F for durations of 1, 7, 28 and 90 days (except for Chevron AC-20 and Chevron Modified).

3. Aging in ultraviolet chamber at 140° F for durations of 1, 7, 28 and 90 days.

4. Aging in natural weather conditions on the roof for durations of 6 months, 1 year, 2 years and 3 years (except for Chevron AC-20 and Chevron Modified).

Three replicate specimens were made for each condition thus accounting for the 540 specimens fabricated.

4.2.2 Randomization in Assignment of Treatments

The assignment of specimens to different groups (to be used for different exposure conditions) was done in such a way that the average

Table 4.3 Maximum Specific Gravities of Mixtures

Mixture	Maximum Specific Gravity
Amoco AC-30	2.294
Chevron AC-30	2.336
Belcher AC-30	2.320
Mariani AC-30	2.284
Average	2.309
Texaco 85-100 pen	2.324
Texaco Airblown 85-100 pen	2.313
Boscan 85-100 pen	2.307
Average	2.315
Esso 25-35 pen	2.322
Chevron AC-20	2.298
Chevron AC-20 Modified	2.281
Average	2.289

Table 4.4 Unit Weights and Air Void Contents of Marshall Specimens

Asphalt Type	Average Unit Wt. (pcf)	Standard Deviation (pcf)	Average Air Voids (%)	Standard Deviation (%)
Mariani AC-30	136.71	0.79	5.09	0.55
Amoco AC-30	136.84	0.44	5.00	0.30
Belcher AC-30	136.55	0.55	5.21	0.38
Chevron AC-30	136.52	0.53	5.23	0.37
Texaco 85-100 pen	137.21	0.60	5.26	0.36
Texaco Airblown 85-100 pen	137.30	0.60	4.94	0.41
Boscan 95-100 pen	136.54	0.49	5.47	0.34
Esso 25-35 pen	136.50	0.45	5.79	0.31
Chevron AC-20	137.21	0.60	3.94	0.42
Chevron AC-20 Mod	137.53	0.65	3.71	0.46

density of the specimens for the same asphalt type was approximately the same. This was done so that the effects of different aging environments would not be obliterated by the effects of different air voids. The assignment of groups and subgroups to respective conditions and durations of exposure was done in a completely random manner. Table A-2 in the Appendix presents the assignment of specimens along with the average values of unit weight for every triplicate set assigned.

4.2.3 Tests on Marshall Specimens

Tests were run on the aged Marshall specimens to determine their resilient moduli and fracture energy. These tests were restricted to four asphalts, i.e., Amoco AC-30, Mariani AC-30, Chevron AC-20 and Chevron AC-20 Modified. Specimens corresponding to the Amoco and Mariani asphalts were aged for 0, 7, 28 and 90 days. Specimens corresponding to Chevron and Chevron Modified were aged for 0, 28 and 90 days, aging conditions being normal oven and ultraviolet chamber only. This abridgement of scope was necessary considering the available resources.

Indirect tensile tests were run on all the aged Marshall specimens.

4.2.4 Tests on Asphalt Residues

The asphalt residues were recovered from the aged samples and the following tests conducted on them

1. Absolute Viscosity at 140° F (60° C)
2. Penetration at 77° F (25° C)
3. Infrared spectral analysis
4. Schweyer Rheometer at 59° F (15° C) and 77° F (25° C).

4.2.5 Resilient Modulus Test

4.2.5.1 General. A linear elastic layered model requires two material properties as input parameters which are the elastic modulus E and Poisson's ratio ν. The most common "idealized" E value used in this model is the resilient modulus M_R. The resilient modulus is defined as the ratio of the applied stress to the recoverable strain when a repeated dynamic load is applied. It can be expressed as

$$M_R = \sigma/\epsilon_r \tag{4.1}$$

where σ = Applied stress

ϵ_r = Recoverable strain

Basically, the test method involves application of pulse loads of relatively short duration of time and recording the instantaneous deformation using strain gages or linear variable differential transformers (LVDTs). The resilient moduli are then calculated from the stresses induced and resultant strains. In essence, the resilient modulus is the instantaneous elastic modulus of a viscoelastic material.

A simple diametral compression test procedure to determine the resilient modulus of asphaltic concrete was developed by Schmidt [34]. In this method, standard Marshall specimens were used and a pulsating load of 0.1 second duration was applied every 3 seconds, and the corresponding horizontal deformation measured. Derivation of an expression for calculating M_R from the applied load and the induced deformation is based on the analytical work of Timoshenko and Goodier [35] on an elastic thin disk. By assuming the specimen to be linearly elastic and in a plane stress condition, Schmidt [34] derived the following relationship between M_R of the specimen and the induced horizontal deformation d_h.

$$M_R = P(\nu + \frac{4}{\pi} - 1)/t\ d_h \tag{4.2}$$

where P = Applied load

μ = Poisson's ratio

t = Thickness of specimen

The procedure has been standardized in ASTM D4123-82 and recommends the application of compressive loads with a haversine or suitable wave form. The load is applied vertically in the vertical diametral plane of a cylidrical specimen through a loading strip of 1/2 inch width. The resulting horizontal deformation of the specimen is measured and, with an assumed Poisson's ratio, is used to calculate a resilient modulus.

Interpretation of the deformation data has resulted in two resilient modulus values being used. The instantaneous resilient modulus is calculated using the recoverable deformation that occurs instantaneously during the unloading portion of one cycle. The total resilient modulus is calculated using the total recoverable deformation which includes both the instantaneous and recoverable and the time-dependent continuing recoverable deformation during the unloading and rest-period portion of one cycle.

The resilient moduli can be calculated by the expressions

$$M_{RI} = P\ (\mu_{RI} + 0.27)/td_{RI} \qquad (4.3)$$

$$M_{RT} = P(\mu_{RT} + 0.27)/td_{RT} \qquad (4.4)$$

where

M_{RI} = instantaneous resilient modulus of elasticity, psi (or MPa),

M_{RT} = total resilient modulus of elasticity, psi (or MPa,

μ_{RI} = instantaneous resilient Poisson's ratio,

μ_{RT} = total resilient Poisson's ratio,

P = repeated load, lbf (or N),

t = thickness of specimen, in (or mm),

d_{RI} = instantaneous recoverable horizontal deformation, in (or mm),

d_{RT} = total recoverable horizontal deformation, in (or mm)

A value of 0.35 for Poisson's ratio has been found to be reasonable for asphalt mixtures at 77° F (25° C) [34]. This is also stated in ASTM D4123-82.

The diametral resilient modulus test used in this study was essentially the one proposed by Schmidt [34] and later standardized in ASTM D4123-82, the horizontal deformation being used to calculate the resilient modulus of the test specimen. Tia [36] presents a comprehensive study of the theoretical background for this test.

4.2.5.1 Theoretical Background. In the diametral resilient modulus test, dynamic pulse loads are applied diametrally to the Marshall size specimens, and the induced vertical and horizontal deformations are recorded and used to calculate the resilient moduli. The test is based on the assumption that the specimen behaves as a linear elastic material under dynamic loads. Timoshenko and Goodier [35] and Frocht [37] had analyzed the stresses in an elastic circular disk subjected to a diametral loading condition. Based on their works, Schmidt [34] derived the relationship between the resilient modulus and the induced horizontal deformation of the specimen.

Hondros [36] analyzed the stresses in a circular disk loaded through a short strip. The stress components and notations are illustrated in Figure 4.1. His equation for the stresses along the horizontal diameter is

$$\sigma_{\theta x} = -\frac{2p}{\pi}\left[\frac{(1 - r^2/R^2)\sin 2\alpha}{(1 + 2r^2/R^2 \cos 2\alpha + r^4/R^4)} + \tan^{-1}\left(\frac{(1 - r^2/R^2)}{(1 + r^2/R^2)}\tan\alpha\right)\right] \tag{4.5}$$

$$\sigma_{rx} = +\frac{2p}{\pi}\left[\frac{(1 - r^2/R^2)\sin 2\alpha}{(1 + 2r^2/R^2 \cos 2\alpha + r^4/R^4)} - \tan^{-1}\left(\frac{(1 - r^2/R^2)}{(1 + r^2/R^2)}\tan\alpha\right)\right] \tag{4.6}$$

$$\tau_{r\theta} = 0 \tag{4.7}$$

According to the elastic stress-strain relationship, the strains along the horizontal diameter can be expressed as

$$\varepsilon_{\theta x} = \frac{1}{E}(\sigma_{\theta x} - \mu\sigma_{rx}) \tag{4.8}$$

$$\varepsilon_{rx} = \frac{1}{E}(\sigma_{rx} - \mu\sigma_{\theta x}) \tag{4.9}$$

The total horizontal displacement d_h is the integration of the horizontal strains along the horizontal diameter and can be expressed as

$$d_h = 2\int_0^R \varepsilon_{rx}\, dr \tag{4.10}$$

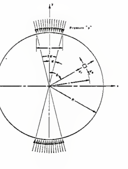

Figure 4.1 Stress Components in a Circular Disk

A complete expression for d_h can be obtained by substituting Equation 4.5 and 4.6 into 4.9, which is then substituted into Equation 4.10.

For a specimen diameter of 4 inches and width of loading strip of 1/2 inch, the following relationships can be established

$$\alpha = .124 \text{ radian } (7.125 \text{ degrees}) \qquad (4.11)$$

$$p = \frac{2P}{(1 \text{ inch})\, t} \qquad (4.12)$$

The expression in integral form for d_h, using these values for α and p, can be solved by the method of incremental summations, yielding

$$d_h = \frac{p}{\pi t E} (.941 + 3.141\, \nu) \qquad (4.13)$$

The elastic modulus can then be expressed as

$$E = \frac{P\,(0.27 + \nu)}{t\, d_h} \qquad (4.14)$$

which is the same as the expression used by Schmidt [34].

4.2.5.2 Experimental Procedure. The procedure for the resilient modulus test consisted of the following steps:

1. The height of the specimen was measured and then the specimen was left in a temperature controlled room for at least 12 hours so as to stabilize at 77° F (25° C). A dummy specimen with a thermister inserted inside was placed in the same condition as that of the test specimens and used to measure the test temperature of the test specimens just before the test. The test temperature in this case was 77° F (25° C).

2. The specimen was placed in the resilient modulus test equipment, care being taken to ensure that the specimen was well centered in the testing apparatus and the two LDVTs on either side bore firmly on the sides of the specimen. The top loading strip was brought down carefully and adjusted in position such that it no more than just touched the specimen.

3. A pulsating haversine load of 100 lbs was then applied every one second i.e., at a loading frequency of 1.0 Hz, with a duration of 0.1 second. This was done 10 times to precondition the specimen. The level of load and number of repetitions were decided upon after preliminary trial runs, checking to see that the resilient deformations were stable. Thereafter, 10 haversine pulse loads of 200 lbs. were applied at a loading frequency of 1.0 Hz with a duration of 0.1 second. The level of load was decided so as to induce approximately 10 to 15 percent of the tensile strength as determined from a destructive test.

4. Loads were measured with an electronic load cell and the horizontal deformations measured by the two LVDTs. Both load and deformation were plotted on the chart recorder. A typical load-pulse deformation trace is shown in Figure 4.2 along with notations indicating load-time terminology.

5. During the load application, the changes in the output voltages of the LVDTs were converted to movements of the recording pens. The sensitivities of the recorder channels and the positions of the pens were adjusted to obtain recordings within the chart. The speed of chart movement was set at 0.8 in/sec (2cm/sec).

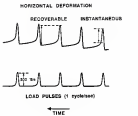

Figure 4.2 Typical Load-Pulse Deformation Trace

6. After the deformations for the 10 pulse loads were taken, the loading cycle was stopped. The specimen was rotated by 90 degrees and tested again as per the same procedure above. If large differences were found between deformation values for the two positions, the specimen was tested at a third position and the unreasonable results were discarded.

7. The recoverable horizontal deformations were measured over at least three loading cycles after the repeated resilient deformation became stable. The average values were used for the calculation of the resilient moduli.

4.2.6 Indirect Tensile Test

4.2.6.1 General. The indirect tensile test was developed in Brazil [39] and independently in Japan [40]. In this test, cylindrical specimens are failed by applying compressive loads along a diametral plane through two opposite loading heads. This type of loading produces a relatively uniform tensile stress acting perpendicular to the applied load plane. Using photoelastic analyses of plastic disks, a simplified mathematical treatment was given by Frocht [37].

The advantages of this test are [41]

1. It is simple.
2. Marshall specimen may be used.
3. Surface irregularities do not seriously effect the results.
4. The coefficient of variation of the test results is low.

4.2.6.2 Theoretical Background. The test assumes an isotropic and homogenous material with a linear elastic behavior. Although an asphalt mixture is not ideally so, it is thought that the random distribution of aggregate particles in an asphalt mixture tends to minimize the effect of heterogeneity [42]. Further, at a fast rate of loading, an asphalt mixture would, most likely, exhibit reasonable elastic properties.

The test also assumes plane stresses in the specimen, which while not being totally valid, yields approximations which are close. Notwithstanding these discrepancies between theory and application, the advantages of the test outweigh the limitations.

The stress distribution using loading strips of width less than 0.1 times the specimen diameter results in a compressive stress along the vertical diameter, three times that of the tensile stress. The test is thus applicable to materials like asphaltic mixtures which are at least three times stronger in compression than in tension.

On the basis of the maximum load at failure P, applied through a loading strip of width 1/2 in., the tensile strength at failure S_t, can be calculated by the expression

$$S_t = 1.96P / \pi td \qquad (4.15)$$

where t = Specimen thickness

d = Specimen diameter

For a constant diameter of specimen of 4 in. the expression reduces to

$$S_t = 0.156P/t \qquad (4.16)$$

which has been used in all the calculations.

4.2.6.3 Experimental Procedure. The procedure for the indirect tensile test, in brief, consisted of the following steps:

1. The height of the test specimen was measured and then the specimen was left in a temperature controlled room for at least 12 hours so as to stabilize at 77° F (25° C). A dummy specimen with a thermister inserted inside was placed in the same condition as that of the test specimen and used to measure the test temperature of the test specimens just before the test. The test temperature in this case was 77° F (25° C).

2. The specimen was placed in the indirect tensile test equipment, care being taken to ensure that the specimen was well centered in the testing apparatus and the two LVDTs on either side bore firmly on the sides of the specimen. The top loading strip was brought down carefully and adjusted in position such that it no more than just touched the specimen.

3. Load was then applied at a rate of 2 inches per minute until failure and measured with an electronic load cell. Horizontal deformations were measured by the two LVDTs. Both load and deformation were plotted on the chart recorder.

4. During the load application, changes in the output voltages of the LVDTs were converted to movements of the recording pens. The sensitivities of the recorder channels and the positions of the pens were so adjusted to obtain recordings within the chart.

5. The load at failure was used to calculate the indirect tensile strength.

4.2.7 Fracture Energy

The induced horizontal strain and applied vertical stress were used to establish fracture energy (F_E) values using the relation

$$F_E = \sigma \varepsilon \qquad (4.17)$$

where σ = applied vertical tensile stress, Pa

ε = induced horizontal strain

On the load and horizontal deformation plots recorded for the indirect tensile test, ten ordinates were chosen on the load curve and values of load measured. The first measurement was zero load and the tenth measurement was the failure load. Corresponding values of horizontal deformation were also measured.

Applied stress was calculated for each value of the load using Equation 4.16. Using the corresponding value of horizontal deformation, the elastic modulus was calculated using Equation 4.14. Poisson's ratio was taken as 0.35.

Using the calculated values of applied stress and elastic modulus, the induced strain was obtained by the relation

$$\varepsilon = \frac{E}{\sigma} \qquad (4.18)$$

Thus, for each specimen tested, ten data points became available, defining the relationship between applied vertical stress and induced horizontal strain. The area under this curvilinear relationship was calculated using the trapezoidal rule, which yielded the value of fracture energy.

4.2.8 Schweyer Rheometer Test

4.2.8.1 General. Rheology involves the study and evaluation of the time-temperature dependent response of materials which are stressed or subjected to an applied force. Low temperature (25° C or less) rheological properties of bitumens have been evaluated in various research investigations using testing equipment such as the sliding plate microviscometer, co-axial viscometer, mechanical spectrometer, Schweyer constant stress rheometer etc. In this study, the Schweyer constant stress rheometer was used to define the low temperature rheological properties of asphalts recovered from laboratory compacted mixtures and field cores.

4.2.8.2 Theoretical Background. Tia and Ruth [43] have presented a comprehensive study on the theoretical background for the Schweyer constant stress rheometer and application of rheological concepts proposed by H. E. Schweyer, a pioneer in this field. Major points from this milestone paper are summarized as follows:

1. Experimental data have shown that shear stress (τ) and shear rate ($\dot{\gamma}$) of asphalts can generally be related by the power law function, $\tau = \eta_1 \dot{\gamma}^C$.
2. Asphalts often exhibit Newtonian-like (Shear Susceptibility, C = 1.0) flow behavior, at or near conventional mix temperatures.
3. Asphalts tested at low temperatures and low shear stresses generally exhibit pseudoplastic ($C < 1.0$) flow behavior.
4. When tested at high temperatures and high stress levels, asphalts may exhibit dilatant ($C > 1$) flow behavior.

5. The Schweyer constant stress rheometer offers a correct and efficient method for measuring the properties of asphalt over a wide range of temperature and stress levels.
6. When a viscosity is computed at a shear rate considerably different from that of the test value, a substantial error may be induced. The use of a constant power viscosity eliminates the need for extrapolation of viscosity from one shear rate to another, since the viscosity can be computed at the test condition. A constant power input of 100 w/m^3 is usually used and found to give reliable results.

4.2.8.3 Experimental Procedure. The procedure for Schweyer constant stress rheometer test, in brief, consisted of the following steps:

1. A sample tube was filled right to the top.
2. The plunger was seated and forced into the sample tube for about 5 mm.
3. The entire assembly was placed into the metal block which was then cooled to either 77° F (25° C) or 59° F (15° C), the two test temperatures used in this study.
4. Once the temperature stabilized, the gas pressure was preset and the gas cylinder activated to apply force to the plunger and asphalt sample.
5. Through the data acquisition system, the creep curve was recorded for each stress level until the response became linear.
6. Tests were conducted at a minimum of five stress levels, usually between 100 psi and 20 psi.

7. Using the system software developed by Tia and Ruth (unpublished), the shear stress versus shear rate relationship was obtained. It was seen that log shear stress versus log shear rate plot, within experimental error, is a straight line (conforming to the power law).
8. The system software also computed the shear susceptibility (C) which is the slope of the regressed line relating log shear stress to log shear rate. The corresponding R^2 value was also indicated. In addition, the system software computed viscosity at shear rate = 1.0 sec^{-1} ($\eta_{1.0}$) and constant power viscosity (η_J) .

4.2.9 Infrared Absorption Spectral Test

Considering the relative novelty of infrared techniques in the characterization of asphalts, a comprehensive background study on the subjects has been presented earlier in Chapters 2 and 3. However, before dealing with the experimental procedure, two aspects merit discussion. They are quantitative and qualitative analyses, which are briefly discussed in subsequent paragraphs.

4.2.9.1 Infrared Quantitative Analysis. Quantitative analysis in the infrared region is based on the relationship between concentration of the compound (or the functional group) and the radiation absorbed. However, there are certain problems in infrared quantitative analysis that are worthy of mention [44].

First, it is quite common to encounter situations in which there are overlapping absorption bands. Secondly, even the determination of a value for absorbance can pose some difficulty. Using known techniques and exercising due care, one can perform quantitative analyses at precision levels between 1 and 5 percent [44]. However, it has to be emphasized that quantitative methods in determining the structure of chemical compounds are largely empirical, the certainty with which predictions of structure can be made depends greatly on the information and experience of the investigator.

4.2.9.2 Infrared Qualitative Analysis. The aim of qualitative analysis is to determine the presence of individual components. Even qualitative identification of the components of a system may be of interest and importance, and for this purpose the methods of infrared analysis are often useful. As stated earlier, if a large enough library of spectra is available, it is possible to identify compounds, and in favorable instances, even mixtures of compounds, by comparison with such reference spectra [45]. For this purpose, modern computer storage and retrieval facilities are used to great advantage.

4.2.9.3 Experimental Procedure. The following is a brief description of the testing procedure which was adopted for the infrared spectral test.

1. The asphalt specimen was weighed out in a 3 dram glass vial, the weight of asphalt being approximately 0.20 gms. Figure 3.16 illustrates the type of vial used. The weight was accurately measured to a thousandth of a gram.
2. HPLC grade Tetrahydrofuran (THF) was used to make a 5 percent (W/V) solution. Petersen [20] reports that the use of THF eliminates the interference from hydrogen bonding on the carbonyl absorption region which helps in the determination of ketones, carboxylic acids, anhydrides and 2-quinolone types.

This was confirmed by preliminary runs on specimens made with THF at a concentration of 5% (W/V), a level which gave satisfactory spectra with minimal amount of noise interference. Due to the difficulty in dissolving a large concentration of asphalt in the solvents, the minimun concentration level of 5% was selected. The solution in the vial was tightly stoppered and left for ten minutes. During this period, the vial was occasionally shaken up to accelerate the dissolving of the aphalt sample.

3. The two Teflon stoppers were removed from the sealed cell. Approximately 2 ml of THF was drawn into a 3 cc Luer Lock syringe. Figure 3.16 illustrates the type of syringe used. (WARNING: THF is toxic, read Product Data and Safety Sheets.) The syringe was inserted into the lower fitting of the cell. The cell was flushed out twice, gently depressing the plunger of the syringe when injecting the solvent in. Then the cell was filled with THF making sure that no air bubbles are entrapped. The syringe was removed and the Teflon plugs inserted with a twisting motion. If the liquid filled the top part, it was sponged off with a piece of clean tissue. If the part is left full when the second plug is inserted, excessive pressure may distort or rupture the cell.
4. The cell was then inserted into the cell holder which is positioned within the chamber on the optical bench. The chamber was closed.
5. The system software was operated to scan the solvent, generating the background spectum for THF. It is essential to gene-

rate the background spectrum on every occasion that the test is run.

6. The background spectrum was stored on the disk facilities.
7. The sealed cell was removed from the chamber. The Teflon plugs were removed and using the Luer syringe, the solvent was emptied and blown dry with a draft of Nitrogen. To avoid serious damage to the cell windows, it should be scrupulously ensured that not even a trace of moisture gets into the sealed cell. The syringe was also shaken and blown dry.
8. Steps at Serials 3 and 4 were gone through again, with the difference that instead of the solvent, the 5 percent (W/V) solution of asphalt was inserted into the sealed cell.
9. The system software was operated to scan the solution, generating the spectrum for the solution. Using software commands, the background spectrum was ratioed out, yielding the spectrum of the asphalt sample, which was stored on the disk facilities.
10. Using various software commands, the analysis of the spectrum of the asphalt was done, so as to obtain the values of absorbance at different wavenumbers.
11. These figures were utilized in the computation of Carbonyl Ratios and Ketone Factors.
12. A hardcopy of the spectrum was also obtained on a connected plotter.
13. The sealed cell and syringe were rinsed out with THF until thoroughly clean and put away when done for the day. The cell should be stored in a dry dessicated chamber.

CHAPTER 5
THIN FILM AND ROLLING THIN FILM OVEN TESTS

5.1 Introduction

With the general aim of assessing the extent of hardening of the selected asphalts when subjected to exposure in the Thin Film and Rolling Thin Film Ovens, an experimental program was devised and run. For each of the asphalts, TFOT (ASTMD1754-78) and RTFOT (ASTMD2872-80) were performed at 285° F, 325° F and 365° F. Parameters measured before and after the tests were as follows:

1. Penetration at 77° F.
2. Absolute Viscosity at 140° F.
3. Kinematic Viscosity at 275° F.

The specific objectives of the experiment were as follows:

1. To carry out statistical analyses of the results obtained and determine
   - (a) differences between asphalts
   - (b) differences between the effects of the three levels of temperature
   - (c) difference between the effects of TFOT and RTFOT on the various parameters
2. To carry out regression analyses and establish relationships between the effects of TFOT and RTFOT.
3. To establish patterns of change for the response parameters over increasing temperature levels, for each asphalt.

The TFOT and RTFOT procedures and the physical tests on the asphalt residues before and after the tests were performed by the personnel of the Bureau of Materials and Research, Florida Department of Transportation, under the supervision of Messrs. Ken Murphy and Phil Eunice.

5.2 Results

Results obtained have been tabulated in Tables 5.1 through 5.3. Percentages Penetration Retained and Viscosity Ratios of 140° F have been calculated and presented in Tables 5.4 and 5.5, respectively.

5.3 Analysis of Results

5.3.1 Statistical Model

The test results as listed in Tables 5.1 to 5.5 were analyzed as results of a factorial experiment comprising of eleven types of asphalts (ASPHALT), three levels of temperature (TEMP) and two types of test (OVEN). In the study, the concern is only in these eleven asphalts, three temperatures and two tests. Thus ASPHALT, TEMP and OVEN are regarded as fixed effects. The experiment has 66 treatment combinations.

The following linear model is assumed for any single measurement in the experiment:

$$Y_{ijk} = m + A_i + T_j + O_k + AT_{ij} + AO_{ik} + TO_{jk} + \varepsilon_{ijk} \qquad (5.1)$$

where

Y_{ijk} = the response of the ith ASPHALT,
jth TEMP and kth OVEN.
m = the grand mean.
A_i = the main effect of ASPHALT i.

Table 5.1 TFOT and RTFOT Effects on Penetration

Asphalt	Test	Original	Penetration at 77° F		
			Oven Temperature (° F)		
			285	325	365
Chevron AC-30	TFOT	68	52	45	35
	RTFOT		47	41	33
Belcher AC-30	TFOT	87	53	43	34
	RTFOT		48	38	34
Amoco AC-30	TFOT	73	55	45	34
	RTFOT		50	41	34
Mariani AC-30	TFOT	62	47	41	35
	RTFOT		46	38	35
Marathon AC-30	TFOT	65	48	40	32
	RTFOT		43	37	31
Chevron AC-20	TFOT	75	56	47	44
	RTFOT		53	43	39
Chevron AC-20 Modified	TFOT	102	84	73	58
	RTFOT		76	60	57
Texaco 85-100	TFOT	88	65	51	39
	RTFOT		60	48	43
Texaco Airblown 85-100	TFOT	82	70	63	52
	RTFOT		69	64	57
Esso 25-35	TFOT	27	24	22	20
	RTFOT		24	21	18
Boscan 85-100	TFOT	76	54	44	31
	RTFOT		54	42	32

Table 5.2 TFOT and RTFOT Effects on Absolute Viscosity

Asphalt	Test	Original	Absolute Viscosity at 140° F		
			Oven Temperature (° F)		
			285	325	365
Chevron AC-30	TFOT	3100	6145	9748	22710
	RTFOT		7711	14389	32855
Belcher AC-30	TFOT	2753	5597	8854	23176
	RTFOT		6628	11321	21644
Amoco AC-30	TFOT	3301	5847	9760	23586
	RTFOT		6958	10451	18045
Mariani AC-30	TFOT	2967	5101	7513	13550
	RTFOT		5802	8489	14122
Marathon AC-30	TFOT	2981	5661	9504	23803
	RTFOT		7570	11743	26027
Chevron AC-20	TFOT	2135	3944	6246	12855
	RTFOT		4414	8399	10201
Chevron AC-20 Modified	TFOT	2576	3802	4930	10138
	RTFOT		5078	9101	12199
Texaco 85-100	TFOT	1064	1611	2327	4048
	RTFOT		1889	2499	3256
Texaco Airblown 85-100	TFOT	1931	2648	3588	5935
	RTFOT		2866	3426	4761
Esso 25-36	TFOT	17885	26258	38309	70260
	RTFOT		28639	48601	116060
Boscan 85-100	TFOT	3810	8579	17910	81525
	RTFOT		9082	19090	53140

Table 5.3 TFOT and RTFOT Effects on Kinematic Viscosity

Asphalt	Test	Original	Kinematic Viscosity at 275° F		
			Oven Temperature (° F)		
			285	325	365
Chevron AC-30	TFOT	506	653	851	1187
	RTFOT		734	993	1321
Belcher AC-30	TFOT	489	637	786	1196
	RTFOT		704	848	1073
Amoco AC-30	TFOT	593	783	947	1531
	RTFOT		847	1018	1332
Mariani AC-30	TFOT	542	666	802	1038
	RTFOT		720	839	1000
Marathon AC-30	TFOT	550	667	792	1183
	RTFOT		731	873	1195
Chevron AC-20	TFOT	412	541	655	885
	RTFOT		565	747	778
Chevron AC-20 Modified	TFOT	539	671	742	1017
	RTFOT		716	926	1030
Texaco 85-100	TFOT	268	309	358	433
	RTFOT		315	370	418
Texaco Airblown 85-100	TFOT	365	413	456	524
	RTFOT		403	433	480
Esso 25-35	TFOT	937	1180	1380	1866
	RTFOT		1156	1437	2172
Boscan 85-100	TFOT	649	1006	1333	2751
	RTFOT		943	1360	2190

Table 5.4 TFOT and RTFOT Effects on Penetration Retained

Asphalt	Test	% Penetration Retained		
		Oven Temperature (° F)		
		285	325	365
Chevron AC-30	TFOT	76.5	66.2	51.5
	RTFOT	69.1	60.3	48.5
Belcher AC-30	TFOT	79.1	64.2	50.7
	RTFOT	68.7	56.7	50.7
Amoco AC-30	TFOT	75.3	61.6	46.6
	RTFOT	68.5	56.2	46.8
Mariani AC-30	TFOT	75.8	66.1	56.5
	RTFOT	74.2	61.3	56.6
Marathon AC-30	TFOT	73.8	61.5	49.2
	RTFOT	66.2	56.9	47.7
Chevron AC-20	TFOT	74.7	62.7	58.7
	RTFOT	70.7	57.3	52.0
Chevron AC-20 Modified	TFOT	82.4	71.6	56.9
	RTFOT	74.5	58.8	55.9
Texaco 85-100	TFOT	73.9	58.0	44.3
	RTFOT	68.2	54.5	48.9
Texaco Airblown 85-100	TFOT	85.4	76.8	63.4
	RTFOT	84.1	78.0	89.5
Esso 25-35	TFOT	86.9	81.5	74.1
	RTFOT	66.9	77.8	66.7
Boscan 85-100	TFOT	71.1	57.9	40.8
	RTFOT	71.1	55.3	42.1

Table 5.5 TFOT and RTFOT Effects on Absolute Viscosity Ratio

Asphalt	Test	Absolute Viscosity Ratio		
		Oven Temperature (° F)		
		285	325	365
Chevron AC-30	TFOT	1.98	3.14	7.33
	RTFOT	2.49	4.64	10.60
Belcher AC-30	TFOT	2.03	3.23	8.42
	RTFOT	2.41	4.11	7.86
Amoco AC-30	TFOT	1.77	2.96	7.15
	RTFOT	2.11	3.17	5.47
Mariani AC-30	TFOT	1.72	2.57	4.57
	RTFOT	1.96	2.86	4.76
Marathon AC-30	TFOT	1.90	3.19	7.98
	RTFOT	2.54	3.94	8.73
Chevron AC-20	TFOT	1.85	2.93	6.02
	RTFOT	2.07	3.93	4.78
Chevron AC-20 Modified	TFOT	1.48	1.91	3.54
	RTFOT	1.97	3.53	4.74
Texaco 85-100	TFOT	1.51	2.19	3.80
	RTFOT	1.78	2.35	3.06
Texaco Airblown 85-100	TFOT	1.37	1.86	3.07
	RTFOT	1.48	1.77	2.47
Esso 25-35	TFOT	1.47	2.14	3.93
	RTFOT	1.60	2.72	6.49
Boscan 85-100	TFOT	2.36	4.70	21.40
	RTFOT	2.38	5.01	13.95

β_j = the main effect of TEMP j.

O_k = the main effect of OVEN k.

AT_{ij} = the interaction of $ASPHALT_i$ x $TEMP_j$.

AO_{ik} = the interaction of $ASPHALT_i$ x $OVEN_k$.

TO_{jk} = the interaction of $TEMP_j$ x $OVEN_k$.

ε_{ijk} = the experimental error.

Analysis of variance (ANOVA) was performed on the test results using the linear model above. The SAS/STAT computer software was used to perform these analyses.

5.3.2 Penetration

The most important results of an ANOVA are the p-values for the factors considered. Basically, the P value for a factor indicates the probability of error of the statement that the factor has a significant effect on the measured parameter. For example, if a factor A has a P value of 0.05, the statement that factor A is significant will have a probability of error of 0.05. A lower P value indicates a higher level of significance. In this study, a probability of error (α level) of 0.05 was used. If the P value of a factor is equal or less than 0.05, the factor is considered to be significant.

Results of ANOVA on the penetration data are summarized in Table 5.6. From Table 5.6 it is seen that all main effects and interaction effects are significant. It follows that

1. Comparison of ASPHALT must be made at each level of TEMP, for each OVEN type separately.
2. Comparison of TEMP must be made by ASPHALT, for each OVEN type separately, and

Table 5.6 Result of ANOVA on Penetration Data

Source	df	MS	F-Value	P
ASPHALT	10	912.03	339.69	0.0001
TEMP	2	1387.29	516.71	0.0001
OVEN	1	101.88	37.95	0.0001
ASPHALT * TEMP	20	15.25	5.68	0.0001
ASPHALT * OVEN	10	8.51	3.17	0.0135
TEMP * OVEN	2	23.65	8.81	0.0018
ERROR	20	2.68		

R-SQUARE 0.996

3. Comparison of OVEN type must be made at each level of TEMP, for each ASPHALT separately.

Since it is known that the asphalts have a variety of Penetration values in the original state, comparison of asphalts by Penetration values after TFOT and RTFOT would be better done if the percent penetration retained is considered.

5.3.3 Percent Penetration Retained

Results of ANOVA on the percent Penetration Retained (the data in Table 5.4) are summarized in Table 5.7. From Table 5.7 it is seen that all three main effects and the TEMP * OVEN interaction effect are significant.

Since ASPHALT does not interact with the other two factors, the asphalts can be evaluated by comparing the mean responses for the eleven asphalts, averaged over the other two factors. This was done by Duncan's multiple-range test at a level of significance of 0.05. The results are summarized in Table 5.9. It can be seen from Table 5.8 that the following asphalts are significantly better on the basis of percent Penetration Retained:

1. Esso 25-35
2. Texaco Airblown 95-100
3. Chevron AC-20 Modified
4. Mariani AC-30

It should be noted that Esso 25-35 is a roofing asphalt. Among the paving asphalts, Serials 2, 3 and 4 indicated better percent Penetration Retained. Serials 3 and 4 are not different from each other.

Since the factor TEMP interacts with the factor OVEN, it is appropriate to compare the TEMP means separately for each OVEN type averaged

Table 5.7 Result of ANOVA on Percent Penetration Retained

Source	df	MS	F-Value	P
ASPHALT	10	332.08	69.74	0.0001
TEMP	2	2659.35	558.51	0.0001
OVEN	1	201.43	42.30	0.0001
ASPHALT * TEMP	20	9.19	1.93	0.0750
ASPHALT * OVEN	10	11.12	2.34	0.0510
TEMP * OVEN	2	32.47	6.82	0.0055
ERROR	20	95.23		

R-SQUARE 0.990

Table 5.8 Grouping of Asphalts on the Basis of Percent Penetration Retained from Duncan's Test

Asphalt	Mean	Duncan's Grouping
Esso 25-35	79.65	A
Texaco Airblown 85-100	76.20	B
Chevron AC-20 Mod	66.68	C
Mariani AC-30	65.07	C D
Chevron AC-20	62.68	D E
Chevron AC-30	62.02	E
Belcher AC-30	61.68	F E
Marathon AC-30	59.22	F G
Amoco AC-30	59.13	F G
Texaco 85-100	57.97	G
Boscan 85-100	56.38	G

NOTE: Means with the same letter are not significantly different (alpha = 0.05).

over the factor ASPHALT. This was done by Duncan's test at a level of significance of 0.05. The results are summarized in Table 5.9. From Table 5.9, it can be seen that for both the TFO and RTFO processes, different oven temperatures produced different effects on the asphalts on the basis of percent Penetration Retained.

Similarly, since the factor OVEN interacts with the factor TEMP, it is appropriate to compare the OVEN means separately for each TEMP with Duncan's test at a level of significance of 0.05. The results are summarized in Table 5.10. From Table 5.10, it can be seen that, for oven temperatures of 285 and 325° F, the RTFO process is more severe than the TFO process. However, for an oven temperature of 365° F, the two processes are not different from one another on the basis of percent Penetration Retained.

Plots of percent Penetration Retained after TFOT v.s. Oven Temperature for different asphalts are shown in Figure 5.1 and similar plots for RTFOT are shown in Figure 5.2. It can be seen clearly that the effects of oven temperature are significant.

5.3.4 Absolute Viscosity at 140° F

Results of ANOVA on the Absolute Viscosity at 140° F (the data in Table 5.2) are summarized in Table 5.11. From Table 5.11, it is seen that the main factors ASPHALT and TEMP and the interaction ASPHALT * TEMP are significant. OVEN type is not significant. Since it is known that the asphalts are quite different from each other in their viscosities, comparison of asphalts by viscosity values after TFOT and RTFOT would be better done if the Viscosity Ratios are considered.

Table 5.9 Grouping of Temperature by Oven Type on the Basis of Percent Penetration Retained from Duncan's Test

Oven Type	Temp (° F)	Mean	Duncan's Grouping
TF	285	77.90	A
TF	325	66.19	B
TF	365	53.88	C
RTF	285	73.11	A
RTF	325	61.19	B
RTF	365	53.19	C

NOTE: Means with the same letter are not significantly different (alpha = 0.05)

Table 5.10 Grouping of Oven Type by Temperature on the Basis of Percent Penetration Retained from Duncan's Test

Temp (° F)	Oven Type	Mean	Duncan's Grouping
285	TF	77.90	A
285	RTF	73.11	B
325	TF	66.19	A
325	RTF	61.19	B
365	TF	53.88	A
365	RTF	53.19	A

Note: Means with the same letter are not significantly different (alpha = 0.05)

Table 5.11 Results of ANOVA on Absolute Viscosity

Source	df	MS	F Value	P
ASPHALT	10	1368334926	32.02	0.0001
TEMP	2	2423126777	56.70	0.0001
OVEN	1	55363041	1.30	0.2685
ASPHALT * TEMP	20	265295059	6.21	0.0001
ASPHALT * OVEN	10	70157798	1.64	0.1657
TEMP * OVEN	2	3545673	0.08	0.9207
ERROR	20	42736422		

R-SQUARE 0.966

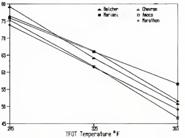

Figure 5.1 Relation Between Percent Penetration Retained and Oven Temperature for TFOT

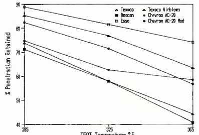

Figure 5.1--continued

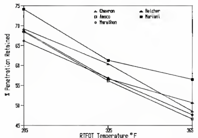

Figure 5.2 Relation Between Percent Penetration Retained and Oven Temperature for RTFOT

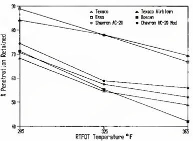

Figure 5.2--continued

5.3.5 Absolute Viscosity Ratio

Results of ANOVA on the Absolute Viscosity Ratio (the data in Table 5.5) are summarized in Table 5.12. From Table 5.12, it is seen that the main factors ASPHALT and TEMP and the interaction ASPHALT * TEMP are significant while the effect of oven type is not significant.

Since ASPHALT interacts with TEMP (and not OVEN), comparison of asphalts must be made at each level of temperature, averaged over the two types of OVEN. This was done by Duncan's test at a level of significance of 0.05. The results are summarized in Table 5.13. For convenience in presentation, asphalts have been coded as follows.

Boscan 85-100	BO
Chevron AC-30	CH
Belcher AC-30	BE
Marathon AC-30	MT
Chevron AC-20	OI
Amoco AC-30	AM
Mariani AC-30	MA
Chevron AC-20 (Mod)	DM
Texaco 85-100	TX
Esso 25-35	SO
Texaco Airblown 85-100	TA

From Table 5.13, it can be seen that the following paving asphalts had a better Absolute Viscosity Ratio

For Oven Temperature of 285° F

1. Texaco Airblown 85-100*
2. Texaco 85-100*
3. Chevron AC-20 Modified

Table 5.12 Results of ANOVA on Absolute Viscosity Ratio

Source	df	MS	F Value	P
ASPHALT	10	18.00	15.31	0.0001
TEMP	2	144.74	123.11	0.0001
OVEN	1	0.52	0.44	0.5135
ASPHALT * TEMP	20	8.85	7.53	0.0001
ASPHALT * OVEN	10	1.70	1.44	0.2317
TEMP * OVEN	2	1.69	1.43	0.2633
ERROR	20	1.18		

R-SQUARE 0.966

Table 5.13 Grouping of Asphalts by Temperature on the Basis of Absolute Viscosity Ratio from Duncan's Test

Temp 285° F

Asphalt	BO	CH	BE	MT	DI	AM	MA	DM	TX	SO	TA
Mean	2.37	2.24	2.22	2.22	1.96	1.94	1.84	1.73	1.65	1.54	1.43
	A	A	A	A			D	D	D	D	
		B	B	B	B	B		E	E	E	E
					C	C	C	C	C		

Temp 325° F

Asphalt	BO	CH	BE	MT	DI	AM	DM	MA	SO	TX	TA
Mean	4.86	3.89	3.67	3.57	3.43	3.07	2.72	2.72	2.43	2.27	1.82
	A	B	B	B	B	B	E	E	E	E	E
			C	C	C	C	C	C			
						D	D	D	D	D	

Temp 365° F

Asphalt	BO	CH	MT	BE	AM	DI	SO	MA	DM	TX	TA
Mean	17.7	8.97	8.36	8.14	6.31	5.40	5.21	4.67	4.34	3.43	2.77
	A	B	B	B	B	B	B	B	B		
				C	C	C	C	C	C	C	
					D	D	D	D	D	D	D

Note Means with the same letters are not significantly different (alpha = 0.05)

For Oven Temperature of 325° F

1. Texaco Airblown 85-100*
2. Texaco 85-100*
3. Mariani AC-30*
4. Chevron AC-20 Modified*

For Oven Temperature of 365° F

1. Texaco Airblown 85-100*
2. Texaco 85-100*
3. Chevron AC-20 Modified*
4. Mariani AC-30*
5. Chevron AC-20*
6. Amsco AC-30*

* Not different from each other.

Since TEMP interacts with ASPHALT (and not with OVEN), comparison of TEMP means must be made separately for each ASPHALT, averaged over the two types of OVEN. This, however, is not considered useful as it is obvious that higher temperatures would result in increased levels of viscosities and the differential would depend on the asphalt.

Plots of the average Absolute Viscosity Ratio (averaged over both oven types) v.s. Oven Temperature for different asphalts are shown in Figure 5.3. It can be seen from these two figures that

1. the change in Viscosity Ratio between 325° F and 365° F is greater than that between 285° F and 325° F, and
2. the degree of change depends on the type of asphalt.

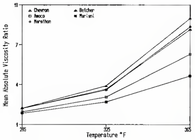

Figure 5.3 Relation Between Mean Absolute Viscosity Ratio and Oven Temperature

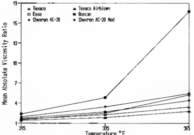

Figure 5.3--continued

5.3.6 Kinematic Viscosity at 275° F

Results of ANOVA on the Kinematic Viscosity (the data in Table 5.3) are summarized in Table 5.14. From Table 5.14, it is seen that the main factors ASPHALT and TEMP and the interaction ASPHALT * TEMP are significant, while the effect of oven type is not significant. This corresponds to what was seen earlier from the analyses of variance done on Absolute Viscosity and Viscosity Ratio at 140° F. As such, no further analysis is considered useful.

5.3.7 Relationship Between RTFOT and TFOT Effects

For each of the response parameters, relationships were established between response after RTFOT and response after TFOT. This was done for each temperature level by a linear regression analysis using SAS/STAT computer software. The results obtained are summarized in Table 5.15. The table also gives the number of samples within multilab reproducibility as specified in ASTM test methods D5, D2170 and D2171.

5.4 Summary of Findings

The major findings from the results of the Thin Film and Rolling Thin Film oven tests are summarized as follows.

1. On the basis of percent Penetration Retained, the RTFOT is a more severe aging process than the TFOT for oven temperatures of 285 and 325° F. However, for an oven temperature of 365° F, the two processes are not different from one another.
2. On the basis of Absolute Viscosity Ratio, the RTFOT and TFOT are not different from one another.

Table 5.14 Results of ANOVA on Kinematic Viscosity

Source	df	MS	F-Value	P
ASPHALT	10	866893.04	121.08	0.0001
TEMP	2	1501248.97	209.68	0.0001
OVEN	1	2546.97	0.36	0.5576
ASPHALT * TEMP	20	86324.74	12.06	0.0001
ASPHALT * OVEN	10	11497.37	1.61	0.1761
TEMP * OVEN	2	22080.79	3.08	0.0680
ERROR	20	7159.59		

R-SQUARE 0.990

Table 5.15 Relationship Between RTFOT and TFOT Effects

Process	$Pen_{(RTF)} = a + b\,Pen_{(TF)} + \varepsilon$			Samples within Reproducibility
Temp (° F)	R^2	a	b	out of 11*
285	0.970	1.687	0.904	6
325	0.934	2.885	0.858	9
365	0.944	-2.322	1.059	9
	$AbsVis_{(RTF)} = a + b\,AbsVis_{(TF)} + \varepsilon$			
285	0.994	523.846	1.070	2
325	0.981	14.752	1.240	3
365	0.715	33.775	1.070	3
	$KinVis_{(RTF)} = a + b\,KinVis_{(TF)} + \varepsilon$			
285	0.966	70.549	0.938	10
325	0.967	52.236	1.017	7
365	0.891	131.105	0.848	5

* Based on ASTM D5, D2170 & D2171, respectively.

3. When the Absolute Viscosity Ratios are used to give relative ratings to asphalts, using a different oven temperature can produce different results. For example, asphalt A may have a higher Viscosity Ratio than that of asphalt B for oven temperature of 285° F and a lower Viscosity Ratio than that of asphalt B for oven temperature of 325° F.
4. Differences in asphalts of comparable grade, when evaluated by Duncan's test, tend to minimize as the oven temperature increases on the basis of Absolute Viscosity Ratio. However, differences in absolute terms increase.
5. The Penetration, Absolute Viscosity and Kinematic Viscosity after TFOT can be related to the same measured parameters after RTFOT.

CHAPTER 6

INFRARED ABSORPTION SPECTROSCOPY ON RESIDUES FROM TFO AND RTFO TESTS

6.1 Introduction

In the recommendations made on the basis of preliminary investigations [46], it was brought out that IR spectroscopy appears to be a viable technique to identify and quantify changes in asphalt composition due to oxidation and age hardening. In order to study this aspect more deliberately, an experimental program was devised and run on the original asphalts and residues obtained after TFOT and RTFOT, for each of the asphalts used in this study. Section 5.1 gives details of the TFO and RTFO tests run.

The specific objectives of the experiment using IR spectroscopy were as follows

1. To study the possibility of expressing the level of oxidation as a ratio of two absorbances, one of which varies with the amount of oxidation, the other remaining constant throughout the oxidation process.
2. To devise a measure which would enable quantifying relative degrees of change brought about by oxidation and hardening.
3. To carry out statistical analyses of the quantified effects and determine
    - (a) difference between asphalts
    - (b) differences between the three levels of temperature

   (c) differences between the effects of TFOT and RTFOT on the various parameters.

4. To compare results based on IR spectral analysis with those based on percent Penetration Retained and Absolute Viscosity Ratio.

6.2 Examination of IR Absorption Spectra

The asphalts and residues were dissolved in Tetrahydrofuran at a concentration of 5 percent (W/V) and evaluated in the FTIR spectrophotometer using procedures described in Section 4.2.9.3. A sealed cell with 0.1mm pathlength and sodium chloride windows was used. Figures 6.1 to 6.11 display the IR absorption spectra of the original asphalts in the region between 1800 cm^{-1} and 1500 cm^{-1}.

Study of the spectra by asphalts, indicates a definite increase in the level of oxidation as indicated by increases in carbonyl absorption in the 1700 cm^{-1} region, which is due to increasing concentration of ketones and anhydrides. Also, carbonyl absorption of acid types occurs at about 1730 cm^{-1}. As stated earlier in Section 2.5.4, ketones and anhydrides are formed on oxidative aging and carboxylic acids occur naturally in the asphalt but increase on oxidative aging. Since these three functional groups are the most significant chemical functionalities which can be related to oxidative aging, examination of the spectra in this study, was done with particular reference to them.

The spectra also indicated that the band centering at about 1600 cm^{-1} which results primarily from aromatic carbon-carbon double bonds, can be assumed to be fairly constant, because the group is present in highly condensed stable molecules [47]. As such, it will be possible to

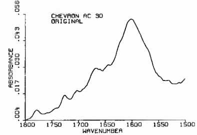

Figure 6.1 IR Spectrum of Original Asphalt Chevron AC-30

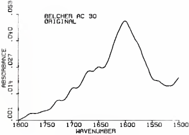

Figure 6.2 IR Spectrum of Original Asphalt Belcher AC-30

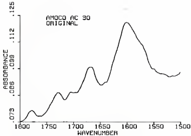

Figure 6.3 IR Spectrum of Original Asphalt Amoco AC-30

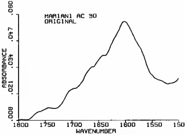

Figure 6.4 IR Spectrum of Original Asphalt Mariani AC-30

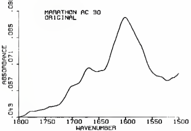

Figure 6.5 IR Spectrum of Original Asphalt Marathon AC-30

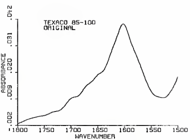

Figure 6.6 IR Spectrum of Original Asphalt Texaco 85-100

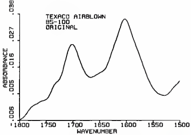

Figure 6.7 IR Spectrum of Original Asphalt Texaco Airblown BS-100

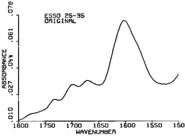

Figure 6.8 IR Spectrum of Original Asphalt Esso 25-35

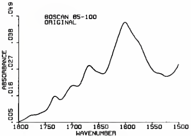

Figure 6.9 IR Spectrum of Original Asphalt Boscan 85-100

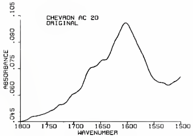

Figure 6.10 IR Spectrum of Original Asphalt Chevron AC-20

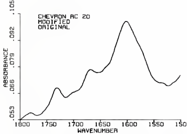

Figure 6.11 IR Spectrum of Original Asphalt Chevron AC-20 Modified

express the level of oxidation as a ratio of absorbances at 1700 cm^{-1} and 1600 cm^{-1}. This may be referred to as Carbonyl Ratio at 1700 cm^{-1}.

Measured absorbances at the peaks corresponding to 1700 cm^{-1} and 1600 cm^{-1} wavenumbers have been documented, using the coding adopted earlier in Section 5.3.5, for each of the asphalts and asphalt residues in Table 6.1. Ratios of absorbances have been calculated and presented as Carbonyl Ratio at 1700 cm^{-1} in Table 6.2. Plots of Carbonyl Ratio at 1700 cm^{-1} v.s. TFOT and RTFOT temperatures for different asphalts are shown in Figures 6.12 and 6.13. It can be seen from the table and figures that

1. the increase in Carbonyl Ratio between 325°F and 365°F is generally greater than that between 285°F and 325°F, with a few exceptions.
2. the degree of increase depends on the asphalt type.
3. Texaco Airblown 85-100 has a distinctly higher Carbonyl Ratio as compared to the other asphalts.

In order to quantitatively follow the change in Carbonyl Ratio, a factor is obtained by dividing the Carbonyl Ratios for the residues by the Carbonyl Ratios for the respective original asphalts. Corresponding to Carbonyl Ratio at 1700 cm^{-1}, this factor may be referred to as the Ketone Anhydride Development Factor (KADF). KADF values for the eleven asphalts tested are presented in Table 6.3. Figures 6.14 and 6.15 display the relationships between KADF and the process temperature for the various asphalts after TFOT and RTFOT respectively.

A similar procedure would also be appropriate in respect of carboxylic acids, however, in this study, reference to the carboxylic group would be limited to the extent of just noting the presence or otherwise of a well-defined peak at about 1730 cm^{-1} in the spectra of

Table 6.1 Measured Absorbances at 1600 and 1700 cm^{-1}

Asphalt	ORI	TFOT 285°F	 325°F	 365°F	RTFOT 285°F	 325°F	 365°F
CH	.0496*	.0495	.0839	.0549	.0386	.0489	.0610
	.0141**	.0169	.0309	.0217	.0125	.0179	.0239
BE	.0489	.0369	.0450	.0504	.0520	.0496	.0646
	.0157	.0130	.0165	.0218	.0168	.0173	.0266
AM	.0485	.0402	.0304	.0498	.0529	.0536	.0521
	.0138	.0133	.0112	.0211	.0187	.0194	.0222
MA	.0485	.0496	.0887	.0826	.0522	.0533	.1062
	.0152	.0172	.0339	.0339	.0165	.0192	.0395
MT	.0527	.0517	.0526	.0577	.0594	.0520	.0593
	.0166	.0186	.0203	.0257	.0200	.0191	.0244
01	.0560	.0615	.0582	.0653	.0593	.0661	.0650
	.0158	.0196	.0203	.0262	.0192	.0234	.0236
DM	.0483	.0523	.0495	.0503	.0491	.0619	.0522
	.0136	.0155	.0156	.0181	.0144	.0164	.0187
TX	.0417	.0460	.0449	.0600	.0452	.0602	.0507
	.0106	.0129	.0139	.0220	.0126	.0196	.0172
TA	.0417	.1529	.0363	.0401	.0793	.0563	.0858
	.0312	.1231	.0298	.0355	.0634	.0477	.0736
SO	.0640	.0913	.1169	.0795	.0490	.0902	.0982
	.0230	.0363	.0437	.0373	.0184	.0369	.0465
BO	.0413	.0613	.0203	.0641	.0412	.0438	.0323
	.0151	.0247	.0084	.0301	.0182	.0208	.0148

NOTE * Absorbance at 1600 cm^{-1}

** Absorbance at 1700 cm^{-1}

Table 6.2 Ratio of Absorbances Expressed as Carbonyl Ratio at 1700 cm^{-1}

	Absorbance at 1700 cm^{-1}/Absorbance at 1600 cm^{-1}						
		TFOT			RTFOT		
Asphalt	ORI	285°F	325°F	365°F	285°F	325°F	365°F
CH	.284	.341	.368	.395	.324	.366	.392
BE	.321	.352	.367	.434	.323	.349	.412
AM	.285	.331	.368	.424	.353	.352	.426
MA	.313	.347	.382	.410	.318	.360	.376
MT	.315	.360	.366	.445	.337	.367	.411
DI	.282	.319	.349	.401	.324	.354	.363
OM	.282	.296	.315	.360	.293	.316	.358
TX	.254	.280	.310	.367	.279	.326	.339
TA	.748	.805	.821	.885	.793	.838	.858
SO	.359	.374	.387	.469	.376	.409	.474
BO	.366	.403	.414	.470	.393	.418	.458

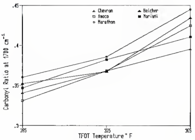

Figure 5.12 Carbonyl Ratio of Asphalt Residue After TFOT v.s. Oven Temperature

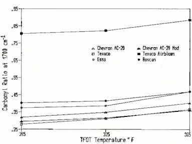

Figure 6.12--continued

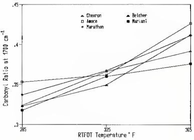

Figure 6.13 Carbonyl Ratio of Asphalt Residue After RTFOT v.s. Oven Temperature

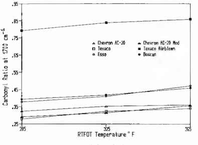

Figure 6.13--continued

Table 6.3 Ketone Anhydride Development Factors

Asphalt	TFOT			RTFOT		
	285°F	325°F	365°F	285°F	325°F	365°F
CH	1.20	1.30	1.39	1.14	1.29	1.38
BE	1.10	1.14	1.35	1.01	1.09	1.28
AM	1.16	1.29	1.49	1.24	1.27	1.49
MA	1.11	1.22	1.31	1.02	1.15	1.20
MT	1.14	1.23	1.41	1.07	1.17	1.30
Ol	1.13	1.24	1.42	1.15	1.26	1.29
OM	1.05	1.12	1.28	1.04	1.12	1.27
TX	1.10	1.22	1.44	1.10	1.28	1.33
TA	1.08	1.10	1.18	1.08	1.12	1.15
SO	1.04	1.08	1.31	1.05	1.14	1.32
BO	1.10	1.13	1.28	1.07	1.14	1.25

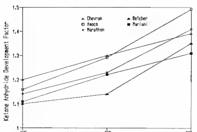

Figure 5.14 Ketone Anhydride Development Factor of Asphalt Residue After TFOT v.s. Oven Temperature

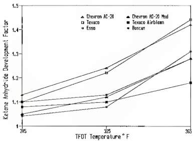

Figure 6.14--continued

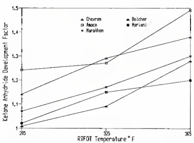

Figure 6.15 Ketone Anhydride Development Factor of Asphalt Residue After RTFOT v.s. Oven Temperature

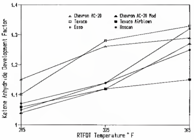

Figure 6.15--continued

the original asphalts. From Figures 6.1 to 6.11 it is seen that the following asphalts show distinct peaks at wavenumber of about 1630 cm^{-1}, corresponding to carbonyl absorption of acid types:

1. Chevron AC-30
2. Belcher AC-30
3. Amoco AC-30
4. Esso 25-35
5. Chevron AC-20 Modified

6.3 Analysis of Results

6.3.1 Statistical Model

The test results as listed in Table 6.3 were analyzed as results of a factorial experiment, in a manner and using a model identical to that done in Section 5.3.1.

6.3.2 Ketone Anhydride Development Factor

In Section 5.3, a probability of error (= level) of 0.05 was used. However, in this portion of the study, considering the relative innovation of the methods adopted, it is more appropriate to use a lower value of α. This will ensure a higher level of confidence when rejecting the null hypothesis. As such, an α value of 0.01 was adopted. In other words, the statement that a particular factor is significant will have a probability of error of 0.01, thus rendering the statistical tests much more conservative.

Results of ANOVA on the data are summarized in Table 6.4, from where it can be seen that all main effects are significant and the interaction effect ASPHALT*TEMP is significant. Since ASPHALT interacts with TEMP (and not OVEN), comparison of asphalts must be made at each

Table 5.4 Results of ANOVA on Ketone Anhydride Development Factor

Source	df	MS	F Value	P
ASPHALT	10	0.0256	34.34	0.0001
TEMP	2	0.2840	380.41	0.0001
OVEN	1	0.0122	16.44	0.0006
ASPHALT*TEMP	20	0.0024	3.27	0.0055
ASPHALT*OVEN	10	0.0022	2.94	0.0192
TEMP*OVEN	2	0.0036	4.85	0.0192
ERROR	20	0.0007		

R-SQUARE 0.984

level of temperature, averaged over the two types of OVEN. This was done by Duncan's test at a level of significance of 0.05. The results are summarized in Table 6.5. For convenience in presentation, asphalts have been coded as described earlier in Section 5.3.5.

From Table 6.5, it can be seen that the following paving asphalts have a better Ketone Anhydride Development Factor, in that the said factor is the lowest, thereby possibly indicating better durability and/or greater resistance to hardening.

For Oven Temperature of 285°F

1. Chevron AC-20 Modified
2. Belcher AC-30
3. Mariani AC-30
4. Texaco Airblown 85-100
5. Boscan 85-100
6. Texaco 85-100
7. Marathon AC-30

For Oven Temperature of 325°F

1. Texaco Airblown 85-100
2. Belcher AC-30
3. Chevron AC-20 Modified
4. Boscan 85-100
5. Mariani AC-30

For Oven Temperature of 365°F

1. Texaco Airblown 85-100

Table 6.5 Grouping of Asphalts by Temperature on the Basis of Ketone Anhydride Development Factor

Temp 285°F

Asphalt	AM	CH	OI	MT	TX	BO	TA	MA	BE	DM	SO
Means	1.200	1.170	1.140	1.050	1.100	1.085	1.070	1.065	1.055	1.045	1.045
	A	A	A								
		B	B	B	B	B					
			C	C	C	C	C	C	C		
				D	D	D	D	D	D	D	D

Temp 325°F

Asphalt	CH	AM	TX	OI	MT	MA	BO	DM	BE	TA	SO
Mean	1.295	1.280	1.250	1.250	1.200	1.185	1.135	1.120	1.115	1.110	1.110
	A	A	A	A							
			B	B	B	B					
					C	C	C				
						D	D	D	D	D	D

Temp 365°F

Asphalt	AM	TX	CH	MT	OI	BE	SO	DM	BO	MA	TA
Mean	1.490	1.385	1.385	1.355	1.355	1.315	1.315	1.275	1.265	1.255	1.165
	A										
		B	B	B	B	B	B				
				C	C	C	C	C	C		
						D	D	D	D	D	
											E

Note Means with the same letters are not significantly different (alpha = 0.05)

Since TEMP interacts with ASPHALT (and not OVEN), comparison of TEMP means must be made separately for each ASPHALT, averaged over the two types of OVEN. This, however is not considered useful as it is obvious that higher temperatures would result in increased levels of oxidation and the differential would depend on the asphalt.

Since OVEN does not interact with either ASPHALT or TEMP, comparison of OVEN means can be made averaged over all asphalts and over all temperature conditions. This was done by Duncan's test at a level of significance of 0.05. It was seen that the TFOT and RTFOT processes are not different from one another.

On the basis of Tables 6.3, 6.5 and Figures 6.14 and 6.15, it may be concluded that Ketone Anhydride Development Factor is a suitable measure of asphalt hardening, since prima facie, there is correlation between this factor and the two parameters discussed earlier, that is percent Penetration Retained and Absolute Viscosity Ratio.

6.3.3 Correlation Between Parameters

Even in the initial stages of this study it was apparent that potential hardening characteristics of asphalts caused by excessive loss of volatiles would possibly escape detection by methods such as IR spectroscopy. In order to confirm this aspect, Flash Point and Smoke Point tests were run on the eleven asphalts. These tests were performed by the personnel of the Bureau of Materials and Research, Florida Department of Transportation. Results obtained are presented in Table 6.6.

From Table 6.6, it can be seen that Amoco AC-30 and Boscan 85-100 have the lowest Smoke Points (290 and 270° F respectively), as also the lowest Flash Points. This property of asphalt could have contributed to

Table 6.6 Results of Flash and Smoke Point Tests

Asphalt	Smoke Point °F	Flash Point °F
Chevron AC-30	350	600
Belcher AC-30	350	605
Amoco AC-30	290	510
Mariani AC-30	385	590
Marathon AC-30	345	600
Texaco 85-100	380	600
Texaco Airblown 85-100	395	600
Esso 25-35	385	610
Boscan 85-100	270	470
Chevron AC-20	350	600
Chevron AC-20 Mod	340	610

the high loss of penetration as measured by percent Penetration Retained, which was presented earlier in Table 6.8. It can be seen that Boscan 85-100 and Amoco AC-30 are both in the last group (with high loss of penetration). Interestingly, when considering Absolute Viscosity Ratio from Table 5.13, Boscan 85-100 still remains at the end of the spectrum of asphalts considered (with high Absolute Viscosity Ratio), but Amoco AC-30 moves into a median group.

While comparing the relative rating of asphalts, it is best to remove the anomolous ones, i.e., those which suffer hardening due to a low Smoke and Flash Point, and then see whether there is any association between percent Penetration Retained, Absolute Viscosity Ratio and Ketone Anhydride Development Factor. Table 6.7 presents comparative data at the median temperature level of 325°F. Contents of Tables 5.8, 5.13, and 6.5 have been used to compile Table 6.7.

It can be seen from Table 6.7 that barring Texaco 85-100 and Belcher AC-30, there is a certain measure of correlation between the three parameters. Using Spearman's coefficient of rank correlation method, coefficients of correlation were calculated between each pair of the three different parameters. The coefficients of correlation between Absolute Viscosity Ratio and KADF, between Absolute Viscosity Ratio and Percent Penetration Retained, and between KADF and Percent Penetration Retained were 0.49, 0.43 and 0.67 respectively.

Although this method has drawbacks, it is very handy for obtaining a quick approximate estimate of the coefficient of correlation. The results indicate that the best correlation exists between Ketone Anhydride Development Factor and percent Penetration Retained, with a coefficient of correlation of 0.67.

Table 6.7 Comparative Rating of Asphalts Based on Penetration, Absolute Viscosity and Spectral Measurement

Absolute Viscosity Ratio	TA	TX	SO	MA	DM	DI	MT	BE	CH
Ketene Anhydride Development Factor	SO	TA	BE	DM	MA	MT	DI	TX	CH
Percent Penetration Retained	SO	TA	DM	MA	DI	CH	BE	MT	TX

6.3.4 Effect of Low Smoke Point

As brought out earlier, a low Smoke Point would result in hardening which may or may not be attributable to the base constituents in the asphalt. For example, Boscan 85-100 and Amoco AC-30 both have the greatest penetration losses and appear in the last group in Table 5.8. Interestingly, in Table 6.5, Amoco goes back into the lower group when considering Ketone Anhydride Enhancement Factor, whereas Boscan appears in the desirable group having the better test results.

The above observation may indicate that Boscan 85-100 hardens primarily because of rapid loss of the volatile constituents, whereas Amoco AC-30, in contrast, hardens partly due to volatiles lost and partly due to changes in the chemical structure of the hydrocarbon compounds.

6.4 Summary of Findings

The major findings from the results of the spectral studies are summarized as follows

1. It is possible to express the level of oxidation as a ratio of two absorbances, one corresponding to the peak at 1700 cm^{-1}, which is due to the formation of ketones and anhydrides, and the other corresponding to the peak at 1600 cm^{-1}, which is fairly constant and due to aromatic carbon-carbon double bonds. This ratio of absorbances may be referred to as Carbonyl Ratio at 1700 cm^{-1}.

2. In order to follow changes in the level of oxidation, a factor may be used which is obtained by dividing the ratio of absorbance at 1700 cm^{-1} for the aged asphalt residue by the ratio of absorbance at 1700 cm^{-1} for the original asphalt. This factor may be termed as Ketone Anhydride Development Factor, which increases with increasing levels of oxidation.

3. On the basis of Ketone Anhydride Development Factor, TFOT and RTFOT are not different from one another.

4. When Ketone Anhydride Development Factors are used to give relative ratings to asphalts, using a different oven temperature can produce different results.

5. Differences in asphalts of comparable grade, when evaluated by Duncan's test, tend to maximize as the oven temperature increases on the basis of Ketone Anhydride Development Factors.

6. At an oven temperature of 325°F, a positive correlation exists between Ketone Anhydride Development Factor and percent Penetration Retained, with a coefficient of correlation of 0.67. Correlation between Ketone Anhydride Development Factor and Absolute Viscosity Ratio was lower at 0.49 and correlation between Absolute Viscosity Ratio and percent Penetration Retained was the least with a value of 0.43. All correlations above exclude asphalts which have a smoke point less than 300°F.

7. Considering the low levels of absorbance recorded, it is considered appropriate to use a sealed cell with a greater path length. This would increase the absorbance and also improve the signal-to-noise ratio.

CHAPTER 7
RESULTS OF MIXTURE STRENGTH TESTS

7.1 Introduction

An experimental program to assess the effects of different aging conditions on strength, moduli and energy using 50-blow Marshall compacted specimens was devised and performed. Details have been previously presented in Chapter 4.

The specific objectives of the experiment were as follows:

1. Perform Indirect Tensile and Resilient Moduli Tests for evaluation of age hardening effects on the tensile strength and resilient moduli.

2. Evaluate Fracture Energy and determine the effect of age hardening.

3. Conduct statistical analyses to establish the significance and relationships between test parameters. This will be done by performing analyses of variance and/or regression analyses. Specifically, the analyses will establish relationships and/or determine

(a) differences between the effects of the three exposure test conditions.

(b) differences between asphalts in their properties and response to age hardening.

7.2 Results

Results of the Indirect Tensile Test by asphalt, type of exposure and duration of exposure are tabulated in Appendix B-1. The results are presented on ten pages, one page corresponding to each of the asphalts tested. Test results include data on each replicate tested as also the average of the three replicates tested for each type and duration of exposure.

Results of the Resilient Modulus Test with respect to the four asphalts tested i.e., Mariani AC-30, Amoco AC-30, Chevron AC-20 and Chevron AC-20 Modified, have been tabulated in Appendix B-2.

The results are presented separately for the two types of exposure conditions viz oven and ultraviolet. The tabulation includes data on instantaneous recoverable, total recoverable and total deformations as also moduli calculated both on the basis of instantaneous and total recoverable deformations. Test results cover data on each replicate tested, average values of moduli and measured deformations along the two directions in which the specimens were tested.

Computed values of Fracture Energy, with respect to the four asphalts on which the modulus tests were conducted, are presented in Appendix B-3. Test results include data on each replicate tested as also the average of the three replicates tested for each type and duration of exposure.

7.3 Analysis of Results

7.3.1 Indirect Tensile Test

7.3.1.1 Statistical Model. The test results as tabulated in Appendix B-1 were analyzed as results of a factorial experiment comprising of eight asphalts (ASPHALTS), (since the scope of the experiment was abridged with respect to two asphalts i.e., Chevron AC-20 and Chevron AC-20 Modified, in that specimens corresponding to these two asphalts were not subjected to exposure in the Forced Draft environment, data on these two asphalts were excluded from the analysis of variance, resulting in data pertaining to eight ASPHALTS), three conditions of exposure (EXPOSURE) and five levels of duration of exposure (DURATION). ASPHALT, EXPOSURE and DURATION are regarded as fixed effects (as opposed to random effects) since, in this study, concern is only in the chosen asphalts, conditions of exposure and durations of exposure. The experiment has 380 treatment combinations.

The following linear model is assumed for any single measurement in the experiment:

$$\begin{aligned} Y_{ijkl} = m + A_i + B_j + C_k + (AB)_{ij} + (AC)_{ik} \\ + (BC)_{jk} + (ABC)_{ijk} + e_{ijkl} \end{aligned} \qquad (7.1)$$

where

m = overall mean.

A_i = effect of the i^{th} asphalt.

B_j = effect of the j^{th} exposure condition.

C_k = effect of the k^{th} exposure duration.

$(AB)_{ij}$ = joint effect of the i^{th} asphalt and j^{th} exposure condition.

$(AC)_{ik}$ = joint effect of the i^{th} asphalt and k^{th} exposure duration.

$(BC)_{jk}$ = joint effect of the j^{th} exposure condition and k^{th} exposure duration.

$(ABC)_{ijkl}$ = joint effect of the i^{th} asphalt, j^{th} exposure condition and k^{th} exposure duration on the l^{th} replicate.

ϵ_{ijkl} = random error.

7.3.1.2 Analysis of Variance. Analysis of variance (ANOVA) was performed on the test data using SAS/STAT computer software. Results of ANOVA on the Indirect Tensile Test data are summarized in Table 7.1. A probability or error (α level) of 0.05 was used, which corresponds to a 95 percent level of confidence. All main effects and interaction effects given in Table 7.1 are significant, since the P values are less than 0.05. It therefore follows that

1. Comparison of ASPHALT must be made at each EXPOSURE, for each level of DURATION.
2. Comparison of EXPOSURE must be made by ASPHALT, for each level of DURATION.
3. Comparison of level of DURATION must be made for each EXPOSURE, for ASPHALT separately.

7.3.1.3 Comparison of Means. Items 1 and 2 are of greater interest than 3 because the effects produced by long-term aging conditions are of primary interest. Consequently, effects at the 90 day DURATION were subjected to a detailed study in preference to those at shorter durations of exposure. A comparison of means for EXPOSURE, for each ASPHALT at 90 days DURATION was performed using Duncan's test at a level of significance of 0.05. The results are summarized in Table 7.2. Similarly, a comparison of means for ASPHALT, for each EXPOSURE at 90 days DURATION was performed using Duncan's test, at the same level of significance. These results are summarized in Table 7.3.

Table 7.1 Result of ANOVA on Indirect Tensile Strength

Source	df	MS	F-Value	P
ASPHALT	7	73177.21	1049.15	0.0001
EXPOSURE	2	1609.45	23.07	0.0001
DURATION	4	77420.74	1109.99	0.0001
ASPHALT * EXPOSURE	14	194.95	2.80	0.0007
ASPHALT * DURATION	28	636.96	9.12	0.0001
EXPOSURE * DURATION	8	340.50	4.88	0.0001
ASPHALT * EXP * DUR	56	122.61	1.76	0.0020
ERROR	240	69.75		

Note

df - degrees of freedom
MS - Mean Square
F-Value - Mean Square/Error Mean Square
P - Probability of error

Table 7.2 Grouping of Type of Exposure by Asphalt for 90 Day Duration on the Basis of Indirect Tensile Strength

Asphalt Code	Means (psi)		
	Forced Draft	Ultraviolet	Oven
CH	199.23 (A)	183.75 (B)	185.66 (B)
BE	202.63 (A)	199.23 (A)	185.13 (A)
AM	229.56 (A)	226.21 (A)	223.85 (A)
MA	231.28 (A)	203.98 (A)	210.21 (A)
TX	225.68 (A)	206.03 (B)	209.45 (B)
TA	131.80 (A)	112.77 (A)	121.16 (A)
SO	316.84 (A)	277.97 (B)	302.28 (A) (B)
BO	197.06 (A)	193.80 (A)	202.46 (A)
DI	Not Tested	198.97 (A)	202.15 (A)
DM	Not Tested	185.16 (A)	184.46 (A)

Note: Row means with the same letter are not significantly different (alpha = 0.05).

Table 7.3 Grouping of Asphalts by Type of Exposure for 90 Day Duration on the Basis of Indirect Tensile Strength

Forced Draft

Asphalt Code	SD	MA	AM	TX	BE	CH	BO	TA
Means (psi)	316.84	231.28	229.56	225.68	202.63	199.23	197.06	131.80
Group	A	B	B	B	C	C	C	D

Oven

Asphalt Code	SD	AM	MA	TX	BO	CH	BE	TA
Means (psi)	302.28	223.85	210.21	209.45	202.46	185.65	185.13	121.16
Group	A	B	B	B	D	D	D	E
			C	C	C			

Asphalt Code	OI	OM
Means (psi)	202.16	184.46
Group	A	A

Ultraviolet

Asphalt Code	SD	AM	TX	MA	BE	BO	CH	TA
Means (psi)	277.97	226.21	206.03	203.98	199.23	193.80	183.75	112.77
Group	A	B	C	C	C	C		
					D	D	D	E

Asphalt Code	OI	OM
Means (psi)	198.97	185.16
Group	A	A

Note Row means with the same letter are not significantly different (alpha = 0.05).

To differentiate between Chevron AC-20 and Chevron AC-20 Modified on the basis of Indirect Tensile Strength, a separate comparison of means was performed for the 90 day data. These results have also been included in Tables 7.2 and 7.3.

7.3.1.4 Regression Analysis. Preliminary analyses revealed that a relationship defined by the following model would best fit the data.

$$\text{Dependent Response} = \theta_0 + \theta_1(\log_{10}\text{ days}) + \theta_2(\log_{10}\text{ days})^2 + \text{Random Error} \quad (7.2)$$

On this basis, data in Appendix B-1 was used to plot relationships between Indirect Tensile Strength and duration of exposure (log scale) for each type of exposure, by asphalt and are presented in Figure 7.1.

Since the regression equations would be useful in relating response due to aging in the laboratory with response of samples aged on the roof, it was considered appropriate to regress the data for each asphalt but not by type of exposure. In other words, one equation per asphalt was sought, regardless of exposure type. Such an equation represents an average effect of the three types of exposure.

Using SAS/STAT software, regression analyses resulted in coefficients presented in Table 7.4.

7.3.1.5 General Observations and Findings. Considering the significance ($\alpha = 0.05$) of asphalt, duration and type of exposure as also their interaction, it can be stated that strength response is a function of all three variables independently as also in combinations of these variables. Comparison of means done at a 90 day DURATION indicate that

1. Forced draft exposure results in a significantly higher strength ($\alpha = 0.05$) over that caused by ultraviolet or oven with

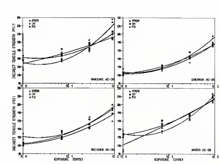

7.1 Relation Between Indirect Tensile Strength and Duration of Exposure

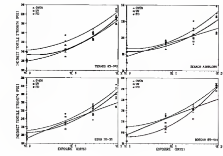

Figure 7.1--continued

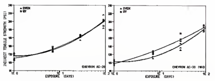

Figure 7.1--continued

Table 7.4 Regression Coefficients for Relation Between Indirect Tensile Strength and Duration of Exposure

Asphalt Code	β_0	β_1	β_2	R^2
CH	114.81	-1.344	20.260	0.95
BE	119.71	-0.223	20.036	0.91
AM	129.11	12.544	18.566	0.91
MA	143.60	-4.948	21.147	0.85
TX	131.99	4.657	18.839	0.88
TA	82.25	5.079	7.647	0.78
SD	202.98	21.896	13.742	0.87
BD	112.98	-9.782	26.890	0.93

Note:

Indirect Tensile Strength = $\beta_0 + \beta_1 (\log_{10} \text{days}) + \beta_2 (\log_{10} \text{days})^2$

respect to the following asphalts

(a) Chevron AC-30

(b) Texaco 85-100

2. Effects caused by ultraviolet and oven are about the same.
3. On the basis of forced draft exposure, it is seen that Mariani AC-30 and Amoco AC-30 result in higher strengths compared to Belcher AC-30 and Chevron AC-30 ($\alpha = 0.05$).
4. On a similar basis, it is seen that Texaco 85-100 results in higher strength than Boscan 85-100, which in turn is higher than Texaco Airblown 85-100.
5. The relationship between Indirect Tensile Strength and duration of exposure in days can be defined by a polynominal expression of the second order, the independent variable being the common logarithm of the number of days. R-Square values range from 0.76 to 0.95.

7.3.2 Resilient Modulus Test

7.3.2.1 Deformation. Tabulated results in Appendix B-2 were used to develop relationships between the horizontal deformation and duration of exposure for the four asphalts and the two types of exposure (oven and ultraviolet). Deformations were measured corresponding to both instantaneous and total recoveries as also the total deformation including the non-recoverable component. Recoverable deformations were included in the plots and developed relationships, which are presented as Figure 7.2.

7.3.2.2 Modulus. Similarly, relationships were plotted between Resilient Modulus (psi) and duration of exposure for the four asphalts

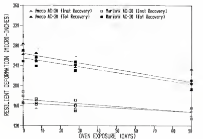

Figure 7.2 Relation Between Horizontal Deformation and Duration of Exposure

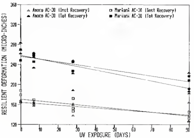

Figure 7.2--continued

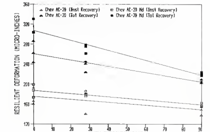

Figure 7.2--continued

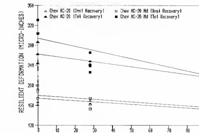

Figure 7.2--continued

and the two types of exposure. Moduli relationships corresponding to both instantaneous and total recoveries are presented in Figure 7.3.

7.3.2.3 Regression Equations. Data for the four asphalts were regressed using the following model:

$$\text{Dependent Response} = \beta_0 + \beta_1 \text{ (days)} + \text{Random Error} \qquad (7.3)$$

This model was chosen after examining other options. The analysis was done with data corresponding to instantaneous and total recovery, for each type of exposure, all separately. Using SAS/STAT software, the analysis resulted in coefficients presented in Table 7.5.

7.3.2.4 General Observations and Findings. Trends in the plotted relationship between horizontal deformation and duration of exposure, as shown in Figure 7.2 indicate that

1. As the asphalt hardens, deformations decrease and differences between total deformation and total recoverable deformation decrease. In other words, the magnitude of the creep component is reduced as viscosity increases. This behavior is reasonable and as anticipated.
2. Differences in the deformation characteristics of comparable asphalts diminish with increased durations of exposure.
3. Chevron AC-20 Modified in comparison to Chevron AC-20, exhibits greater recoverable and total deformations.
4. Ultraviolet and oven exposures result in a generally similar pattern of responses.

Trends in the plotted relationship between Resilient Modulus and duration of exposure as shown in Figure 7.3 indicate that

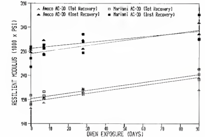

Figure 7.3 Relation Between Resilient Modulus and Duration of Exposure

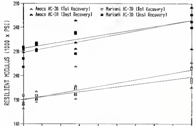

Figure 7.3--continued

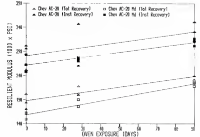

Figure 7.3--continued

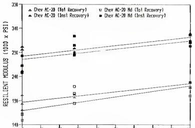

Figure 7.3--continued

Table 7.5 Regression Coefficients for Relation Between Resilient Modulus and Duration of Exposure

Asphalt Code	Type of Exposure	Based On Instantaneous Recovery			Based On Total Recovery		
		B_0	B_1	R^2	B_0	B_1	R^2
AM	Oven	296233	399.96	0.61	185934	560.35	0.76
AM	UV	296762	647.59	0.47	190178	688.12	0.59
MA	Oven	285786	544.82	0.53	192220	556.12	0.87
MA	UV	287976	745.02	0.73	191028	515.34	0.83
DI	Oven	280624	560.20	0.37	187681	568.19	0.84
DI	UV	282150	444.35	0.59	186817	434.88	0.80
DM	Oven	261616	527.10	0.81	158401	721.62	0.96
DM	UV	275358	432.53	0.46	169280	575.77	0.62

Note

Resilent Modulus = B_0 + B_1 (Exposure in Days)

1. As the asphalt hardens, the Modulus increases.
2. Chevron AC-20 in comparison to Chevron AC-20 Modified gave higher values of Moduli.
3. Ultraviolet and oven exposures result in a generally similar pattern of responses.

The relationship between Resilient Modulus and duration of exposure in days can be defined by a linear relationship, the independent variable being the number of days. R-Square values range from 0.37 to 0.81 for Moduli based on instantaneous recovery and 0.59 to 0.96 for values using total recovery.

7.3.3 Fracture Energy

Tabulated results in Appendix B-3 were used to develop relationships between the Fracture Energy (Pascals) and duration of exposure for the four asphalts and the two types of exposure (oven and ultraviolet). Preliminary analyses revealed that a relationship defined by the following model, would best fit the data

$$\text{Dependent Response} = \beta_0 + \beta_1\,(\text{days}) + \beta_2\,(\text{days})^2 + \text{Random Error} \qquad (7.4)$$

The model defined by Equation 7.4 was used in the data and the individual relationships were plotted and regressed as shown in Figure 7.4. Regression coefficients for relationships between Fracture Energy and duration of exposure in Table 7.6.

Trends in the plotted relationship between Fracture Energy and duration of exposure as shown in Figure 7.4 indicate that

1. As the asphalt hardens, energy values tend to increase up to a maximum and then decrease.

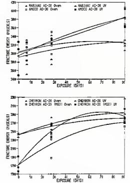

Figure 7.4 Relation Between Fracture Energy and Duration of Exposure

Table 7.6 Regression Coefficients for Relation Between Fracture Energy and Duration of Exposure

Asphalt	Type of Exposure	β_0	β_1	β_2	R^2
AM	Oven	3033.89	7.713	0.0154	0.66
AM	UV	2948.07	13.600	-0.0416	0.73
MA	Oven	2911.66	7.252	-0.0359	0.22
MA	UV	3019.28	8.299	-0.0643	0.18
DI	Oven	2421.20	10.886	-0.0674	0.64
DI	UV	2421.20	8.421	-0.0456	0.86
DM	Oven	1710.70	20.491	-0.1042	0.85
DM	UV	1710.70	35.534	-0.2543	0.92

Note:

$$\text{Fracture Energy} = \beta_0 + \beta_1\,(\text{days}) + \beta_2\,(\text{days})^2$$

2. Since the tests were run at 77° F (25° C), such a trend appears reasonable. Should the tests be run at temperatures lesser than 77° F (25° C), it is likely that the decreasing trend would manifest sooner in the aging period. In other words, decreasing trends are likely even when the asphalt just starts to harden.
3. Mixes made with Amoco AC-30 have greater Fracture Energy at 90 days aging for both oven and ultraviolet exposures in comparison to those made with Mariani AC-30.
4. Similarly, the Chevron AC-20 mixes have marginally higher Fracture Energy at 90 days as compared to those made with Chevron AC-20 Modified. However, in the initial stages of hardening, there is considerable difference in the energy levels of the two asphalts, the Modified asphalt generating very low energy.
5. At a level of exposure of 90 days, oven and ultraviolet exposures result in a generally similar pattern of responses.

The relationship between Fracture Energy and duration of exposure in days can be defined by a polynominal expression of the second order, the independent variable being the number of days. R-Square values vary from 0.18 to 0.92, the two lowest values of 0.18 and 0.22 pertaining to Mariani AC-30. Otherwise, the variation is between 0.64 to 0.92. Low R-Square values in respect of Mariani AC-30 have been caused by a high variation between replicate samples.

CHAPTER 8
RESULTS OF CONSISTENCY AND RHEOLOGY TESTS ON RECOVERED ASPHALT RESIDUES

8.1 Introduction

An experimental program to assess the effects of different aging conditions on Absolute Viscosity at 140° F (60° C), Penetration at 77° F (25° C) and viscosities at a constant power (j) of 100 W/m^3 at 77° F (25° C) and 59° F (15° C), was devised and performed. Refer to Sections 3.5 and 4.2.8.

The specific objectives of the experiment were as follows:

1. Perform tests on the recovered asphalt residues to determine Absolute Viscosity at 140° F (60° C) and Penetration at 77° F (25° C), for evaluation of age hardening effects on the consistency of asphalts.
2. Perform Schweyer Rheometer Tests on the recovered ashpalt residues to determine viscosities at a constant power of 100 W/m^3 at two temperatures, 77° F (25° C) and 59° F (15° C), for evaluation of age hardening effects with reference to temperature conditions.
3. Conduct statistical analyses to establish the significance and relationship between test parameters. This will be done by performing analyses of variance and/or regression analyses. Specifically, the analyses will establish relationships and/or determine

(a) differences between the effects of the three exposure test conditions.

(b) differences between asphalts in their properties and response to age hardening.

8.2 Results

Results of the Absolute Viscosity Tests by asphalt, type of exposure and duration of exposure are tabulated in Appendix C-1. Results of the Penetration and Rheometer Tests have been tabulated in Appendix C-2. The results are presented on ten pages, one page corresponding to each of the asphalts tested. Test results include Constant Power Viscosities (n_J) at two temperatures and corresponding values of Shear Susceptibility (C).

Test measurements are made one per sample residue i.e., with single replicate. Although the Marshall specimens were fabricated, aged and tested for strength in replicates of three, recovery of asphalt from the replicate was done as a single combined residue, the sample representing an average of the effects on the asphalt in the individual specimens comprising the replicates. This was necessitated by resource constraints.

Effects of the three exposure conditions and durations of exposure of Absolute Viscosity and Penetration are presented in the form of bar charts in Figures 8.1 and 8.2 respectively, one chart corresponding to each of the asphalts.

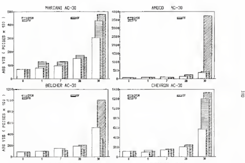

Figure 8.1 Effect of Type and Duration of Exposure on Absolute Viscosity

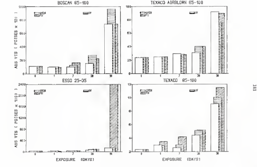

Figure 8.1--continued

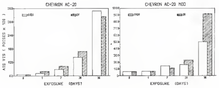

Figure 8.1--continued

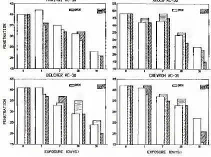

Figure 8.2 Effect of Type and Duration of Exposure on Penetration

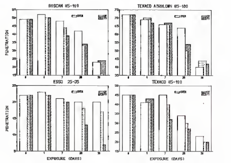

Figure 8.2--continued

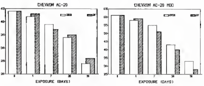

Figure 8.2--continued

8.3 Analysis of Results

8.3.1 Absolute Viscosity Test

8.3.1.1 Statistical Model. The test results as tabulated in Appendix C-1 were analyzed in a manner similar to that described in Section 7.3.1.1 ante. In consideration of the fact that only single replicate measurements were made, the following linear model is assumed for any single measurement in the experiment

$$y_{ijk} = m + A_i + B_j + C_k + (AB)_{ij} + (AC)_{ik} + (BC)_{jk} + e_{ijk} \qquad (8.1)$$

where

m = overall mean

A_i = effect of the i^{th} asphalt

B_j = effect of the j^{th} exposure condition

C_k = effect of the k^{th} exposure duration

$(AB)_{ij}$ = joint effect of the i^{th} asphalt and j^{th} exposure condition

$(AC)_{ik}$ = joint effect of the i^{th} asphalt and k^{th} exposure duration

$(BC)_{jk}$ = joint effect of the j^{th} exposure condition and k^{th} exposure duration

e_{ijk} = random error

8.3.1.2 Analysis of Variance. ANOVA was performed on the test results using SAS/STAT computer software. Results of ANOVA are summarized in Table 8.1. A probability of error (α level) of 0.05 was used which corresponds to a 95 percent level of confidence. Only the main effect DURATION is significant, and all other main and interaction effects are not. It there follows that

Table 8.1 Result of ANOVA on Absolute Viscosity

Source	df	MS	F-Value	P
ASPHALT	7	7.35E+10	1.79	0.1073
EXPOSURE	2	6.26E+10	1.53	0.2264
DURATION	4	1.14E+11	2.79	0.0350
ASPHALT * EXPOSURE	14	4.14E+10	1.01	0.4582
ASPHALT * DURATION	28	4.83E+10	1.18	0.2968
EXPOSURE * DURATION	8	6.04E+10	1.47	0.1886
ERROR	56	4.11E+10		

1. Since ASPHALT does not interact with the other two factors, the effects of asphalts can be compared by comparing the mean responses for the eight asphalts, averaged over the other two factors.
2. Since EXPOSURE does not interact with the other two factors, the relative effects caused by the three conditions of exposure can be assessed by comparing the mean responses for the three conditions, averaged over the other two factors.

8.3.1.3 Comparison of Means. A comparison of means for ASPHALT averaged over the other two factors, was performed using Duncan's test at a level of significance of 0.05. The results are summarized in Table 8.2. Similarly, a comparison of means for EXPOSURE averaged over the other two factors, was performed. These results are summarized in Table 8.3.

To differentiate between Chevron AC-20 and Chevron AC-20 Modified, a separate comparison of means was performed. The result has also been included in Table 8.2.

8.3.1.4 Regression Analysis. Preliminary analysis revealed that a relationship defined by the following model would best fit the data.

$$\log_{10} (\text{Dependent Response}) = \beta_0 + \beta_1 (\text{days}) + \text{Random Error} \qquad (8.2)$$

On this basis, data in Appendix C-1 was used to plot relationships between Absolute Viscosity at 140° F (60° C), expressed in Pa.s (log scale) and duration of exposure, for each asphalt separately. These are presented in Figure 8.3, wherein regression lines represent an average effect of the three types of exposure.

Using SAS/STAT software, regression analysis resulted in coefficients presented in Table 8.4.

Table 8.2 Grouping of Asphalts on the Basis of Absolute Viscosity

Asphalt Code	Means (Poises)	Grouping
SO	215981	A
AM	35219	B
CH	32641	B
BO	27419	B
BE	22408	B
MA	17260	B
TX	4751	B
TA	4003	B
OM	23280	C
01	14562	C

Note Means with the same letter are not significantly different (alpha = 0.05).

Table 8.3 Grouping of Exposure Type on the Basis of Absolute Viscosity

Type of Exposure	Means (Poises)	Grouping
Forced Draft	91102	A
Ultraviolet	24468	A
Oven	20810	A

Note. Means with the same letter are not significantly different (alpha = 0.05).

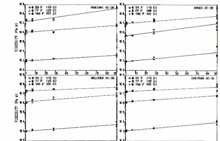

Figure A.3 Relation Between Viscosity and Duration of Exposure for Different Levels of Temperature

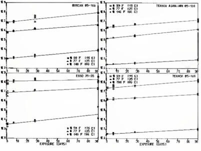

Figure 8.3--continued

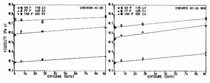

Figure 8.3--continued

Table B.4 Regression Coefficients for Relation Between Absolute Viscosity and Duration of Exposure

Asphalt Code	B_0	B_1	R^2
CH	4.07	0.010	0.95
BE	4.01	0.008	0.87
AM	3.92	0.011	0.76
MA	3.97	0.007	0.89
TX	3.45	0.006	0.91
TA	3.40	0.006	0.98
SO	4.52	0.012	0.68
BO	4.03	0.010	0.96
OI	3.89	0.007	0.94
DM	3.90	0.011	0.91

Note: $\log_{10}$ (Absolute Viscosity) = $B_0 + B_1$ (Exposure in Days)

8.3.1.5 General Observations and Findings. Results of ANOVA indicate that only the main effect DURATION is significant ($\alpha = 0.05$). Comparison of means indicate that

1. Measurements of Absolute viscosity do not reveal differences between the three types of exposure ($\alpha = 0.05$).
2. It is seen that Esso 25-35 stands significantly different ($\alpha = 0.05$) compared to the other asphalts on the basis of Absolute Viscosity.

The relationship between Absolute Viscosity and duration of exposure in days can be defined by a linear expression, the dependent variable being the common logarithm of the Absolute Viscosity. R-Square values range from 0.68 (for Esso 25-35) to 0.98 (for Texaco Airblown 85-100).

8.3.2 Penetration Test

8.3.2.1 Statistical Model. The test results from Appendix C-2 were analyzed in a manner similar to that done for Absolute Viscosity in Section 8.3.1.1.

8.3.2.2 Analysis of Variance. ANOVA was performed on the test results using SAS/STAT software. Results of ANOVA are summarized in Table 8.5. A probability of error (α level) of 0.05 was used, which corresponds to a 95 percent level of confidence. All main effects and the ASPHALT * DURATION interaction effect are significant. It therefore follows that

1. Since the factor ASPHALT interacts with the factor DURATION, it is appropriate to compare the ASPHALT means separately for each DURATION, averaged over the factor EXPOSURE. However, the

Table 8.5 Result of ANOVA on Penetration

Source	df	MS	F-Value	P
ASPHALT	7	1970.37	215.77	0.0001
EXPOSURE	2	58.80	6.44	0.0030
DURATION	4	1867.45	204.50	0.0001
ASPHALT * EXPOSURE	14	7.04	0.77	0.6949
ASPHALT * DURATION	28	32.31	3.54	0.0001
EXPOSURE * DURATION	8	10.23	1.12	0.3643
ERROR	56	9.13		

effects produced by long-term aging being of primary interest, comparisons may be restricted to the 90 day duration.

2. Since EXPOSURE does not interact with the other two factors, the relative effects caused by the three conditions of exposure can be assessed by comparing the mean responses for the three conditions, averaged over the other two factors.

8.3.2.3 Comparison of Means. A comparison of means for ASPHALT, at a DURATION of 90 days, averaged over the factor EXPOSURE was performed using Duncan's test at a level of significance of 0.05. The results are summarized in Table 8.6. Similarly, a comparison of means for EXPOSURE, averaged over the other two factors, was performed. These results are summarized in Table 8.7.

To differentiate between Chevron AC-20 and Chevron AC-20 Modified, a separate comparison of means was performed. These results have also been included in Table 8.6.

8.3.2.4 Regression Analysis. Preliminary analyses revealed that a relationship defined by the following model would best fit the data.

$$\text{Dependent Response} = \beta_0 + \beta_1 \text{ (days)} + \beta_2 \text{ (days)}^2 + \text{Random Error} \qquad (8.3)$$

On this basis, data in Appendix C-2 was used to plot relationships between Penetration and duration of exposure. These are presented in Figure 8.4, wherein regression lines represent an average effect of the three types of exposure.

Using SAS/STAT software, regression analyses resulted in coefficients presented in Table 8.8.

8.3.2.5 General Observations and Findings. Considering the significance ($\alpha = 0.05$) of asphalt, type and duration of exposure as also

Table B.6 Grouping of Asphalts for 80 Day Duration on the Basis of Penetration

Asphalt code	Mean	Grouping
TA	42.00	A
BE	23.33	B
MA	21.67	B C
CH	21.33	B C
AM	21.00	B C
TK	21.00	B C
BO	21.00	B C
SO	14.67	C
OM	30.50	D
OI	25.00	D

Note Means with the same letter are not significantly different (alpha = 0.05)

Table 8.7 Grouping of Exposure Type on the Basis of Penetration

Type of Exposure	Mean	Grouping
Oven	38.225	A
Ultraviolet	36.725	B
Forced Draft	35.825	B

Note: Means with the same letter are not significantly different (alpha = 0.05).

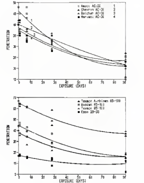

Figure 8.4 Relation Between Penetration and Duration of Exposure

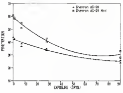

Figure B.4--continued

Table 8.8 Regression Coefficients for Relation Between Penetration and Duration of Exposure

Asphalt Code	β_0	β_1	β_2	R^2
CH	40.61	-0.281	0.0008	0.89
SE	39.32	-0.388	0.0023	0.87
AM	46.77	-0.600	0.0035	0.90
MA	38.19	-0.367	0.0020	0.89
TX	43.45	-0.581	0.0037	0.89
TA	70.63	-0.621	0.0034	0.93
SO	23.26	-0.293	0.0022	0.50
BO	49.41	-0.564	0.0028	0.92
DI	42.69	-0.373	0.0020	0.96
DM	59.73	-0.822	0.0056	0.98

Note

Penetration = $\beta_0 + \beta_1$ (Exposure in Days) + β_2 (Exposure in Days)^2.

the interaction of asphalt with duration, it can be stated that Penetration is a function of all three variables independently and when comparison of asphalts is done, for each duration separately, averaged over the types of exposure. Comparison of means for grouping of asphalts for 90 day duration on the basis of Penetration reveals that Texaco Airblown is significantly different (α = 0.05) from the other asphalts. Grouping of type of exposure indicates greater hardening is caused by ultraviolet and forced draft exposure, compared to Oven exposure.

The relationship between Penetration and duration of exposure in days can be defined by a polynomial expression of the second order. R-Square values start from 0.50 (for Esso 25-35), the others between 0.87 to 0.98.

8.3.3 Schweyer Rheometer Tests

8.3.3.1 Statistical Model. The test results from Appendix C-2 were analyzed in a manner similar to that done for Absolute Viscosity in Section 8.3.1.1 ante. The same linear model was used.

8.3.3.2 Analysis of Variance. ANOVA was performed on the constant power viscosity (η_c) corresponding to the test temperature of 77° F (25° C). This was chosen in preference to results at the test temperature of 59° F (15° C), since generally, viscosities measured at a higher temperature are likely to suffer less dispersion than those at a comparatively lower temperature. SAS/STAT software was used and results of ANOVA are summarized in Table 8.9. A probability of error (α level) of 0.05 was used, which corresponds to a 95 percent level of confidence. Main effects ASPHALT and DURATION are significant. None of the interaction effects are significant. It there follows that:

Table 8.9 Result of ANOVA on Constant Power Viscosity (η_J) at 77° F (25° C)

Source	df	MS	F-Value	P
ASPHALT	7	2.03E + 14	4.54	0.0005
EXPOSURE	2	7.04E + 13	1.58	0.2154
DURATION	4	3.62E + 14	8.12	0.0001
ASPHALT * EXPOSURE	14	4.63E + 13	1.04	0.4325
ASPHALT * DURATION	28	4.92E + 13	1.10	0.3676
EXPOSURE * DURATION	8	7.31E + 13	1.64	0.1344
ERROR	56	4.46E + 13		

1. Since ASPHALT does not interact with the other two factors, the asphalts can be compared by comparing the mean responses for the eight asphalts, averaged over the other two factors.
2. Since EXPOSURE does not interact with the other two factors, the relative effects caused by the three conditions of exposure can be assessed by comparing the mean responses for the three conditions, averaged over the other two factors.

8.3.3.3 Comparison of Means. A comparison of means for ASPHALT averaged over the other two factors, was performed using Duncan's test at a level of significance of 0.05. The results are summarized in Table 8.10. Similarly, a comparison of means for EXPOSURE averaged over the other two factors, was performed. These results are summarized in Table 8.11.

To differentiate between Chevron AC-20 and Chevron AC-20 Modified, a separate comparison of means was performed. These results have also been included in Table 8.10.

8.3.3.4 Regression Analysis. Preliminary analysis revealed that a relationship defined by Equation 8.2 would best fit the data. On this basis, data from Appendix C-2 was used to plot relationships between Constant Power Viscositites (η_J) at 77° F (25° C) and 59° F (15° C), and duration of exposure, for each asphalt separately. These are in Figure 8.3, wherein regression lines represent an average effect of the three types of exposure.

Using SAS/STAT software, regression analyses resulted in coefficients presented in Table 8.12, based on data from test run at 77° F (25° C).

Table 8.10 Grouping of Asphalts on the Basis of Constant Power Viscosity (η_j) at 77° F (25° C)

Asphalt Code	Means	Grouping
SO	12029684	A
AM	6299512	B
BE	3206135	B C
CH	2870794	B C
TX	2511152	B C
MA	2391314	B C
BO	1633718	B C
TA	466376	C

Asphalt Code	Means	Grouping
DM	1870355	D
DI	1735657	D

Note: Means with the same letter are not significantly different. (alpha = 0.05)

Table 8.11 Grouping of Exposure Type on the Basis of Constant Power Viscosity (η_j) at 77° F (25° C)

Type of Exposure	Means	Grouping
Forced Draft	5443070	A
Ultraviolet	3353645	A
Oven	2981618	A

Note: Means with the same letter are not significantly different (alpha = 0.05).

Table 8.12 Regression Coefficients for Relation Between Constant Power Viscosity (n_j) at 77° F (25° C) and Duration of Exposure

Asphalt Code	β_0	β_1	R^2
CH	6.16	0.008	0.94
BE	6.12	0.009	0.84
AM	5.66	0.015	0.73
MA	6.01	0.009	0.81
TX	6.16	0.007	0.89
TA	5.16	0.012	0.99
SO	6.84	0.006	0.63
BO	5.89	0.008	0.93
OI	5.88	0.009	0.82
OM	5.51	0.016	0.91

Note

$\log_{10}$ (CPV @ 25° C) = $\beta_0 + \beta_1$ (Exposure in Days)

8.3.3.5 General Observation and Findings. In view of the significance ($\alpha = 0.05$) of asphalt and duration it can be stated that Constant Power Viscosity (n_J) at 77° F (25° C) is a function of these two variables independently. As noted for Absolute Viscosity, Esso 25-35 stands significantly different ($\alpha = 0.05$) compared to the other asphalts, on the basis of Constant Power Viscosity.

The relationship between Constant Power Viscosity (n_J) at 77° F (25° C) and duration of exposure can be defined by a linear expression, the dependent variable being the common logarithm of the Viscosity. R-Square values range from 0.63 (for Esso 25-35) to 0.93 (for Texaco Airblown 85-100).

CHAPTER 9
RESULTS OF INFRARED ABSORPTION SPECTROSCOPY ON RECOVERED ASPHALT RESIDUES

9.1 Introduction

An experimental program to assess the effects of different aging conditions on Ketone Anhydride Development Factor (henceforth referred to as Ketone Factor) was devised and performed. Refer Sections 3.6 and 4.2.9.

The specific objectives of the experiment were as follows

1. Perform infrared spectral tests on the recovered asphalt residues to determine Ketone Factors for evaluating age hardening effects on the absorption characteristics of asphalts.
2. Conduct statistical analyses to establish significance and relationship between test parameters. This will be done by performing analyses of variance and/or regression analyses. Specifically, the analyses will establish relationships and/or determine
   (a) differences between the effects of the three exposure test conditions
   (b) differences between asphalts in their properties and response to age hardening
   (c) differences between two techniques of measurement to determine Ketone Factors.

8.2 Results

Results of the spectral tests by asphalt, type of exposure and duration of exposure are tabulated in Appendix D-1. Test measurements are one per sample residue i.e., single replicate. In Chapter 6, all spectral measurements were made with reference to the absorption at wavenumber of 1800 cm^{-1}. Noting the relative stability of the region around 1900 cm^{-1}, it was decided to now make all measurements with reference to the absorption at 1900 cm^{-1}. In order to improve the quality of spectral measurements, a sealed cell with 1 mm path length and sodium chloride windows was used. It may be recalled that a sealed cell with 0.1 mm path length was used in the work reported in Chapter 6.

As an alternative to the absorption band centering at 1600 cm^{-1} resulting primarily from aromatic carbon-carbon double bonds which was used as a reference measurement in Chapter 6, it was decided to evaluate the absorption band centering at 1375 cm^{-1} resulting primarily from carbon - methyl bond, a C-H scissoring band (48). Ketone Factors calculated with respect to both these reference measurements have been included in the tabulations.

Comparison of the two measures of relative absorbance, one at 1600 cm^{-1} and the other at 1375 cm^{-1}, has been presented as bar graphs in Appendix D-2. One bar graph represents one asphalt with the absorbance levels shown at four durations of aging, and in turn, for the three types of exposure.

9.3 Analysis of Results

9.3.1 Statistical Model

The test results as tabulated in Appendix D-1 were analyzed as results of a factorial experiment comprising of eight asphalts (ASPHALTS), three conditions of exposure (EXPOSURE), five levels of duration (DURATION) and two types of measurements (MEASURE). ASPHALT, EXPOSURE, DURATION and MEASURE are regarded as fixed effects, the experiment has 240 treatment combinations.

The following linear model is assumed for any single measurement in the experiment.

$$\begin{aligned} y_{ijkl} = m &+ A_i + B_j + C_k + D_l \\ &+ AB_{ij} + AC_{ik} + AD_{il} \\ &+ BC_{jk} + BD_{jl} + CD_{kl} \\ &+ \varepsilon_{ijkl} \end{aligned} \tag{9.1}$$

where notations are on similar lines as those described after Equation 7.1.

9.3.2 Analysis of Variance

Analysis of variance (ANOVA) was performed on the test data using SAS/STAT computer software. Results of ANOVA on the Ketone Factors are summarized in Table 9.1. A probability of error (α level) of 0.05 was used. All main effects are significant and except for EXPOSURE * MEASURE, all interaction effects are significant, since P values are less than 0.05. It therefore follows that

1. Comparison of ASPHALT must be made at each EXPOSURE, for each level of DURATION by type of MEASURE.
2. Comparison of EXPOSURE must be made by ASPHALT, for each level of DURATION averaged over the factor MEASURE.

Table 9.1 Result of ANOVA on Ketone Factors

Source	df	MS	F-Value	P
Asphalt	7	2.16	265.04	0.0001
Exposure	2	0.07	8.62	0.0003
Duration	4	5.00	612.21	0.0001
Measure	1	0.23	28.67	0.0001
Asphalt * Exposure	14	0.03	3.29	0.0001
Asphalt * Duration	28	0.11	14.04	0.0001
Asphalt * Measure	7	0.31	38.48	0.0001
Exposure * Duration	8	0.04	4.54	0.0001
Exposure * Measure	2	0.003	0.39	0.6808
Duration * Measure	4	0.17	21.06	0.0001
Error	162	0.008		

3. Comparison of MEASURE must be made by ASPHALT, for each level of DURATION averaged over the factor EXPOSURE.

9.3.3 Comparison of Means

A comparison of means for ASPHALT, by EXPOSURE, by DURATION and by MEASURE will not be possible since the source of error will have zero degrees of freedom. This is because of single replicate measurements. To overcome this problem, it was decided to ignore the significance of effect ASPHALT * MEASURE and perform comparisons for ASPHALT, by EXPOSURE and by DURATION but averaged over MEASURE. This was done by Duncan's test at a level of significance of 0.05. The effects at 90 days DURATION were subjected to a detailed study in preference to those at shorter durations of exposure. The results are summarized in Table 9.2. Similarly, a comparison of means for EXPOSURE, for each ASPHALT at 90 days DURATION, averaged over the factor MEASURE, was performed using Duncan's test at the same level of significance. These results are summarized in Table 9.3. Finally, comparisons on the same lines, for the two types of MEASURE, for each ASPHALT at 90 days DURATION, averaged over the factor EXPOSURE are presented in Table 9.4.

To differentiate between Chevron AC-20 and Chevron AC-20 Modified on the basis of Ketone Factors, a separate comparison of means was performed for the 90 day data. These results have also been included in Tables 9.2 through 9.4.

9.3.4 Regression Analysis

Preliminary analyses revealed that a relationship defined by the following model would best fit the data:

$$\text{Dependant Response} = \beta_0 + \beta_1\,(\text{days}) + \beta_2\,(\text{days})^2 + \text{Random Error} \qquad (9.2)$$

Table 9.2 Grouping of Asphalts by Type of Exposure for 80 Day Duration on the Basis of Ketone Factors

Forced Draft

Asphalt Code	MA	BE	TX	AM	SO	CH	BO	TA
Means	2.83	2.59	2.49	2.43	2.21	1.83	1.70	1.14
Grouping	A	A	A	A	A	C	C	C
		B	B	B	B	B	B	

Oven

Asphalt Code	TX	MA	BE	SO	AM	BO	CH	TA
Means	2.48	2.28	2.28	2.10	1.88	1.71	1.68	1.11
Grouping	A	A	A	A				D
		B	B	B	B			
				C	C	C	C	

Asphalt Code	DI	DM
MEANS	2.68	2.27
Grouping	A	A

Ultraviolet

Asphalt Code	BE	MA	TX	SO	AM	BO	CH	TA
Means	2.61	2.51	2.46	2.08	1.92	1.74	1.70	1.29
Grouping	A	A	A	A	A			
			B	B	B	B	B	
					C	C	C	C

Asphalt Code	DI	DM
Means	2.74	2.43
Grouping	A	A

Note Means with the same letter are not significantly different (alpha = 0.05)

Table 9.3 Grouping of Type of Exposure by Asphalt for 90 Day Duration on the Basis of Ketone Factors

Asphalt Code	Means		
	Forced Draft	Ultraviolet	Oven
CH	1.826 (A)	1.699 (A)	1.690 (A)
RE	2.592 (A)	2.609 (A)	2.275 (A)
AM	2.434 (A)	1.923 (A)	1.861 (A)
MA	2.929 (A)	2.511 (A)	2.280 (A)
TX	2.490 (A)	2.461 (A)	2.483 (A)
TA	1.141 (A)	1.266 (A)	1.109 (A)
SO	2.210 (A)	2.040 (A)	2.103 (A)
80	1.696 (A)	1.735 (A)	1.714 (A)
OI	Not Tested	2.742 (A)	2.675 (A)
DM	Not Tested	2.425 (A)	2.268 (A)

Note Row means with the same letter are not significantly different (alpha = 0.05).

Table 9.4 Grouping of Types of Measure by Asphalt for 90 Day Duration on the Basis of Ketone Factors

Asphalt Code	KF1	KF2
AM	1.86 (A)	2.30 (A)
BE	2.11 (A)	2.87 (B)
BO	1.76 (A)	1.67 (B)
CH	1.58 (A)	1.90 (B)
MA	2.29 (A)	2.86 (B)
SO	2.03 (A)	2.23 (B)
TA	1.26 (A)	1.09 (B)
TX	2.44 (A)	2.52 (B)
DM	2.14 (A)	2.55 (A)
DI	2.41 (A)	3.00 (B)

Note: Row means with the same letter are not significantly different (alpha = 0.05)

On this basis, data in Appendix D-1 was used to plot relationships between Ketone Factors (calculated with reference measurements at 1600 cm^{-1}) and duration of exposure. These are presented by asphalt and by type of exposure in Figure 9.1. However, one regression per asphalt type was developed, representing an average effect of the three types of exposure.

Using SAS/STAT software, regression analyses resulted in coefficients presented in Table 9.5.

9.4 General Observations and Findings

The main effects are significant ($\alpha = 0.05$) which confirms that asphalt, type and duration of exposure and the technique used to measure the response, all influence Ketone Factors independently. They also have an influence, in combination, except the interaction between the type of exposure and technique used to measure the response.

Comparisons of means ($\alpha = 0.05$) done at a 90 day duration indicate that

1. The three types of exposures result in responses which are not different.
2. The two techniques of measurement result in responses which are different in the case of asphalts coded as BE, BD, CH, MA, SO, TA, TX.

The relationship between Ketone Factor (with reference to absorption at 1600 cm^{-1}) and duration of exposure in days can be defined by a polynomial expression of the second order. R-Square values range from 0.78 to 0.98.

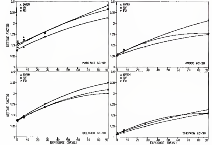

Figure 9.1 Relation Between Ketone Factors and Duration of Exposure

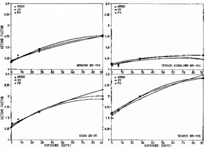

Figure 9.1--continued

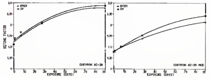

Figure 9.1--continued

Table 9.5 Regression Coefficients for Relation Between Ketone Factors (reference measurements at 1600 cm^{-1}) and Duration of Exposure

Asphalt Code	β_0	β_1	β_2	R^2
CH	1.069	0.0088	-0.000036	0.98
BE	1.372	0.0138	-0.000062	0.97
AM	1.272	0.0108	-0.000048	0.91
MA	1.461	0.0118	-0.000028	0.92
TX	1.577	0.0160	-0.000071	0.95
TA	1.106	0.0056	-0.000042	0.78
SO	1.308	0.0140	-0.000069	0.97
RO	1.182	0.0103	-0.000043	0.99
DI	1.624	0.0186	-0.00011	0.98
DM	1.396	0.0136	-0.000059	0.98

Note:

$$\text{Ketone Factor} = \beta_0 + \beta_1 \text{ (days)} + \beta_2 \text{ (days)}^2$$

CHAPTER 10
INTERPRETATION OF FIELD DATA

10.1 Introduction

The field testing program involved the acquisition of samples and cores from three selected sections of newly laid asphalt concrete pavements in Hernando County in the state of Florida. The locations of these sections are fully described in Figures 10.1 and 10.2. Characteristics of the pavements have been summarized in Table 10.1.

10.2 Field Sampling and Testing

The work shown below was performed at the plant site.

1. Four quarts of the original asphalt (AC-20) was sampled from the hot storage tank to be used for measurement of viscosities and penetration.
2. Two box samples, each approximately 3 kilograms of the hot mixture were sampled from the pugmill (truck) and the paving machine, for asphalt recovery, from each of the sites. Average temperatures of the hot mix were as follows

    (a) I-75 Pugmill 293° F
    (b) I-75 Paver 285° F
    (c) US-301 Pugmill 285° F
    (d) US-301 Paver 275° F

On the I-75 section, the roadway density control strip worksheet indicated that 99.3 percent of the laboratory density was obtained, with

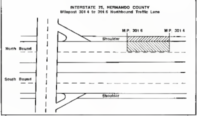
INTERSTATE 75, HERNANDO COUNTY
Milepost 301.4 to 301.6 Northbound Traffic Lane
M.P. 301.6
M.P. 301.4
Shoulder
North Bound
South Bound
Shoulder

Figure 10.1 Location Plan of Interstate-75 Test Sections

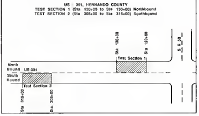

Figure 10.2 Location Plan of US-301 Test Sections

Table 10.1 Characteristics of Test Pavements in Hernando County

Test Road	Mile Post/Station Number	Year*	Thickness of Surface Layer (in)
I-75	301.4 to 301.6 Northbound Lane	1985	2.0 (Type S-I Mix)
US-301 Section 1	130 + 00 to 120 + 00 Northbound Lane	1986	1 1/4 (Type S-III Mix)
US-301 Section 2	305 + 00 to 315 + 00 Southbound Lane	1986	1 1/4 (Type S-III Mix)

* Year represents the latest year of reconstruction.

an average core density of 134.8 pcf. On the US-301 Test Section No. 1, the control strip did not meet the required 95 percent of laboratory density. It was 91.8 percent with an average core density of 128.3 pcf. An additional test section was scheduled on the southbound lane where the control strip density indicated that 98.8 percent of the laboratory density was obtained with an average core density of 137.8 pcf. This section was designated as Test Section No. 2 and used for detailed study.

Evaluation of the asphalts recovered from cores taken out from the two pavement sections was done periodically. Cores were extracted both from wheel paths from between wheel paths and air void contents determined. The core samples of asphalt concrete were heated and broken down for extraction using Method B (Reflux) of ASTM D 2172 for Quantitative Extraction of Bitumen from Bituminous Paving Mixtures. The asphalt cement was recovered using the Abson method, ASTM D 1856.

The following test were performed on the recovered asphalts

1. Absolute Viscosity at 77° F (25° C)
2. Penetration at 77° F (25° C)
3. Spectral analysis.

The sampling, coring, recovery, TFOT/RTFOT procedures and the physical tests on the asphalts and residues were performed by the personnel of the Bureau of Materials and Research, Florida Department of Transportation, under the supervision of Messrs. Ken Murphy, Phil Eunice and Ed Leitner.

10.3 Hardening Trends

Initially, Penetration at 77° F (25° C) and Absolute Viscosity at 140° F (60° C) were determined for the original asphalts. Thereafter, the original asphalts were subjected to TFOT and RTFOT procedures at 285° F, 325° F and 365° F and Absolute Viscosity and/or Penetration determined on the residues. Tables 10.2 and 10.3 summarize the results for the I-75 and US-301 test sections respectively.

Results of the tests on recovered samples from I-75 are presented in Table 10.4 and those in respect of US-301 are presented in Table 10.5. Absolute Viscosity, Penetration and Ketone Factor have all been plotted in the form of scatter graphs, for the two test pavements, against duration of aging. These are presented as Figures 10.3 to 10.8 respectively.

The air void contents were computed for the I-75 project after 90 days and 6 months of traffic exposure. The average air void content was 5.8 percent at 90 days, reducing to 4.8 percent at 6 months, when measured on wheel path areas. Between wheel paths, the figures were 6.1 and 5.5 respectively. On the US-301 project, air void contents were computed after 14 days and 90 days of traffic movement. In wheel path areas, the figure was 6.6 percent, reducing to 3.5 percent. Between wheel path areas started with 9.8 percent, reducing to 3.4 percent.

For purposes of discussion, it may be reasonable to reckon the air voids contents to be around five percent for both the test pavements.

Figures 10.3, 10.4 and 10.6 confirm that the TFOT procedure run at 325° F yields residues which closely represent the hardening characteristics of the asphalt residues recovered from mixtures discharged at the pugmill and prior to paving operations. The pugmill temperatures, (it may be re-called) were in the region of 290° F.

Table 10.2 Viscosity and Penetration Tests on Asphalts and Residues from I-75 Project

Test	Temperature	Kinematic Viscosity (Cs)	Absolute Viscosity (Poises)	Kinematic Viscosity Ratio	Absolute Viscosity Ratio
TFOT	285° F	517	3539	1.2	1.7
TFOT	325° F	641	6382	1.5	3.0
TFOT	365° F	939	15663	2.3	7.4
RTFOT	285° F	602	5467	1.4	2.6
RTFOT	325° F	736	9307	1.8	4.4
RTFOT	365° F	993	18660	2.4	8.8

Type of Asphalt: Chevron AC-20
Kinematic Viscosity @ 275° F: 416 Cs
Absolute Viscosity @ 140° F: 2111 Poises
Penetration @ 77° F: 75

Table 10.3 Viscosity and Penetration Tests on Asphalts and Residues from US-301 Project

Test	Temperature	Kinematic Viscosity (Cs)	Absolute Viscosity (Poises)	Pene-tration	Kinematic Viscosity Ratio	Absolute Viscosity Ratio
TFOT	285° F	530	4002	57	1.3	1.8
TFOT	325° F	653	6224	46	1.6	2.8
TFOT	365° F	878	13011	38	2.1	5.8
RTFOT	285° F	625	5601	49	1.5	2.5
RTFOT	325° F	754	9316	42	1.8	4.1
RTFOT	355° F	945	16682	36	2.2	7.4

Type of Asphalt, Marathon AC-20
Kinematic Viscosity @ 275° F 424
Absolute Viscosity @ 140° F 2246
Penetration @ 77° F 73

Table 10.4 Results of Tests on Samples From Interstate - 75

Specimen BR #	Location	Age in days or months	Pen at 77° F (25° C)	Absolute Viscosity at 140° F (60° C) (Poises)	Ketone Factor	Average Percentage Air Voids
3248	-	Original	75	2111	1.0	
-	-	Pugmill	49	6287	-	
-	-	Paver	47	10416	-	
3333	WP	10 days	39	9984	1.491	
3334	WP	10 days	36	18156*	1.514	
3335	WP	10 days	34	19058*	1.557	
3340	BWP	10 days	49	6225	1.290	
3341	BWP	10 days	50	6185	1.332	
4375	WP	90 days	35	12081	-	
4376	WP	90 days	40	11692	1.452	WP 5.6
4377	WP	90 days	36	13516	1.574	
4378	WP	90 days	37	13312	1.545	
4380	BWP	90 days	32	18611	1.572	BWP 6.1
4381	BWP	90 days	43	8407	1.440	
4382	BWP	90 days	30	30894*	1.709	
4781	WP	6 months	41	8727	1.377	WP 4.9
4782	BWP	6 months	34	14061	1.520	BWP 5.5
6442	WP	12 months	41	8002	1.373	
6443	WP	12 months	39	8356	-	
6444	WP	12 months	39	9446	1.416	
6445	BWP	12 months	34	14380	1.586	
6446	BWP	12 months	35	14308	-	
6447	BWP	12 months	38	9701	1.478	
0444	WP	18 months	48	6342	1.270	
0442	BWP	18 months	34	14539	1.511	

Note: * Data points ignored while plotting relationships.

Table 10.5 Results of Tests on Samples from US - 301 (Section No. 2)

Specimen HR #	Location	Age in days or months	Pen at 77° F (25° C)	Absolute Viscosity at 140° F (60° C) (Poises)	Ketone Factor	Average Percentage Air Voids
3620	-	Original	73	2246	1.0	
-	-	Pugmill	53	5690	-	
-	-	Paver	38	7980	-	
4122	WP	14 days	35	14269	1.565	WP 6.6
4123	BWP	14 days	56	7466	1.559	BWP 9.8
4786	WP	90 days	38	10165	1.621	WP 3.5
4787	BWP	90 days	35	17234	1.575	BWP 3.4
5451	WP	6 months	40	8869	1.530	
5452	WP	6 months	41	7407	1.367	
5453	WP	6 months	37	10166	1.661	
5448	BWP	6 months	39	10300	1.478	
5449	BWP	6 months	40	11340	1.589	
5450	BWP	6 months	38	8797	1.539	
0123	WP	12 months	39	10231	1.518	
0124	WP	12 months	38	11233	1.617	
0125	BWP	12 months	35	14500	1.704	
0126	BWP	12 months	36	13058	1.830	
1307	BWP	18 months	27	36559*	-	
1310	BWP	18 months	48	6840	-	
1312	WP	18 months	42	8870	-	

Note: * Data point ignored while plotting relationships.

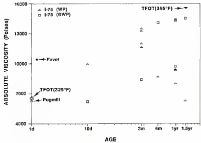

Figure 10.3 Relation Between Absolute Viscosity and Duration of Field Aging on I-75

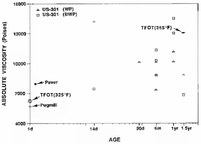

Figure 10.4 Relation Between Absolute Viscosity and Duration of Field Aging on US-301

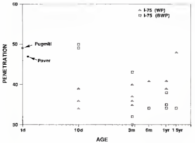

Figure 10.5 Relation Between Penetration and Duration of Field Aging on I-75

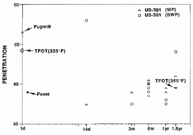

Figure 10.6 Relation Between Penetration and Duration of Field Aging on US-301

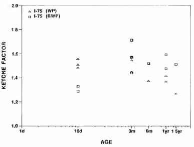

Figure 10.7 Relation Between Ketone Factor and Duration of Field Aging on I-75

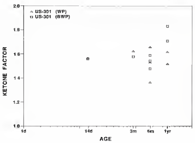

Figure 10.8 Relation Between Ketone Factor and Duration of Field Aging on US-301

However, Figures 10.3 to 10.7 indicate that variations in air void contents of core samples and possibly testing variations produced substantial scatter of data points. This may also be associated with the thicknesses of the layer (2 in. and 1 1/4 in.). Trends may begin to establish over a longer time period and reliable relationships would then be possible.

10.4 Comparisons of Field and Laboratory Aging

The Chevron AC-20 used in the laboratory study closely corresponds to the Chevron AC-20 used on the I-75 project and the Marathon AC-20 used on the US-301 project, when comparing original properties and properties of TFOT/RTFOT residues. It will not be unreasonable therefore, to establish equivalence of field and laboratory data on this basis.

Initial analyses revealed that a 28 day aging period in the laboratory would represent an approximate duration of 12 months or more of pavement aging in the field. Using this as a starting point, a comparison of acquired data is presented in Table 10.6. The figures for laboratory data are an average of the responses under the two test conditions of exposure. To balance out the effects of scatter in the data from the field, averages have been taken over data for 6, 12 and 18 months, the average value considered representative of conditions at 12 months. Air voids in wheel paths would diminish with pavement densification and so it is preferable to base comparisons on data from areas between wheel paths. It may be recalled that the Chevron AC-20 specimens were compacted to an average air void content of 3.94 percent.

The comparison in Table 10.6 confirms that a period of 28 days aging in the laboratory would result in a state of hardening which

Table 10.6 Comparison of Hardening Effects due to Field and Laboratory Aging

Property	I-75 1 Year field aging*	US-301 1 Year field aging@	Laboratory aging£ 28 days
Absolute Viscosity at 140° F (Poises)	13400	10806	15523
Penetration at 77° F	35	39	36
Ketone Factor	1.53	1.63	2.0

* Chevron AC-20

@ Marathon AC-20

£ Chevron AC-20

closely approximates the conditions reached after 12 months, when the unit of measure is Penetration. However, longer durations of aging in the field would be necessary to bring the Absolute Viscosities and Ketone Factors to the level of 28 day aging in the laboratory. It is probable that another six to twelve months of field aging may be necessary to see the Absolute Viscosities and Ketone Factors reach the levels at 28 days laboratory aging.

CHAPTER 11
ANALYSIS AND DISCUSSION OF RESULTS

11.1 Introduction

In the previous chapters, some general observations and findings were presented immediately after the respective analyses. This portion of the study links and interrelates some of the previously presented observations and findings by the establishment of correlations, equivalences and comparisons between major parameters of interest. A discussion is presented on infrared spectroscopic techniques for the evaluation of asphalt hardening. Finally, a framework for improved specifications is suggested.

11.2 TFOT and RTFOT Procedures

Page et al. (11) have noted that the change in properties (after artificial aging by the TFOT) of the asphalt binder is definitely related to the degree of age hardening that will occur over a period of time in the field. They suggested that the TFOT procedure be performed at different temperatures for the purpose of characterizing loss and hardening, which ultimately could result in modification of existing specifications.

Study of the changes in properties due to TFOT and RTFOT procedures discussed earlier in Chapter 5, has demonstrated that higher oven temperatures result in increased differentials in properties. For example, the change in Viscosity Ratio between 325° F and 365° F is greater than that between 285° F and 325° F. In other words, a higher test temperature like 365° F would magnify the potential to suffer hardening and might be a better indicator of performance, as compared to the present level of 325° F.

The limited test data presented in Figures 10.3, 10.4 and 10.6 confirm that the TFOT procedure run at 365° F yields residues which would correspond to aging of approximately 18 months in the field. It is probable that 28 day aging at 140° F in the laboratory, TFOT procedure at 365° F and 18 months aging in the field, would result in approximately the same hardening effects on a typical paving grade asphalt, in Florida. This comparison, however, is a rough estimate and would obviously depend on many factors.

It has been seen in Chapter 5 that for an oven temperature of 365° F, TFOT and RTFOT processes are not different from one another ($\alpha = 0.05$). No particular reason therefore exists to favor the RTFOT process over the TFOT process, particularly if the test temperature is raised to 365° F. In this context, work reported by Kemp and Predoehl (17) is of interest, wherein a new procedure has been developed which simulates to a reasonable degree, what is apparently the most severe California weathering condition, a desert climate. The new test was based primarily on the Rolling Thin Film procedure with the difference that the temperature was lowered to 235.4° F (113° C) and the weathering period extended to 168 hours (7 days). Lowering the temperature caused the asphalt to build up in the bottles and this problem was addressed by tilting the oven so that the front was slightly higher. The method as proposed, was designated California Tilt-oven Asphalt Durability Test and is recommended by them to predict asphalt hardening caused in two years in one of their typical desert test sites. The lowering of temperature and extension of the weathering period are both positive features of the test.

11.3 Relationships Between Mixture Properties and Asphalt Viscosity

11.3.1 Indirect Tensile Strength

The average tensile strengths at 77° F (25° C), from tabulations in Appendix 9-1 were plotted against corresponding Constant Power Viscosities (n_j) at 77° F (25° C). The relationship is illustrated in Figure 11.1 and can be defined by the equation

$$S_t = \beta_0 + \beta_1 \log_{10}(n_j) + \beta_2[\log_{10}(n_j)]^2 \qquad (11.1)$$

where

S_t = Indirect Tensile Strength, Pa

n_j = Constant Power Viscosity, Pa.s

$\beta_0 = 755.40$, $\beta_1 = -274.65$, $\beta_2 = 28.50$

$R^2 = 0.90$

Ruth, Roque and Puyena (49) have developed a relationship from an extensive test program in Florida. The prediction equation is

$$S_t = 4217.94\ (n_j)^{0.3570} \qquad (11.2)$$

where

S_t = Indirect Tensile Strength, Pa

$n_j < 1.16$ E8 Pa.s.

Although the loading rate used by Ruth et al. was 0.05 in/min as against 2.0 in/min used in this study, the predicted values, as illustrated in Figure 11.1, closely follow the trend of results from this study. The higher rate of loading has resulted in correspondingly higher values of

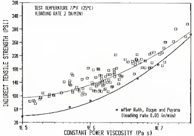

Figure 11.1 Relation Between Indirect Tensile Strength and Asphalt Viscosity

strength, the effects of rate of loading diminishing with increased viscosity. This is reasonable and anticipated, since creep components of failure diminish with increased viscosity of the binder.

11.3.2 Resilient Modulus

The average moduli at 77° F (25° C) calculated on the basis of both instantaneous recoverable and total recoverable deformations from tabulations in Appendix B-2 were plotted against corresponding Constant Power Viscosities (η_3) at 77° F (25° C). The linear relationship is illustrated in Figure 11.2 and can be defined by the equation

$$\text{Modulus} = \beta_0 + \beta_1 \log_{10}(\eta_3) \qquad (11.3)$$

where the parameter estimates are

	Instantaneous	Total
β_0	89111	-44789
β_1	35289	40889
R^2	0.48	0.66

Some scatter in the data, which may be attributable to the inherent limitations in the diametral test notwithstanding, a clear trend emerges with moduli increasing linearly with binder viscosity. The near parallel regression lines on the basis of instantaneous and total recovery are notable. It may be recalled that the test procedure adopted for this study used a cyclic loading of 1 cycle/sec with load duration of 0.1 second.

In an identical test program completed recently by Manzione (50), a cyclic loading of 2 cycles/sec was used with a load duration of 0.1 second. However, the specimens tested in that study were cores from airfield pavements which had aged substantially, viscosities running well above 10^7 Pa.s. Using the relationship proposed by Manzione and inserting the appropriate percentage air voids content, a predictor line is placed on Figure 11.2. Although the line is extrapolated downwards and outside Manzione's database, the approximation is satisfactory, particularly in the region of 10^7 Pa.s. At lower viscosities, moduli depend more on aggregate properties than on binder characteristics and therefore the divergence in moduli is perhaps acceptable.

11.3.3 Fracture Energy

The average fracture energies at 77° F (25° C) from tabulations in Appendix B-3 were plotted against corresponding Constant Power Viscosities (η_3) at 77° F (25° C). The relationship is illustrated in Figure 11.3. Scatter in the data may be attributable to the relatively high temperature of the test and consequent lower viscosities, at which conditions, the tests were performed. With increasing viscosity, response of the asphalt would be better isolated from the characteristics and performance of the aggregates matrix, resulting in lesser variability in the energy measurements.

11.4 Comparison of Laboratory Exposure Types

Conventional oven, ultraviolet chamber and forced draft oven were evaluated by measuring strength, consistency and IR spectral responses at a level of significance of 0.05. Indirect Tensile Strength Tests results indicated that certain asphalts could harden more in a forced draft environment compared to the other two. Effects caused by the ultraviolet and conventional oven are about the same. Penetration tests indicated that greater hardening is caused by ultraviolet and forced draft exposure, as compared with oven exposure. IR Spectral test results rated the three types of exposure as causing near similar responses.

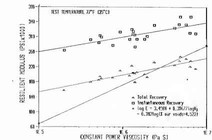

Figure 11.2 Relation Between Resilient Modulus and Asphalt Viscosity

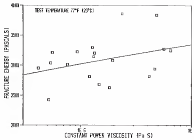

Figure 11.3 Relation Between Fracture Energy and Asphalt Viscosity

In general, it therefore emerges that at a duration of exposure of 90 days, the forced draft oven can cause a marginally higher response in certain parameters, compared to the ultraviolet and oven exposures. Since the average air void content in the specimens was approximately 5 percent, the limited effect of the draft appears reasonable. It is possible that higher air voids would increase the effect of the draft. Nonetheless, trends in the various graphical relationships presented earlier do suggest that for durations of 90 days and beyond, the differences in response caused by forced draft would further increase and could result in comparisons which are statistically significant at the 0.05 level.

The effects of ultraviolet exposure might be more predominant on the outer periphery of the specimens. The interiors would be relatively less influenced and so the effects would be diluted when the whole specimen is subjected to recovery of the asphalt. This appears to be one of the reasons for statistical equivalence between all responses except Penetration, caused by ultraviolet and oven exposures.

It therefore follows that an effective simulated aging process for evaluating mixtures could well be a combination of all three exposure types. This would best simulate the environment in the field where the effects of heat, light and air are experienced. The ultraviolet chamber, modified to permit a rated airflow, uniformly diffused and streaming upwards, would be an ideal environment for testing Marshall type specimens, cores, briquettes and so on.

11.5 Effect of Natural Weathering

Marshall specimens which were subjected to natural weathering over a period of six months were tested for Indirect Tensile Strength at 77° F (25° C). Absolute Viscosity at 140° F (60° C), Penetration at 77° F (25° C) and IR spectral tests were run on the recovered asphalt residues. Table 11.1 summarizes the results obtained.

Using the regressed relationships obtained earlier, between Indirect Tensile Strength, Absolute Viscosity, Penetration and Ketone Factor and duration of exposure, it is possible to obtain the equivalence between six months natural weathering and duration of laboratory aging. Table 11.2 presents the computed equivalences.

It is seen that six months of natural weathering could bring about changes which correspond to average laboratory durations of aging varying from 16.2 to 36.2 days, depending upon the type of test used. The mean of the four column averages in Table 11.2 works out to 26.4. Ketone Factors appear to increase rapidly with initial aging and slow down subsequently, which has resulted in comparatively smaller values of equivalence in days, corresponding to six months of natural weathering. Leaving aside the computed value of 16.2 days for Ketone Factor in Table 11.2, the mean of the three column averages works out to 29.8 days, which is approximately equal to say 28 days.

It was brought out earlier in Section 10.4 and Section 11.4 that 28 day aging in the laboratory and 12 to 24 months months aging in the field would probably result in approximately identical hardening effects. Natural weathering of Marshall specimens for a period of six months also results in hardening effects which are approximately equivalent to 28 day aging in the laboratory. In other words, Marshall

Table 11.1 Results of Tests After Six Months of Natural Weathering

Asphalt Code	Indirect Tensile Strength (psi)	Absolute Viscosity (poises)	Penetration	Ketone Factor
CH	150.62	32004	29	1.16
BE	160.69	21207	30	1.62
AM	169.22	16008	34	1.48
MA	168.30	99950@	33	1.64
TX	169.73	4536	30	1.77
TA	109.11	4162	63	1.16
SO	252.75	70574	17	1.49
BO	161.17	30860	32	1.41

@ result appears erroneous, hence ignored in analysis

Table 11.2 Equivalence Between 6 Months Natural Weathering and Aging in Laboratory

	Equivalent Laboratory Aging in Days Based On			
Asphalt Code	Indirect Tensile Strength	Absolute Viscosity	Penetration	Ketone Factor
CH	22.9	43.5	47.8	10.8
BE	27.5	39.6	29.01	19.7
AM	14.8	25.8	24.9	21.3
MA	15.8	-	15.4	15.8
TX	19.5	34.4	28.2	12.8
TA	37.2	36.6	35.2	10.5
SO	18.6	27.4	26.7	13.9
BD	24.5	45.9	38.1	24.7
Average	22.6	36.2	30.7	16.2

specimens allowed to weather naturally for six months would harden approximately two to four times as much as the mixtures when placed and compacted as a pavement layer. This is understandable considering the area of surface exposed to weather in a Marshall specimen compared to a core of similar dimensions extracted from the pavement.

11.6 Assessment of Ketone Factor

Analysis of spectra requires measurements which are relatively simple and capable of identifying and following the investigated responses. Ratios of absorbances at two wavenumbers, one of which remains relatively stable and constant appears to be a viable technique. This approach has been endorsed by Conway, Norris and Bodwell (51) who have also referred to other publications wherein ratios on data obtained at two different wavelengths for estimating the composition of materials have been used. Interestingly, this approach has also been used recently in the development of a compact instrument for the estimation of body composition in humans. The principle is called infrared interactance and is based on the effects of light absorption, reflection and near-infrared spectroscopy (51). In fact, earlier research conducted by the United States Department of Agriculture in the area of near infrared reflectance and transmittance has led to the development of the infrared interactance method (51).

On the basis of this study, it emerges that Ketone Factor is a useful measure to follow changes in the level of oxidation. The technique to quantify such changes as ratios and factors is a simple and comparatively reliable method. Reference measurements at 1600 cm^{-1} were compared to those at 1375 cm^{-1}. Analysis of variance reveals no interaction between the technique of measurement and type of exposure. In other words, when comparing the effects due to the three types of exposure, it does not matter which technique of measurement is used. This is a good basis to conclude that one technique of measurement is as good as the other. However, it was seen that the peak at 1600 cm^{-1} was better and more typically formed but the peak at 1375 cm^{-1} was inconsistent in shape and intensity. Further, the presence of other features in the 1375 cm^{-1} region could cause some confusion to an inexperienced analyst.

Appendix 0-2 demonstrates the differences in absorbances as measured by the two alternatives. Except for differences in the absolute values of Ketone Factors calculated by the two techniques, there appears no reason to prefer 1375 cm^{-1} over 1600 cm^{-1} as the frequency for the reference measurement.

Figure 9.1 clearly demonstrates what obviously appears to be a limitation in spectral measurements. Increases in Ketone Factors would be pronounced over initial periods of hardening, thereafter changes in Ketone Factors tend to diminish. This may result in insensitivity of the parameter to detect hardening, which otherwise would be seen when running conventional tests. This suggests that Ketone Factor would be more useful in detecting short term hardening of residues from accelerated weathering tests and in order to make it more critical in its ability to detect change, it is suggested that straight asphalt residues be subjected to this kind of test, in preference to residues recovered from mixtures. The latter may sometimes carry residual effects of solvents and minerals which could detract from the integrity of the obtained spectra.

11.7 IR Spectral Evaluation of Hardening

From results and discussions presented earlier, it becomes clear that infrared spectroscopic studies can be used effectively in the evaluation of asphalt binders. The question remains as to what the Ketone Factor physically represents in terms of conventional parameters. In order to assess this, a multiple regression analysis was performed, the objective being to relate Ketone Factor to changes in Absolute Viscosity at 140° F (60° C), Penetration at 77° F (25° C) and Constant Power Viscosity (η_{J}) at 59° F (15° C). Since changes in these parameters are of interest more than the parameters per se, the ratios of these parameters were taken with respect to those measured on the asphalt in its original, virgin condition. In other words Ketone Factor was related to the Viscosity Ratio, Loss in Penetration Ratio and Absolute Viscosity Ratio.

The three parameters chosen were so done, deliberately, since the ratio in each case represents a particular temperature condition. The Ketone Factor would then be assessed against three physical parameters one at 140° F (60° C), another at 77° F (25° C) and the third at 59° (15° C). This would determine the relevance of Ketone Factor in relation to asphalt properties over a substantially large range of service temperatures.

The multiple regression model used is as follows:

$$\text{Ketone Factor} = \beta_0 + \beta_1\,(\text{Abs Vis Ratio}) + \beta_2\,(\text{Loss of Pen Ratio}) + \beta_3\,(\text{Constant Power Vis Ratio}) + \text{Random Error} \quad (11.4)$$

This equation relates Ketone Factor to the three predictor variables. The ratios were computed from data in Appendix C-1 and C-2. Absolute Viscosities and Penetration data on original asphalts were obtained from

Tables 5.1 and 5.2. Constant Power Viscosities (n_j) at 59° F (15° C) of the original asphalts are presented in Table 11.3. Eight asphalts as listed in Table 11.3 were considered in the analysis. The ratios used in the analysis are listed in Appendix E.

Results of regression analysis with the three independent variables carried out using SAS-SAT software are presented in Table 11.4. R-Square value of 0.54 shows that not all the variation in Ketone Factor can be explained by variation in the independent variables in the model. The F Value indicated whether the complete model containing all three independent variables fits better than the reduced model containing all variables except the one being tested. In the case of Absolute Viscosity Ratio, it is seen that the F value is 0.9395. This indicates the insignificance of the variable and suggests that Absolute Viscosity Ratio may be ignored in the analysis.

Results of regression analysis without Absolute Viscosity Ratio are presented in Table 11.5. Both independent variables demonstrate their influence on Ketone Factor. However, the R-Square value remains at 0.54, emphasizing that only 54 percent of the variation in Ketone Factor can be explained by variation in Constant Power Viscosity Ratio and Loss of Penetration Ratio. A correlation matrix is presented in Table 11.6 which indicates the relative relationships between the four variables under analysis. Values of correlation coefficients, computed on the basis of data which excluded 90 day results, are also indicated in parentheses. The matrix shows that

1. Absolute Viscosity Ratio correlates poorly (less than 0.50) with the other three parameters. When data obtained at 90 days is excluded, the correlation improves.

Table 11.3 Constant Power Viscosities (η_j) at 59° F (15° C) of Original Asphalts

Asphalt Code	η_j (Pa.s)
CH	0.129340E + 8
BE	0.901107E + 7
AM	0.538940E + 7
MA	0.871003E + 7
TX	0.959343E + 7
TA	0.160580E + 7
SO	0.117545E + 9
BO	0.319721E + 7

Table 11.4 Results for Regression with Three Independent Variables

Variable	df	Parameter Estimate	P
Intercept	1	0.923	0.0001
Constant Power Vis Ratio	1	0.006	0.0057
Loss of Pen Ratio	1	1.210	0.0001
Absolute Vis Ratio	1	0.0001	0.9396

R-SQUARE 0.54

Table 11.5 Results of Regression with Two Independent Variables

Variable	df	Parameter Estimate	P
Intercept	1	0.922	0.0001
Constant Power Vfs Ratio	1	0.006	0.0031
Loss of Pen Ratio	1	1.214	0.0001

R-SQUARE 0.54

Table 11.6 Correlation Matrix with Four Variables

	KF	AVR	CPVR	LPR
KF	1.00(1.00)	0.40(0.42)	0.53(0.41)	0.71(0.63)
AVR	0.40(0.42)	1.00(1.00)	0.49(0.51)	0.48(0.75)
CPVR	0.53(0.41)	0.49(0.51)	1.00(1.00)	0.50(0.57)
LPR	0.71(0.63)	0.48(0.75)	0.50(0.57)	1.00(1.00)

Note. N = 104
N = 80 for numbers in parentheses

2. Constant Power Viscosity Ratio also exhibits only limited correlation with the other three parameters.
3. Ketone Factor correlates best with Loss of Penetration Ratio (0.71). Removal of results pertaining to 90 day aging increases the coefficient of correlation with respect to Absolute Viscosity Ratio. However, that reduces the correlation coefficients with respect to the other parameters.

It thus becomes apparent that Absolute Viscosity measurement at the 90 day aging level, gives rise to a lack of correlation, even with the conventional parameters like Penetration and Constant Power Viscosity. This deduction can be further examined by performing a regression analysis on the data excluding the 90 day results, but retaining the Absolute Viscosity Ratio. Results are presented in Table 11.7. P value for Absolute Viscosity Ratio in Table 11.4 was 0.9395, which now has reduced to 0.2981. Increase in P value corresponding to Constant Power Viscosity indicates the relevance of the 90 day data with respect to that parameter in relation to Ketone Factor. Reduction in R-Square value from 0.54 to 0.41 confirms that discarding the 90 day data does not help the overall model, even if that benefits correlations with Absolute Viscosity Ratio.

This discussion establishes merit in considering Ketone Factor as a unique measure of oxidative and age hardening, not completely related to the other conventional parameters, but related generally to the extent the other conventional parameters are related between themselves.

Table 11.7 Results of Regression Excluding 90 Day Data

Variable	df	Parameter Estimate	P
Intercept	1	0.971	0.0001
Constant Power Vis Ratio	1	0.013	0.3941
Loss of Pen Ratio	1	1.166	0.0001
Absolute Vis Ratio	1	-0.020	0.2981

R-SQUARE 0.41

11.8 A Framework for Better Specifications

The study undertaken indicates that some changes to the existing structure of specifications would help eliminate asphalts of low durability. With that object in view, a framework for better specifications is discussed.

11.8.1 The Importance of Smoke Point

The relation of hardening to a low smoke point is obvious. Discussion in Section 6.3.3 demonstrate the necessity to be cognizant of a low smoke point and ensure that such asphalts are avoided. Present specifications in Florida have no criteria in this regard. A tentative minimum Smoke Point temperature at about 350° F appears reasonable, and this is proposed in addition to the existing limit placed on weight loss on heating.

11.8.2 Ratios of Viscosities and Penetration

Present Florida specifications incorporate the Absolute Viscosity Ratio on TFOT (325° F) residue which is a maximum of 4.0. Results in Chapter 5 substantiate the sensitivity of this specification in detecting asphalts which may harden adversely in service. To amplify this specification, the TFOT procedure could be run at a higher temperature (365° F) and/or a similar specification could be incorporated which measures the percentage loss in penetration. Ideally an asphalt should satisfy both criteria to ensure long term durability. Such an enhanced specification would, without being unduly stringent on satisfactory asphalts, be able to identify those which have a tendency to harden rapidly. The elevated temperature would enhance differences and render the specification more restrictive. A suggested cut-off level for Absolute Viscosity Ratio on TFOT (365° F) residue could be 10.0. Loss in Penetration after TFOT (325° F) could be for a start, set at a 40 percent level. Corresponding figure for TFOT (365° F) could be set at a 56 percent level.

Tables 5.4 and 5.5 demonstrate the effect of the suggestions made. For the asphalts in this study, the Boscan 85-100 does not meet the Absolute Viscosity Ratio specifications at both levels of temperature. Boscan 85-100 and Texaco 85-100 do not meet the suggested Loss in Penetration criteria at the lower temperature. In addition, Marathon AC-30 does not meet the criteria at the higher temperature.

II.B.3 Low Temperature Criteria

No specification would be complete without an assessment of the asphalt at or near the lowest temperature which it is likely to experience in service. The relevance of asphalt viscosity measurements, at fairly low temperatures is well known and appreciated. The question is whether Constant Power Viscosities at lower temperatures are adaptable in the form of specifications and if so, in what form.

Work done as part of this study and presented in Appendix C-2 has highlighted the variability in test results which tends to increase as the temperature is lowered. Specifications based on low temperature viscosity have to address the variability of the test results. Two or more tests would have to be specified and the test procedure has to be standardized. Without detracting from the significance and utility of the tests, it is felt that it may be premature to draft specifications which are meaningful in critically isolating asphalts of poor durability and high temperature susceptibility, on the basis of Constant Power

Viscosities. Further studies and developments are necessary in this regard.

11.8.4 Chemical Composition Related to Performance

Aspects of this study on infrared spectral evaluation of age hardening lean heavily on the work done by Petersen and his co-workers (25). They emphasize the undesirability to devise chemical composition specifications and add that such specifications should define the desired performance properties. This indeed has been the guiding principle in developing a possible measure to identify asphalt durability on the basis of infrared spectral tests. Absorbance Ratios and Ketone Factor can follow changes in chemical functionality and yield valuable information, albeit indirectly, on hardening trends. The integration of such a measure into current specifications appears necessary.

The limited database compiled during this study does not permit recommendation of specific limits on Ketone Factors. However, when comparing asphalts, it is recommended that an assessment be made of Ketone Factors on TFOT or RTFOT residues. Of particular interest is the value of this Factor measured on asphalts which are rejected or have performed poorly in service. A compilation of such data will enable development of limits of acceptability.

CHAPTER 12
CONCLUSIONS AND RECOMMENDATIONS

12.1 Conclusions

The following conclusions were derived from the results obtained in this investigation.

1. On the basis of percent Penetration Retained, the RTFOT is a more severe aging process than the TFOT for oven temperatures of 285° F and 325° F. However, for an oven temperature of 365° F, the two processes may be considered identical.
2. On the basis of Absolute Viscosity Ratio, the RTFOT and TFOT procedures may be considered equivalent. Change in Absolute Viscosity Ratio between 325° F and 365° F is greater than between 285° F and 325° F, the degree of change depending on the type of asphalt.
3. On the basis of Indirect Tensile Strength, forced draft exposure could result in higher strength over that caused by ultraviolet or oven, depending upon the asphalt. Effects caused by ultraviolet and oven are about the same.
4. Indirect Tensile Strength can sensitively assess comparative hardening of Marshall specimens fabricated from asphalts of a similar grade. For example, Mariani AC-30 and Amoco AC-30 result in higher strengths compared to Belcher AC-30 and Chevron AC-30, when hardened in the forced draft environment.

5. Horizontal deformations measured in the Resilient Modulus tests, decreased with hardening of the asphalt. Consequently, the Moduli were increased. Differences between total deformation and total recoverable deformation decrease. In other words, the magnitude of the creep component is reduced as viscosity increases. Ultraviolet and oven exposures result in a generally similar pattern of effects on deformation and Moduli.
6. As the asphalts harden, Fracture Energy increased to a maximum and then decreased. The location of this maximum on the aging scale appears to be linked to the test temperature and consequently, to asphalt viscosity.
7. On the basis of Penetration, forced draft and ultraviolet exposures were similar but resulted in higher hardening than obtained by oven exposure.
8. Infrared spectroscopic techniques can be used to sensitively assess changes in the asphalt due to increased levels of oxidation. The factor which can be used to follow these changes was obtained by dividing the ratio of absorbance at 1700 cm^{-1} for the asphalt residue, by the ratio of absorbance at 1700 cm^{-1} of the original asphalt. This value was termed the Ketone Factor, which increases with increasing levels of oxidative hardening of the asphalt. This technique of quantifying age hardening is simple and reliable for the asphalts used in this investigation.
9. Reference measurements for the computation of the ratios of absorbance may be made at wavenumbers of 1600 cm^{-1} or at 1375 cm^{-1}. However, the spectral response at 1600 cm^{-1} is

preferable in the context of shape, consistency of position and intensity.

10. Increases in Ketone Factors may be pronounced in the initial periods of age hardening, but tend to diminish with further oxidation. Therefore, Ketone Factors are most effective in the evaluation of relatively short term hardening.
11. As a rough estimate, it is probable that the 28 day aging of Marshall specimens at 140° F in the laboratory, 6 months of natural weathering of Marshall specimens, TFOT or RTFOT procedure at 365° F and 12 to 24 months field aging after construction, in a well compacted asphalt concrete pavement surface layer, would all give approximately the same degree of hardening for a typical paving grade asphalt cement. This equivalence could vary to some extent depending upon the properties of the asphalt cement.
12. An effective simulated asphalt aging process for evaluating mixtures could be achieved using a combination of the three types of exposure. This would best simulate actual conditions in field service where the combined effects of heat, light and air are experienced.
13. Low temperature rheology tests should be conducted specifically to address the variability of the test results. Such variability would be substantially offset by standardization of the procedure and conduct of the test. In this context, the number of replicate samples to be tested is also of particular interest.

12.2 Recommendations

The findings, discussions thereon and conclusions drawn from this study lead to the following recommendations:

1. The Thin Film Oven Test should be considered to be performed at 365° F since the higher test temperature provides improved detectability of age hardening potential.
2. An investigation should be performed to compare the California Tilt-Oven Test (235.4° F, 7 days) with the Thin Film Oven Test at the elevated temperature of 365° F.
3. An artifical aging chamber should be fabricated incorporating features of the ultraviolet chamber and forced draft oven to provide a uniformly diffused and upward airflow. The chamber should be well-insulated and constructed to maintain the internal temperature at a uniform 140° F. Elevated specimen racks should be arranged to permit ingress of air from all sides. Such a chamber would be ideal for testing the combined environmental effects on Marshall-type specimens, cores, briquittes and the like.
4. A minimum Smoke Point temperature could be specified as part of current specifications.
5. A maximum Absolute Viscosity Ratio for TFOT (365° F) residue could be specified in addition to the current specification with reference to TFOT (325° F). A maximum of 10.0 appears reasonable until additional data can be collected and analyzed.
6. As an auxiliary specification, Loss in Penetration after TFOT (325° F) could be set at a level of 40 percent. The corresponding value for TFOT (365° F) could be set at a level of 55

percent. These values appear reasonable but merit review on the basis of additional data.

7. The recommended levels of acceptance can be optimized on the basis of field performance experience gained over a period of time.
8. All asphalts for acceptance testing should be evaluated on the basis of infrared spectral tests measuring Ketone Factors on TFOT or (RTFOT) residues at the current and proposed temperature levels. A record of these data should be maintained for subsequent analysis with the object of establishing acceptance criteria. Such tests would be valuable to identify asphalts which may be poor performers in the field. A reasonably large database would be necessary for development of acceptance limits.
9. As an extension of this study, a comprehensive test program should be undertaken to study the relationship between low temperature rheological measurements and hardening potential as recognized on the basis of consistency tests on TFOT (or RTFOT) residues. The experimental design should limit the statistical variability of the test data. The object of this extended study would be to develop specifications based on viscosities measured in the Constant Stress Rheometer, at a temperature level appropriate to the low pavement temperatures experienced in Florida.
10. The interrelationship between aging in the field, that in the laboratory and in a natural environment needs to be evaluated over a period of at least three years.

APPENDIX A

PROPERTIES OF MARSHALL SPECIMENS

Table A.1 Density and Voids of Marshall Specimens

CHEVRON AC-30

Spec#	Unit Wt (pcf)	% Voids in Mix	Spec#	Unit Wt (pcf)	% Voids in Mix
CH 33	137.78	4.353	CH 31	136.45	5.274
CH 10	137.72	4.396	CH 57	136.38	5.327
CH 34	137.37	4.641	CH 60	136.37	5.334
CH 43	137.31	4.680	CH 28	136.36	5.341
CH 39	137.29	4.695	CH 37	136.32	5.364
CH 24	137.28	4.703	CH 46	136.32	5.367
CH 44	137.19	4.764	CH 58	136.32	5.368
CH 35	137.18	4.770	CH 20	136.31	5.370
CH 36	137.18	4.770	CH 18	136.27	5.402
CH 40	137.13	4.802	CH 25	136.26	5.409
CH 6	137.11	4.817	CH 22	136.22	5.435
CH 14	137.11	4.821	CH 29	136.22	5.438
CH 42	137.00	4.893	CH 16	136.20	5.447
CH 45	136.91	4.955	CH 26	136.16	5.478
CH 59	136.88	4.978	CH 41	136.15	5.482
CH 52	136.87	4.984	CH 9	136.13	5.495
CH 48	136.86	4.989	CH 23	136.10	5.522
CH 3	136.85	5.002	CH 11	136.09	5.529
CH 5	136.84	5.009	CH 12	136.05	5.554
CH 4	136.82	5.021	CH 38	136.05	5.556
CH 1	136.81	5.026	CH 15	136.04	5.558
CH 49	136.75	5.068	CH 50	136.01	5.580
CH 51	136.64	5.146	CH 56	135.92	5.641
CH 32	136.64	5.147	CH 8	135.83	5.708
CH 13	136.63	5.152	CH 30	135.79	5.734
CH 54	136.61	5.168	CH 55	135.74	5.772
CH 19	136.60	5.169	CH 21	135.70	5.799
CH 2	136.58	5.186	CH 53	135.60	5.867
CH 47	136.54	5.215	CH 7	135.59	5.870
CH 27	136.49	5.247	CH 17	135.59	5.871

Note:

Asphalt Content %	6.5
Theoretical SG	2.309
Combined Aggregate SG	2.483

Table A.1--continued

BELCHER AC-30

Spec#	Unit Wt (pcf)	% Voids in Mix	Spec#	Unit Wt (pcf)	% Voids in Mix
BE 46	137.88	4.282	BE 32	136.69	5.107
BE 39	137.30	4.685	BE 13	136.63	5.151
BE 60	137.20	4.754	BE 58	136.62	5.161
BE 14	137.18	4.768	BE 40	136.61	5.165
BE 52	137.17	4.780	BE 24	136.53	5.223
BE 11	137.12	4.812	BE 42	136.51	5.233
BE 17	137.06	4.851	BE 10	136.48	5.256
BE 15	137.06	4.854	BE 27	136.46	5.272
BE 35	137.06	4.855	BE 26	136.40	5.314
BE 59	137.02	4.878	BE 37	136.38	5.325
BE 51	137.00	4.897	BE 49	136.37	5.329
BE 38	136.95	4.927	BE 25	136.27	5.403
BE 36	136.94	4.933	BE 6	136.26	5.409
BE 30	136.92	4.947	BE 44	136.23	5.426
BE 21	136.92	4.950	BE 12	136.23	5.429
BE 53	136.88	4.978	BE 20	136.20	5.447
BE 19	136.88	4.981	BE 41	136.17	5.470
BE 43	136.87	4.984	BE 28	136.16	5.478
BE 16	136.86	4.993	BE 1	136.16	5.481
BE 4	136.85	4.997	BE 8	136.14	5.495
BE 5	136.85	4.998	BE 34	136.07	5.537
BE 9	136.82	5.021	BE 56	136.04	5.562
BE 22	136.81	5.025	BE 57	136.04	5.564
BE 45	136.80	5.030	BE 55	135.89	5.667
BE 33	136.79	5.038	BE 48	135.79	5.734
BE 18	136.79	5.041	BE 31	135.64	5.837
BE 23	136.77	5.051	BE 2	135.51	5.927
BE 47	136.76	5.059	BE 7	135.32	6.062
BE 29	136.74	5.072	BE 3	135.16	6.173
BE 54	136.73	5.081	BE 50	134.77	6.444

Note:

Asphalt Content %	6.5
Theoretical SG	2.309
Combined Aggregate SG	2.483

Table A.1--continued

AMOCO AC-30

Spec#	Unit Wt (pcf)	% Voids in Mix	Spec#	Unit Wt (pcf)	% Voids in Mix
AM 39	137.70	4.406	AM 29	136.88	4.976
AM 11	137.66	4.437	AM 48	136.84	5.003
AM 7	137.53	4.526	AM 26	136.80	5.036
AM 14	137.45	4.583	AM 37	136.76	5.062
AM 16	137.42	4.603	AM 35	136.74	5.073
AM 24	137.39	4.622	AM 51	136.73	5.083
AM 20	137.38	4.629	AM 52	136.73	5.085
AM 13	137.36	4.644	AM 25	136.72	5.087
AM 2	137.27	4.705	AM 15	136.71	5.095
AM 9	137.27	4.710	AM 22	136.68	5.115
AM 5	137.24	4.729	AM 3	136.66	5.129
AM 19	137.22	4.739	AM 4	136.63	5.151
AM 38	137.19	4.761	AM 18	136.62	5.159
AM 10	137.18	4.766	AM 6	136.61	5.166
AM 43	137.16	4.781	AM 57	136.58	5.187
AM 28	137.14	4.795	AM 32	136.54	5.213
AM 45	137.14	4.800	AM 54	136.54	5.216
AM 55	137.13	4.807	AM 23	136.51	5.237
AM 49	137.12	4.810	AM 36	136.50	5.245
AM 8	137.12	4.813	AM 47	136.48	5.257
AM 46	137.11	4.817	AM 50	136.48	5.258
AM 30	137.10	4.823	AM 34	136.45	5.275
AM 27	137.09	4.833	AM 17	136.35	5.347
AM 40	137.00	4.896	AM 59	136.29	5.384
AM 53	136.96	4.925	AM 56	136.18	5.466
AM 1	136.95	4.929	AM 31	136.18	5.467
AM 44	136.94	4.933	AM 33	136.05	5.553
AM 12	136.91	4.954	AM 21	135.67	5.676
AM 42	136.90	4.962	AM 60	135.81	5.718
AM 41	136.90	4.962	AM 58	135.77	5.751

Note:

Asphalt Content	6.5 %
Theoretical SG	2.309
Combined Aggregate SG	2.483

Table A.1--continued

MARIANI AC-30

Spec#	Unit Wt (pcf)	% Voids in Mix	Spec#	Unit Wt (pcf)	% Voids in Mix
MA 14	138.38	3.825	MA 38	136.60	5.063
MA 7	138.34	3.854	MA 6	136.57	5.082
MA 5	138.03	4.067	MA 39	136.48	5.146
MA 20	137.77	4.250	MA 25	136.45	5.163
MA 21	137.75	4.264	MA 28	136.44	5.170
MA 17	137.73	4.273	MA 53	136.43	5.179
MA 4	137.71	4.289	MA 56	136.42	5.183
MA 27	137.67	4.320	MA 41	136.42	5.186
MA 59	137.64	4.340	MA 12	136.41	5.191
MA 26	137.63	4.343	MA 16	136.41	5.194
MA 3	137.51	4.426	MA 22	136.41	5.196
MA 24	137.44	4.478	MA 51	136.40	5.198
MA 29	137.40	4.502	MA 43	136.37	5.222
MA 1	137.38	4.516	MA 33	136.36	5.226
MA 10	137.38	4.518	MA 34	136.30	5.271
MA 32	137.20	4.642	MA 44	136.21	5.330
MA 54	137.20	4.647	MA 30	136.17	5.357
MA 11	137.18	4.656	MA 60	136.13	5.391
MA 15	137.18	4.658	MA 45	136.07	5.427
MA 19	137.11	4.710	MA 40	136.06	5.440
MA 23	137.08	4.727	MA 37	135.94	5.520
MA 18	137.06	4.729	MA 48	135.91	5.539
MA 8	137.06	4.744	MA 35	135.90	5.546
MA 13	136.95	4.819	MA 52	135.90	5.549
MA 2	136.94	4.822	MA 36	135.86	5.578
MA 31	136.83	4.904	MA 49	135.61	5.748
MA 9	136.77	4.946	MA 46	135.53	5.802
MA 50	136.72	4.979	MA 47	135.37	5.916
MA 58	136.71	4.983	MA 42	134.96	6.201
MA 57	136.60	5.060	MA 55	134.39	6.594

Note:

Asphalt Content %	6.5
Theoretical SG	2.309
Combined Aggregate SG	2.453

Table A.1--continued

TEXACO 85-100

Spec#	Unit Wt (pcf)	% Voids in Mix	Spec#	Unit Wt (pcf)	% Voids in Mix
TX 31	133.30	4.264	TX 32	136.86	5.260
TX 2	133.05	4.433	TX 45	136.83	5.276
TX 4	137.79	4.613	TX 43	136.79	5.305
TX 36	137.65	4.709	TX 30	136.79	5.305
TX 55	137.60	4.749	TX 34	136.79	5.306
TX 9	137.50	4.812	TX 48	136.78	5.315
TX 44	137.43	4.866	TX 19	136.76	5.324
TX 58	137.41	4.878	TX 52	136.73	5.348
TX 42	137.41	4.880	TX 22	136.57	5.456
TX 16	137.37	4.903	TX 12	136.57	5.459
TX 29	137.37	4.903	TX 60	136.55	5.471
TX 3	137.37	4.908	TX 25	136.54	5.478
TX 8	137.22	5.010	TX 7	136.51	5.502
TX 41	137.21	5.017	TX 18	136.46	5.532
TX 1	137.17	5.047	TX 24	136.45	5.545
TX 59	137.13	5.072	TX 13	136.42	5.566
TX 28	137.12	5.076	TX 26	136.38	5.592
TX 46	137.10	5.094	TX 20	136.35	5.610
TX 33	137.09	5.101	TX 57	136.34	5.619
TX 53	137.08	5.108	TX 56	136.32	5.632
TX 40	137.03	5.143	TX 21	136.31	5.641
TX 51	137.02	5.145	TX 10	136.26	5.675
TX 6	137.00	5.163	TX 15	136.25	5.683
TX 47	136.99	5.167	TX 37	136.23	5.695
TX 54	136.99	5.172	TX 50	136.22	5.702
TX 38	136.97	5.183	TX 49	136.20	5.716
TX 35	136.97	5.185	TX 27	136.17	5.737
TX 5	136.94	5.205	TX 17	136.10	5.781
TX 14	136.92	5.217	TX 39	136.10	5.785
TX 23	136.91	5.224	TX 11	135.71	6.053

Note:

Asphalt Content %	6.5
Theoretical SG	2.315
Combined Aggregate SG	2.483

Table A.1--continued

TEXACO AIRBLOWN 85-100

Spec#	Unit Wt (pcf)	% Voids in Mix	Spec#	Unit Wt (pcf)	% Voids in Mix
TA 55	138.47	4.144	TA 15	137.32	4.939
TA 60	138.35	4.229	TA 28	137.25	4.986
TA 32	138.29	4.268	TA 46	137.24	4.995
TA 34	138.20	4.328	TA 9	137.23	5.001
TA 41	138.19	4.338	TA 36	137.19	5.030
TA 50	138.17	4.351	TA 42	137.16	5.049
TA 38	138.14	4.374	TA 14	137.16	5.050
TA 11	138.05	4.435	TA 54	137.04	5.135
TA 45	137.98	4.484	TA 8	137.04	5.135
TA 17	137.96	4.500	TA 57	137.03	5.143
TA 39	137.94	4.511	TA 22	137.02	5.145
TA 35	137.89	4.547	TA 7	136.95	5.198
TA 33	137.87	4.561	TA 56	136.93	5.210
TA 37	137.83	4.584	TA 5	136.92	5.220
TA 53	137.78	4.622	TA 12	136.74	5.342
TA 40	137.76	4.633	TA 18	136.74	5.344
TA 30	137.72	4.660	TA 52	136.74	5.344
TA 31	137.64	4.722	TA 29	136.70	5.372
TA 16	137.62	4.730	TA 23	136.69	5.375
TA 58	137.59	4.753	TA 27	136.68	5.381
TA 10	137.58	4.763	TA 4	136.67	5.338
TA 47	137.56	4.772	TA 24	136.58	5.453
TA 44	137.56	4.775	TA 19	136.53	5.484
TA 25	137.53	4.795	TA 20	136.50	5.509
TA 59	137.45	4.848	TA 3	136.49	5.512
TA 49	137.45	4.853	TA 1	136.49	5.518
TA 43	137.40	4.885	TA 6	136.45	5.540
TA 51	137.39	4.892	TA 21	136.32	5.632
TA 48	137.39	4.892	TA 13	136.27	5.665
TA 26	137.37	4.908	TA 2	135.92	5.912

Note:

Asphalt Content %	6.5
Theoretical SG	2.315
Combined Aggregate SG	2.483

Table A.1--continued

ESSO 25-35

Spec#	Unit Wt (pcf)	% Voids in Mix	Spec#	Unit Wt (pcf)	% Voids in Mix
SO 9	137.84	4.866	SO 2	136.45	5.829
SO 11	137.41	5.163	SO 51	136.44	5.833
SO 15	137.25	5.273	SO 31	136.42	5.845
SO 12	137.23	5.286	SO 46	136.42	5.846
SO 39	137.17	5.328	SO 48	136.42	5.847
SO 8	137.08	5.390	SO 14	136.39	5.867
SO 47	137.02	5.436	SO 50	136.39	5.871
SO 52	137.00	5.446	SO 27	136.37	5.879
SO 16	136.99	5.454	SO 34	136.34	5.903
SO 17	136.99	5.457	SO 13	136.32	5.914
SO 32	136.95	5.485	SO 25	136.27	5.949
SO 7	136.88	5.533	SO 3	136.26	5.955
SO 35	136.87	5.536	SO 20	136.26	5.958
SO 37	136.86	5.543	SO 56	136.16	6.027
SO 43	136.85	5.548	SO 53	136.15	6.034
SO 36	136.77	5.603	SO 19	136.15	6.037
SO 1	136.77	5.609	SO 60	136.13	6.049
SO 18	136.76	5.612	SO 22	136.08	6.083
SO 40	136.69	5.658	SO 26	136.06	6.099
SO 38	136.69	5.663	SO 59	136.04	6.107
SO 44	136.68	5.667	SO 55	136.03	6.115
SO 24	136.68	5.668	SO 58	136.01	6.130
SO 5	136.66	5.685	SO 28	136.00	6.139
SO 10	136.64	5.694	SO 41	135.95	6.171
SO 29	136.61	5.719	SO 54	135.88	6.224
SO 42	136.55	5.758	SO 30	135.86	6.232
SO 57	136.55	5.758	SO 4	135.84	6.247
SO 21	136.50	5.795	SO 33	135.77	6.295
SO 49	136.47	5.811	SO 45	135.74	6.320
SO 6	136.45	5.827	SO 23	135.67	6.368

Note:

Asphalt Content %	6.5
Theoretical SG	2.322
Combined Aggregate SG	2.483

Table A.1--continued

BOSCAN 85-100

Spec#	Unit Wt (pcf)	% Voids in Mix	Spec#	Unit Wt (pcf)	% Voids in Mix
BO 18	137.49	4.820	BO 25	136.55	5.472
BO 39	137.42	4.870	BO 3	136.55	5.472
BO 35	137.29	4.963	BO 41	136.51	5.498
BO 17	137.23	5.012	BO 40	136.50	5.509
BO 30	137.19	5.032	BO 29	136.48	5.524
BO 34	137.10	5.092	BO 1	136.47	5.529
BO 43	137.10	5.094	BO 6	136.47	5.529
BO 10	137.06	5.123	BO 33	136.47	5.532
BO 19	137.06	5.123	BO 9	136.46	5.535
BO 11	137.03	5.141	BO 37	136.42	5.563
BO 45	136.94	5.203	BO 46	136.41	5.571
BO 14	136.93	5.209	BO 38	136.40	5.576
BO 36	136.88	5.242	BO 59	136.37	5.596
BO 31	136.88	5.242	BO 13	136.37	5.597
BO 5	136.88	5.245	BO 12	136.35	5.615
BO 23	136.85	5.266	BO 56	136.32	5.630
BO 48	136.79	5.308	BO 47	136.31	5.640
BO 27	136.77	5.320	BO 32	136.28	5.660
BO 21	136.75	5.332	BO 28	136.23	5.694
BO 15	136.73	5.346	BO 58	136.15	5.752
BO 51	136.71	5.359	BO 53	136.11	5.774
BO 22	136.71	5.360	BO 44	136.10	5.783
BO 42	136.71	5.365	BO 24	136.00	5.856
BO 26	136.69	5.374	BO 55	135.96	5.881
BO 50	136.68	5.381	BO 57	135.92	5.910
BO 4	136.68	5.381	BO 54	135.85	5.960
BO 49	136.68	5.386	BO 52	135.59	6.137
BO 8	136.63	5.417	BO 16	135.44	6.243
BO 7	136.63	5.418	BO 60	135.18	6.421
BO 2	136.59	5.445	BO 20	134.93	6.596

Note.

Asphalt Content %	6.5
Theoretical SG	2.315
Combined Aggregate SG	2.483

Table A.1--continued

CHEVRON AC-20 AND CHEVRON AC-20 (MODIFIED)

Spec#	Unit Wt (pcf)	% Voids in Mix	Spec#	Unit Wt (pcf)	% Voids in Mix
DI 12	138.48	3.05	DM 25	138.71	2.89
DI 11	138.30	3.18	DM 20	138.59	2.97
DI 1	137.84	3.50	DM 7	138.39	3.11
DI 15	137.83	3.50	DM 15	138.29	3.18
DI 7	137.76	3.55	DM 10	138.15	3.28
DI 17	137.70	3.59	DM 8	138.12	3.30
DI 13	137.68	3.61	DM 16	138.07	3.33
DI 6	137.63	3.64	DM 1	137.90	3.46
DI 4	137.57	3.69	DM 4	137.88	3.47
DI 14	137.44	3.78	DM 19	137.88	3.47
DI 2	137.43	3.78	DM 6	137.77	3.54
DI 5	137.35	3.84	DM 18	137.68	3.61
DI 10	137.33	3.85	DM 26	137.44	3.78
DI 3	137.23	3.92	DM 14	137.43	3.78
DI 19	137.15	3.98	DM 21	137.29	3.88
DI 16	137.09	4.02	DM 24	137.28	3.88
DI 18	137.08	4.03	DM 13	137.27	3.90
DI 22	136.99	4.09	DM 11	137.26	3.90
DI 8	136.80	4.23	DM 17	137.24	3.92
DI 20	136.79	4.23	DM 2	137.22	3.93
DI 26	136.77	4.25	DM 12	137.16	3.97
DI 9	136.67	4.32	DM 5	137.06	4.04
DI 23	136.63	4.34	DM 27	137.03	4.06
DI 21	136.52	4.42	DM 23	136.96	4.12
DI 25	136.51	4.43	DM 3	136.94	4.12
DI 24	136.05	4.75	DM 22	136.71	4.28
DI 27	136.05	4.75	DM 9	135.63	5.05

Note:

Asphalt Content	6.5 %
Theoretical SG	2.309
Combined Aggregate SG	2.483

Table A.2 Assignment of Treatments to Marshall Specimens

DURATION	ULTRAVIOLET		FORCED DRAFT		NORMAL OVEN		NATURAL WEATHERING	
DAYS	SPEC #	UNIT WT pcf	SPEC #	UNIT WT pcf	SPEC #	UNIT WT pcf	SPEC #	UNIT WT pcf
0 DAY	CH 6 CH 12 CH 60 AVG	137.11 136.05 136.37 136.51	CH 59 CH 23 CH 1 AVG	136.88 136.10 136.81 136.60	CH 34 CH 21 CH 57 AVG	137.37 135.70 136.39 136.48	CH 44 CH 30 CH 54 AVG	137.19 135.79 136.61 136.53
1 DAY	CH 48 CH 16 CH 25 AVG	136.86 136.20 136.26 136.44	CH 10 CH 17 CH 31 AVG	137.72 135.59 136.45 136.59	CH 52 CH 11 CH 49 AVG	136.87 136.09 136.75 136.57	CH 42 CH 41 CH 51 AVG	137.00 136.15 136.64 136.60
7 DAYS	CH 45 CH 9 CH 32 AVG	136.91 136.13 136.64 136.56	CH 14 CH 38 CH 28 AVG	137.11 136.05 136.35 136.50	CH 5 CH 22 CH 20 AVG	136.84 136.22 136.31 136.46	CH 43 CH 53 CH 47 AVG	137.31 135.60 136.54 136.48
28 DAYS	CH 33 CH 7 CH 27 AVG	137.78 135.59 136.49 136.62	CH 3 CH 26 CH 58 AVG	136.85 136.16 136.32 136.44	CH 36 CH 15 CH 37 AVG	137.18 136.04 136.32 136.52	CH 40 CH 50 CH 46 AVG	137.13 136.01 136.32 136.49
90 DAYS	CH 35 CH 55 CH 19 AVG	137.18 135.74 136.60 136.51	CH 39 CH 56 CH 2 AVG	137.29 135.92 136.58 136.60	CH 24 CH 8 CH 13 AVG	137.28 135.83 136.63 136.58	CH 4 CH 29 CH 18 AVG	136.82 136.22 136.27 136.43

NOTE: 0 DAY, 6 MONTHS, 1 YEAR, 2 YEARS AND 3 YEARS DURATION FOR NATURAL WEATHERING

Table A.2--continued

DURATION	ULTRAVIOLET		NATURAL WEATHERING		FORCED DRAFT		NORMAL OVEN	
DAYS	SPEC #	UNIT WT pcf	SPEC #	UNIT WT pcf	SPEC #	UNIT WT pcf	SPEC #	UNIT WT pcf
0 DAY	BE 15 BE 31 BE 23 AVG	137.18 137.17 137.12 137.16	BE 39 BE 50 BE 32 AVG	136.88 136.88 136.87 136.88	BE 16 BE 49 BE 27 AVG	136.26 136.23 136.23 136.24	BE 17 BE 48 BE 18 AVG	136.16 136.14 136.07 136.12
1 DAY	BE 30 BE 20 BE 45 AVG	137.02 137.00 136.95 136.99	BE 21 BE 41 BE 5 AVG	136.79 136.79 136.77 136.78	BE 11 BE 55 BE 33 AVG	136.61 136.53 136.51 136.55	BE 4 BE 25 BE 26 AVG	135.32 135.15 134.77 135.08
7 DAYS	BE 46 BE 3 BE 54 AVG	137.88 137.30 137.20 137.46	BE 43 BE 44 BE 10 AVG	136.76 136.74 136.73 136.75	BE 35 BE 34 BE 24 AVG	136.48 136.46 136.40 136.44	BE 14 BE 7 BE 29 AVG	136.20 136.17 136.16 136.18
28 DAYS	BE 19 BE 6 BE 37 AVG	136.94 136.92 136.92 136.93	BE 52 BE 57 BE 47 AVG	136.86 136.85 136.85 136.85	BE 60 BE 2 BE 13 AVG	136.69 136.63 136.62 136.65	BE 36 BE 12 BE 22 AVG	135.79 135.64 135.51 135.65
90 DAYS	BE 51 BE 1 BE 58 AVG	137.06 137.06 137.06 137.06	BE 38 BE 8 BE 40 AVG	136.82 136.81 136.80 136.81	BE 53 BE 28 BE 9 AVG	136.38 136.37 136.27 136.34	BE 59 BE 56 BE 42 AVG	136.06 136.04 135.89 135.99

NOTE: 0 DAY, 6 MONTHS, 1 YEAR, 2 YEARS AND 3 YEARS DURATION FOR NATURAL WEATHERING

Table A.2--continued

DURATION	NORMAL OVEN		NATURAL WEATHERING		FORCED DRAFT		ULTRAVIOLET	
DAYS	SPEC #	UNIT WT pcf	SPEC #	UNIT WT pcf	SPEC #	UNIT WT pcf	SPEC #	UNIT WT pcf
0 DAY	AM 39 AM 60 AM 41 AVG	137.70 137.66 137.53 137.63	AM 19 AM 47 AM 37 AVG	136.91 136.90 136.88 136.90	AM 24 AM 59 AM 53 AVG	136.61 136.54 136.54 136.56	AM 8 AM 4 AM 15 AVG	137.12 136.63 136.71 136.82
1 DAY	AM 13 AM 31 AM 44 AVG	137.45 137.42 137.39 137.42	AM 43 AM 54 AM 46 AVG	136.84 136.80 136.76 136.80	AM 49 AM 3 AM 25 AVG	136.18 136.05 135.81 136.01	AM 38 AM 57 AM 27 AVG	137.19 136.58 137.09 136.95
7 DAYS	AM 5 AM 36 AM 26 AVG	137.36 137.27 137.24 137.29	AM 11 AM 58 AM 29 AVG	136.74 136.73 136.72 136.73	AM 7 AM 33 AM 48 AVG	136.69 136.66 136.62 136.65	AM 20 AM 56 AM 1 AVG	137.38 136.19 136.95 136.84
28 DAYS	AM 10 AM 32 AM 40 AVG	137.22 137.18 137.16 137.19	AM 55 AM 6 AM 52 AVG	136.74 136.73 136.72 136.73	AM 2 AM 50 AM 35 AVG	136.51 136.50 136.48 136.49	AM 14 AM 21 AM 42 AVG	135.77 135.87 136.90 136.18
90 DAYS	AM 45 AM 19 AM 22 AVG	137.14 137.14 137.13 137.14	AM 16 AM 17 AM 12 AVG	137.00 136.96 136.94 136.97	AM 28 AM 23 AM 30 AVG	136.48 136.35 136.29 136.37	AM 9 AM 34 AM 51 AVG	137.27 136.45 136.73 136.82

Note: 0 DAY, 6 MONTHS, 1 YEAR, 2 YEARS AND 3 YEARS DURATION FOR NATURAL WEATHERING

Table A.2--continued

DURATION	ULTRAVIOLET		NATURAL WEATHERING		FORCED DRAFT		NORMAL OVEN	
DAYS	SPEC #	UNIT WT pcf	SPEC #	UNIT WT pcf	SPEC #	UNIT WT pcf	SPEC #	UNIT WT pcf
0 DAY	MA 1 MA 44 MA 13 AVG	137.38 136.21 136.95 136.85	MA 10 MA 30 MA 23 AVG	137.38 136.17 137.08 136.88	MA 5 MA 46 MA 6 AVG	138.03 135.53 136.57 136.71	MA 4 MA 36 MA 31 AVG	137.71 135.86 136.83 136.80
1 DAY	MA 14 MA 42 MA 57 AVG	138.39 134.95 136.60 136.65	MA 21 MA 35 MA 50 AVG	137.75 135.90 136.72 136.79	MA 17 MA 52 MA 2 AVG	137.73 135.90 136.94 136.86	MA 19 MA 51 MA 12 AVG	137.11 136.40 136.41 136.64
7 DAYS	MA 54 MA 43 MA 16 AVG	137.20 136.37 136.41 136.66	MA 24 MA 40 MA 25 AVG	137.44 136.06 136.45 136.65	MA 32 MA 60 MA 18 AVG	137.20 136.13 137.06 136.80	MA 20 MA 47 MA 58 AVG	137.77 135.37 136.71 136.62
28 DAYS	MA 27 MA 49 MA 9 AVG	137.67 135.61 136.77 136.68	MA 7 MA 55 MA 38 AVG	138.34 134.39 136.60 136.44	MA 15 MA 22 MA 41 AVG	137.18 136.41 136.42 136.67	MA 29 MA 34 MA 8 AVG	137.40 136.30 137.06 136.92
90 DAYS	MA 3 MA 45 MA 39 AVG	137.51 136.07 136.48 136.69	MA 11 MA 33 MA 56 AVG	137.18 136.36 136.42 136.65	MA 59 MA 37 MA 28 AVG	137.64 135.94 136.44 136.67	MA 26 MA 48 MA 53 AVG	137.63 135.91 136.43 136.66

NOTE: 0 DAY, 6 MONTHS, 1 YEAR, 2 YEARS AND 3 YEARS DURATION FOR NATURAL WEATHERING

Table A.2--continued

DURATION	FORCED DRAFT		NORMAL OVEN		ULTRAVIOLET		NATURAL WEATHERING	
DAYS	SPEC #	UNIT WT pcf	SPEC #	UNIT WT pcf	SPEC #	UNIT WT pcf	SPEC #	UNIT WT pcf
0 DAY	TX 29 TX 57 TX 43 AVG	137.37 136.34 136.79 136.83	TX 1 TX 26 TX 19 AVG	137.17 136.38 136.76 136.77	TX 4 TX 27 TX 45 AVG	137.79 136.17 136.83 136.93	TX 16 TX 10 TX 48 AVG	137.37 136.26 136.76 136.80
1 DAY	TX 31 TX 39 TX 23 AVG	138.30 136.10 136.91 137.10	TX 2 TX 11 TX 32 AVG	138.05 135.71 136.86 136.87	TX 33 TX 60 TX 51 AVG	137.09 136.55 137.02 136.89	TX 8 TX 24 TX 22 AVG	137.22 136.45 136.57 136.75
7 DAYS	TX 41 TX 13 TX 12 AVG	137.21 136.42 136.57 136.73	TX 55 TX 15 TX 5 AVG	137.60 136.25 136.94 136.93	TX 59 TX 20 TX 52 AVG	137.13 136.35 136.73 136.74	TX 53 TX 25 TX 6 AVG	137.08 136.54 137.00 136.87
28 DAYS	TX 28 TX 7 TX 47 AVG	137.12 136.51 136.99 136.87	TX 3 TX 56 TX 30 AVG	137.37 136.32 136.79 136.83	TX 42 TX 21 TX 34 AVG	137.41 136.31 136.79 136.84	TX 44 TX 50 TX 38 AVG	137.43 136.22 136.97 136.87
90 DAYS	TX 58 TX 49 TX 35 AVG	137.41 136.20 136.97 136.86	TX 46 TX 18 TX 40 AVG	137.10 136.46 137.03 136.86	TX 9 TX 37 TX 54 AVG	137.50 136.23 136.99 136.91	TX 36 TX 17 TX 14 AVG	137.65 136.10 136.92 136.89

NOTE: 0 DAY, 6MONTHS, 1 YEAR, 2 YEARS AND 3 YEARS DURATION FOR NATURAL WEATHERING

Table A.2--continued

DURATION	NATURAL WEATHERING		FORCED DRAFT		NORMAL OVEN		ULTRAVIOLET	
DAYS	SPEC #	UNIT WT pcf	SPEC #	UNIT WT pcf	SPEC #	UNIT WT pcf	SPEC #	UNIT WT pcf
0 DAY	TA 55 TA 13 TA 26 AVG	138.47 136.27 137.37 137.37	TA 41 TA 19 TA 51 AVG	138.19 136.53 137.39 137.37	TA 40 TA 29 TA 47 AVG	137.76 136.70 137.56 137.34	TA 17 TA 24 TA 42 AVG	137.96 136.58 137.16 137.23
1 DAY	TA 37 TA 18 TA 25 AVG	137.83 136.74 137.53 137.37	TA 53 TA 52 TA 10 AVG	137.78 136.74 137.58 137.37	TA 16 TA 22 TA 54 AVG	137.62 137.02 137.04 137.23	TA 34 TA 21 TA 48 AVG	138.20 136.33 137.39 137.31
7 DAYS	TA 11 TA 1 TA 43 AVG	138.05 136.49 137.40 137.31	TA 31 TA 5 TA 14 AVG	137.64 136.92 137.16 137.24	TA 50 TA 20 TA 59 AVG	138.17 136.50 137.45 137.37	TA 58 TA 7 TA 8 AVG	137.59 136.95 137.04 137.19
28 DAYS	TA 30 TA 56 TA 57 AVG	137.72 136.93 137.03 137.23	TA 60 TA 2 TA 15 AVG	138.35 135.92 137.32 137.20	TA 32 TA 6 TA 28 AVG	138.29 136.45 137.25 137.33	TA 33 TA 12 TA 44 AVG	137.87 136.74 137.56 137.39
90 DAYS	TA 39 TA 23 TA 46 AVG	137.94 136.69 137.24 137.29	TA 35 TA 27 TA 9 AVG	137.89 136.68 137.23 137.27	TA 45 TA 4 TA 36 AVG	137.98 136.67 137.19 137.28	TA 38 TA 3 TA 49 AVG	138.14 136.49 137.45 137.36

NOTE: 0 DAY, 6 MONTHS, 1 YEAR, 2 YEARS AND 3 YEARS DURATION FOR NATURAL WEATHERING

Table A.2--continued

DURATION	ULTRAVIOLET		NATURAL WEATHERING		FORCED DRAFT		NORMAL OVEN	
DAYS	SPEC #	UNIT WT pcf	SPEC #	UNIT WT pcf	SPEC #	UNIT WT pcf	SPEC #	UNIT WT pcf
0 DAY	SO 32 SO 26 SO 31 AVG	136.95 136.06 136.42 136.47	SO 11 SO 23 SO 2 AVG	137.41 135.67 136.45 136.51	SO 40 SO 25 SO 24 AVG	136.69 136.27 136.68 136.55	SO 35 SO 53 SO 34 AVG	136.87 136.15 136.34 136.45
1 DAY	SO 37 SO 19 SO 13 AVG	136.86 136.15 136.32 136.44	SO 43 SO 60 SO 50 AVG	136.85 136.13 136.39 136.46	SO 36 SO 22 SO 27 AVG	136.77 136.08 136.37 136.41	SO 12 SO 33 SO 49 AVG	137.23 135.77 136.47 136.49
7 DAYS	SO 52 SO 30 SO 57 AVG	137.00 135.86 136.55 136.47	SO 18 SO 56 SO 44 AVG	136.76 136.16 136.68 136.53	SO 16 SO 55 SO 48 AVG	136.99 136.03 136.42 136.48	SO 47 SO 54 SO 42 AVG	137.02 135.88 136.55 136.48
28 DAYS	SO 9 SO 45 SO 6 AVG	137.84 135.74 136.45 136.68	SO 39 SO 28 SO 21 AVG	137.17 136.00 136.50 136.56	SO 8 SO 41 SO 29 AVG	137.08 135.95 136.61 136.55	SO 38 SO 3 SO 5 AVG	136.69 136.25 136.66 136.54
90 DAYS	SO 1 SO 20 SO 10 AVG	136.77 136.26 136.64 136.56	SO 7 SO 59 SO 46 AVG	136.88 136.04 136.42 136.45	SO 15 SO 4 SO 51 AVG	137.25 135.84 136.44 136.51	SO 17 SO 58 SO 14 AVG	136.99 136.01 136.39 136.45

NOTE: 0 DAY, 6 MONTHS, 1 YEAR, 2 YEARS AND 3 YEARS DURATION FOR NATURAL WEATHERING

Table A.2--continued

DURATION	NORMAL OVEN		FORCED DRAFT		ULTRAVIOLET		NATURAL WEATHERING	
DAYS	SPEC #	UNIT WT pcf	SPEC #	UNIT WT pcf	SPEC #	UNIT WT pcf	SPEC #	UNIT WT pcf
0 DAY	BO 10	137.06	BO 39	137.42	BO 23	136.85	BO 15	136.73
	BO 54	135.85	BO 20	134.93	BO 32	136.28	BO 38	136.40
	BO 49	136.68	BO 25	136.55	BO 22	136.71	BO 9	136.46
	AVG	136.53	AVG	136.30	AVG	136.61	AVG	136.53
1 DAY	BO 18	137.49	BO 30	137.12	BO 35	137.29	BO 43	137.10
	BO 60	135.18	BO 24	136.00	BO 52	135.59	BO 57	135.92
	BO 2	136.59	BO 8	136.63	BO 3	136.55	BO 4	136.68
	AVG	136.42	AVG	136.61	AVG	136.48	AVG	136.57
7 DAYS	BO 31	136.88	BO 14	136.93	BO 21	136.75	BO 17	137.22
	BO 56	136.32	BO 58	136.15	BO 46	136.41	BO 16	135.44
	BO 26	136.69	BO 40	136.50	BO 33	136.47	BO 7	136.63
	AVG	136.63	AVG	136.53	AVG	136.54	AVG	136.43
28 DAYS	BO 48	136.79	BO 5	136.88	BO 19	137.06	BO 11	137.03
	BO 59	136.37	BO 47	136.31	BO 53	136.11	BO 44	136.10
	BO 37	136.42	BO 51	136.71	BO 29	136.48	BO 1	136.47
	AVG	136.53	AVG	136.63	AVG	136.55	AVG	136.53
90 DAYS	BO 45	136.94	BO 27	136.77	BO 34	137.10	BO 36	136.88
	BO 28	136.23	BO 13	136.37	BO 55	135.96	BO 12	136.35
	BO 41	136.51	BO 6	136.47	BO 50	136.68	BO 42	136.71
	AVG	136.56	AVG	136.54	AVG	136.58	AVG	136.64

NOTE: 0 DAY, 6 MONTHS, 1 YEAR, 2 YEARS AND 3 YEARS DURATION FOR NATURAL WEATHERING

Table A.2--continued

DURATION	NORMAL OVEN		ULTRAVIOLET		NORMAL OVEN		ULTRAVIOLET	
DAYS	SPEC #	UNIT WT pcf	SPEC #	UNIT WT pcf	SPEC #	UNIT WT pcf	SPEC #	UNIT WT pcf
0 DAY	DI 1 DI 10 DI 25 AVG	137.84 137.33 136.51 137.23			DM 4 DM 17 DM 14 AVG	137.88 137.24 137.43 137.52		
1 DAY	DI 7 DI 2 DI 23 AVG	137.76 137.43 136.63 137.27	DI 15 DI 16 DI 21 AVG	137.83 137.09 136.52 137.15	DM 16 DM 6 DM 12 AVG	138.07 137.77 137.16 137.67	DM 15 DM 24 DM 23 AVG	138.29 137.28 136.96 137.51
7 DAYS	DI 13 DI 18 DI 26 AVG	137.68 137.08 136.77 137.18	DI 17 DI 14 DI 9 AVG	137.70 137.44 136.67 137.27	DM 7 DM 21 DM 3 AVG	138.39 137.29 136.94 137.54	DM 1 DM 19 DM 2 AVG	137.90 137.88 137.22 137.67
28 DAYS	DI 4 DI 8 DI 3 AVG	137.57 136.80 137.23 137.20	DI 6 DI 22 DI 20 AVG	137.63 136.99 136.79 137.14	DM 25 DM 26 DM 9 AVG	138.71 137.44 135.63 137.26	DM 8 DM 11 DM 5 AVG	138.12 137.26 137.06 137.48
90 DAYS	DI 12 DI 19 DI 27 AVG	138.48 137.15 136.05 137.23	DI 11 DI 5 DI 24 AVG	138.30 137.35 136.05 137.23	DM 10 DM 13 DM 27 AVG	138.15 137.27 137.03 137.48	DM 20 DM 18 DM 22 AVG	138.59 137.68 136.71 137.66

APPENDIX B

RESULTS OF MIXTURE STRENGTH TESTS

Table B.1 Results of Indirect Tensile Test

CHEVRON AC-30

DURATION	OVEN				ULTRAVIOLET				FORCED DRAFT			
DAYS	SPEC #	HT in	LOAD lbs	STRESS psi	SPEC #	HT in	LOAD lbs	STRESS psi	SPEC #	HT in	LOAD lbs	STRESS psi
0 DAY	CH 34 CH 21 CH 57 AVG	2.548 2.535 2.551	1981.25 1712.51 1868.75	121.26 105.37 114.26 113.63								
1 DAY	CH 52 CH 11 CH 49 AVG	2.523 2.556 2.526	1812.50 1809.36 1878.13	112.05 110.41 115.86 112.76	CH 46 CH 16 CH 25 AVG	2.535 2.561 2.550	1906.25 1818.75 1881.25	117.29 110.77 115.07 114.37	CH 17 CH 31 CH 10 AVG	2.573 2.522 2.521	1800.00 2025.00 1900.00	109.11 125.23 117.55 117.30
7 DAYS	CH 5 CH 22 CH 20 AVG	2.534 2.552 2.547	2059.38 2212.50 1981.25	126.76 135.22 121.33 127.77	CH 45 CH 9 CH 32 AVG	2.542 2.562 2.519	2075.00 2212.50 2075.00	127.32 134.69 128.46 130.16	CH 14 CH 38 CH 28 AVG	2.516 2.563 2.551	2000.00 2062.50 2125.00	123.89 125.51 129.93 126.44
28 DAYS	CH 36 CH 15 CH 37 AVG	2.450 2.512 2.576	2450.00 2281.30 2500.00	153.47 141.65 151.25 148.79	CH 33 CH 7 CH 27 AVG	2.512 2.582 2.547	2675.00 2500.00 2537.50	166.09 151.02 155.39 157.50	CH 3 CH 58 CH 26 AVG	2.526 2.552 2.552	2687.50 2562.50 2562.50	165.81 156.61 156.61 159.68
90 DAYS	CH 24 CH 8 CH 13 AVG	2.562 2.549 2.538	3087.50 2981.25 3012.50	189.44 182.42 185.13 185.66	CH 35 CH 55 CH 19 AVG	2.525 2.586 2.539	3012.50 3062.50 2937.50	186.08 184.71 180.45 183.75	CH 39 CH 56 CH 2 AVG	2.511 2.534 2.499	3312.00 3250.00 3075.00	205.73 200.04 191.82 199.23

Table 6.1--continued

BELCHER AC-30

DURATION	OVEN				ULTRAVIOLET				FORCED DRAFT			
DAYS	SPEC #	HT in	LOAD lbs	STRESS psi	SPEC #	HT in	LOAD lbs	STRESS psi	SPEC #	HT in	LOAD lbs	STRESS psi
0 DAY	BE 17 BE 48 BE 18 AVG	2.543 2.554 2.556	2062.50 1800.00 2115.63	126.50 109.93 129.10 121.84								
1 DAY	BE 4 BE 25 BE 26 AVG	2.538 2.547 2.549	1937.50 1806.25 1800.00	119.07 110.61 110.14 113.27	BE 30 BE 20 BE 45 AVG	2.541 2.543 2.546	1900.00 1887.50 1812.50	116.63 115.77 111.04 114.48	BE 33 BE 55 BE 11 AVG	2.528 2.556 2.534	2026.50 2150.00 2250.00	125.03 131.09 138.49 131.54
7 DAYS	BE 14 BE 7 BE 29 AVG	2.521 2.559 2.511	2081.25 2062.50 2118.75	128.76 125.71 131.61 128.69	BE 46 BE 3 BE 54 AVG	2.518 2.559 2.522	2350.00 2137.50 2125.00	145.57 130.28 131.42 135.76	BE 24 BE 34 BE 35 AVG	2.553 2.525 2.531	2337.50 2050.00 2262.50	142.81 126.63 139.43 136.29
28 DAYS	BE 36 BE 12 BE 22 AVG	2.524 2.551 2.545	2625.00 2500.00 2550.00	162.21 152.85 156.28 157.11	BE 19 BE 6 BE 37 AVG	2.543 2.553 2.543	2837.50 2650.00 2475.00	174.03 161.90 151.80 162.58	BE 60 BE 2 BE 13 AVG	2.530 2.553 2.538	2912.50 2662.50 2500.00	179.55 162.66 153.64 165.28
90 DAYS	BE 59 BE 56 BE 42 AVG	2.533 2.550 2.548	3187.50 2775.00 3093.75	196.27 169.73 189.38 185.13	BE 51 BE 1 BE 58 AVG	2.534 2.551 2.539	3262.50 3062.50 3412.50	200.81 197.25 209.63 199.23	BE 9 BE 29 BE 53 AVG	2.528 2.505 2.529	3250.00 3175.00 3400.00	200.52 197.69 209.69 202.63

Table 8.1--continued

AMOCO AC-30

DURATION	OVEN				ULTRAVIOLET				FORCED DRAFT			
DAYS	SPEC #	HT in	LOAD lbs	STRESS psi	SPEC #	HT in	LOAD lbs	STRESS psi	SPEC #	HT in	LOAD lbs	STRESS psi
0 DAY	AM 39 AM 60 AM 41 AVG	2.527 2.546 2.530	2500.00 2250.00 2250.00	154.30 137.84 138.71 143.62								
1 DAY	AM 13 AM 31 AM 44 AVG	2.513 2.535 2.518	1612.50 1550.00 2212.50	100.08 95.37 137.05 110.83	AM 38 AM 57 AM 27 AVG	2.514 2.537 2.542	2237.50 2212.50 2125.00	138.82 136.02 130.39 135.07	AM 49 AM 3 AM 25 AVG	2.524 2.530 2.526	2250.00 2137.50 2350.00	139.04 131.77 145.10 138.64
7 DAYS	AM 5 AM 36 AM 26 AVG	2.505 2.539 2.532	2543.75 2487.50 2800.00	158.38 152.81 172.48 161.22	AM 20 AM 56 AM 1 AVG	2.534 2.553 2.521	2675.00 2637.50 2756.25	164.65 161.13 170.53 165.44	AM 7 AM 33 AM 48 AVG	2.516 2.567 2.527	2350.00 2312.50 2362.50	145.68 140.51 145.82 144.00
28 DAYS	AM 10 AM 32 AM 40 AVG	2.535 2.552 2.538	2962.50 2975.00 3000.00	182.27 181.82 184.36 182.82	AM 14 AM 21 AM 42 AVG	2.526 2.572 2.538	3000.00 2850.00 3000.00	185.24 172.83 184.35 180.81	AM 2 AM 50 AM 35 AVG	2.528 2.550 2.546	3037.00 2875.00 2875.00	187.38 175.85 176.13 179.78
90 DAYS	AM 45 AM 18 AM 22	2.532 2.529 2.551	3725.00 3500.00 3700.00	229.46 215.86 226.22 223.85	AM 9 AM 34 AM 51 AVG	2.534 2.552 2.542	3750.00 3562.50 3750.00	230.82 217.73 230.08 226.21	AM 28 AM 23 AM 30 AVG	2.558 2.537 2.551	3875.00 3500.00 3860.00	236.27 215.18 237.23 229.56

Table 6.1--continued

MARIANI AC-30

DURATION	OVEN				ULTRAVIOLET				FORCED DRAFT			
DAYS	SPEC #	HT in	LOAD lbs	STRESS psi	SPEC #	HT in	LOAD lbs	STRESS psi	SPEC #	HT in	LOAD lbs	STRESS psi
0 DAY	MA 4 MA 36 MA 31 AVG	2.503 2.565 2.513	2575.00 2350.00 2337.50	160.46 142.50 145.08 149.48								
1 DAY	MA 19 MA 51 MA 12 AVG	2.510 2.524 2.503	2539.00 2400.00 2450.00	157.71 148.31 152.67 152.50	MA 14 MA 42 MA 57 AVG	2.556 2.550 2.554	2387.50 1987.50 2362.50	145.69 121.57 144.28 137.18	MA 17 MA 52 MA 2 AVG	2.505 2.564 2.496	2350.00 2087.50 2350.50	146.32 126.99 146.88 140.06
7 DAYS	MA 20 MA 47 MA 58 AVG	2.517 2.539 2.524	2562.50 2418.75 2593.75	158.79 148.58 160.28 155.89	MA 54 MA 43 MA 16 AVG	2.514 2.517 2.537	2787.50 2537.50 2668.75	172.94 157.24 164.07 164.75	MA 32 MA 60 MA 18 AVG	2.497 2.539 2.527	2400.00 2350.00 2312.50	149.91 144.36 142.73 145.67
28 DAYS	MA 29 MA 34 MA 8 AVG	2.536 2.529 2.509	3000.00 2812.50 3000.00	184.51 173.46 186.49 181.49	MA 27 MA 49 MA 9 AVG	2.501 2.562 2.526	3025.00 2812.50 2850.00	188.65 171.22 175.98 178.62	MA 15 MA 22 MA 41 AVG	2.528 2.560 2.547	3162.50 2750.00 2825.00	195.12 167.55 173.00 178.55
90 DAYS	MA 26 MA 48 MA 53 AVG	2.508 2.540 2.530	3500.00 3437.50 3275.00	217.66 211.08 201.90 210.22	MA 3 MA 45 MA 39 AVG	2.513 2.558 2.539	3462.50 3237.50 3250.00	214.90 197.40 199.65 203.98	MA 59 MA 37 MA 28 AVG	2.514 2.528 2.537	3975.00 3375.00 3887.50	246.61 208.23 239.00 231.28

Table 9.1--continued

TEXACO 85-100

DURATION	OVEN				ULTRAVIOLET				FORCED DRAFT			
DAYS	SPEC #	HT in	LOAD lbs	STRESS psi	SPEC #	HT in	LOAD lbs	STRESS psi	SPEC #	HT in	LOAD lbs	STRESS psi
0 DAY	TX 1 TX 26 TX 19 AVG	2.531 2.546 2.547	2087.50 2018.75 2112.50	128.64 123.67 129.36 127.23								
1 DAY	TX 2 TX 11 TX 32 AVG	2.500 2.559 2.540	2243.75 2031.25 2250.00	139.98 121.81 138.16 133.98	TX 33 TX 60 TX 51 AVG	2.541 2.543 2.546	1950.00 1931.25 1956.00	119.69 118.45 119.83 119.32	TX 31 TX 39 TX 23 AVG	2.507 2.547 2.548	2406.25 2250.00 2250.00	149.70 137.78 137.73 141.74
7 DAYS	TX 55 TX 15 TX 5 AVG	2.523 2.550 2.536	2493.80 2135.00 2262.50	154.17 129.98 139.15 141.10	TX 58 TX 20 TX 52 AVG	2.540 2.558 2.550	2350.00 2362.50 2375.00	144.30 144.05 145.27 144.54	TX 41 TX 13 TX 12 AVG	2.516 2.520 2.531	2825.00 2625.00 2625.00	175.13 162.47 161.76 166.45
28 DAYS	TX 3 TX 56 TX 30 AVG	2.527 2.543 2.523	2925.00 2750.00 2937.50	180.54 168.27 181.60 176.80	TX 42 TX 21 TX 34 AVG	2.538 2.550 2.515	2887.50 2712.50 2662.50	177.45 165.91 165.12 169.49	TX 7 TX 28 TX 47 AVG	2.531 2.523 2.521	3062.00 2962.00 2875.00	188.69 183.11 177.87 183.23
90 DAYS	TX 46 TX 18 TX 40 AVG	2.525 2.536 2.525	3462.00 3237.00 3487.00	213.85 199.09 215.40 209.44	TX 9 TX 37 TX 54 AVG	2.518 2.538 2.524	3387.00 3250.00 3375.00	209.80 199.73 208.56 206.03	TX 35 TX 49 TX 58 AVG	2.523 2.525 2.520	3675.00 3525.00 3750.00	227.19 217.74 232.10 225.68

Table 6.1—continued

TEXACO AIRBLOWN 85-100

DURATION	OVEN				ULTRAVIOLET				FORCED DRAFT			
DAYS	SPEC #	HT in	LOAD lbs	STRESS psi	SPEC #	HT in	LOAD lbs	STRESS psi	SPEC #	HT in	LOAD lbs	STRESS psi
0 DAY	TA 40	2.517	1353.13	63.85								
	TA 29	2.520	1325.00	62.01								
	TA 47	2.533	1400.00	66.21								
	AVG			64.02								
1 DAY	TA 16	2.521	1418.75	87.78	TA 34	2.510	1250.00	77.68	TA 53	2.532	1400.00	86.24
	TA 22	2.521	1262.50	78.11	TA 21	2.523	1125.00	69.55	TA 52	2.544	1337.50	82.00
	TA 54	2.538	1350.00	62.96	TA 48	2.533	1350.00	63.13	TA 10	2.516	1462.50	90.66
	AVG			62.95	AVG			76.78	AVG			86.30
7 DAYS	TA 50	2.459	1450.00	91.97	TA 59	2.525	1550.00	95.74	TA 31	2.512	1500.00	93.14
	TA 20	2.539	1406.30	66.39	TA 7	2.525	1525.00	94.20	TA 5	2.510	1525.00	94.76
	TA 59	2.526	1462.50	90.30	TA 6	2.525	1512.50	93.43	TA 14	2.522	1575.00	97.40
	AVG			69.56	AVG			94.46	AVG			95.10
28 DAYS	TA 32	2.492	1750.00	109.53	TA 33	2.513	1612.50	100.08	TA 60	2.499	1937.00	120.50
	TA 6	2.536	1612.50	99.17	TA 12	2.540	1562.50	95.95	TA 2	2.534	1500.00	92.33
	TA 28	2.519	1687.50	104.49	TA 44	2.523	1687.50	104.32	TA 15	2.507	1800.00	111.99
	AVG			104.40	AVG			100.12	AVG			108.40
90 DAYS	TA 45	2.509	2100.00	130.55	TA 38	2.450	2025.00	126.84	TA 35	2.504	2225.00	138.59
	TA 4	2.505	1725.00	107.41	TA 3	2.536	1725.00	106.09	TA 27	2.524	2050.00	126.68
	TA 36	2.516	2025.00	125.53	TA 49	2.516	1700.00	105.39	TA 9	2.517	2100.00	130.13
	AVG			121.16	AVG			112.77	AVG			131.80

Table B.1--continued

ESSO 25-35

DURATION	OVEN				ULTRAVIOLET				FORCED DRAFT			
DAYS	SPEC #	HT in	LOAD lbs	STRESS psi	SPEC #	HT in	LOAD lbs	STRESS psi	SPEC #	HT in	LOAD lbs	STRESS psi
0 DAY	SO 35 SO 53 SO 34 AVG	2.529 2.560 2.553	3287.50 3337.50 3262.50	202.75 203.34 199.32 201.80								
1 DAY	SO 12 SO 33 SO 49 AVG	2.533 2.557 2.557	3525.00 3375.00 3212.50	217.05 205.87 195.96 206.29	SO 37 SO 19 SO 13 AVG	2.541 2.552 2.544	3212.50 3087.50 3125.00	197.19 188.70 191.59 192.49	SO 36 SO 22 SO 27 AVG	2.554 2.559 2.532	3375.00 3600.00 3275.00	206.11 219.42 201.74 209.09
7 DAYS	SO 47 SO 54 SO 42 AVG	2.543 2.559 2.547	3531.30 3687.50 3800.00	216.59 224.75 232.70 224.68	SO 52 SO 30 SO 57 AVG	2.547 2.540 2.555	4000.00 3500.00 3762.50	244.95 214.92 229.68 229.85	SO 16 SO 55 SO 48 AVG	2.528 2.553 2.544	4087.00 4112.00 3725.00	252.16 251.22 228.38 243.92
28 DAYS	SO 38 SO 3 SO 5 AVG	2.541 2.557 2.551	4125.00 4362.50 4437.50	253.20 266.10 271.31 263.54	SO 9 SO 45 SO 6 AVG	2.511 2.566 2.549	4375.00 4100.00 4262.50	271.75 249.21 260.82 260.60	SO 8 SO 41 SO 29 AVG	2.511 2.552 2.537	4450.00 4375.00 3862.00	276.41 267.39 237.43 260.41
90 DAYS	SO 17 SO 58 SO 14 AVG	2.522 2.535 2.520	5112.00 4712.00 4875.00	316.15 288.92 300.78 302.28	SO 1 SO 20 SO 10 AVG	2.521 2.537 2.505	4375.00 4388.00 4713.00	270.68 269.77 293.45 277.97	SO 15 SO 4 SO 51 AVG	2.524 2.547 2.541	5237.00 4950.00 5275.00	323.62 303.12 323.79 316.85

Table B.1--continued

ROSCAN 85-100

DURATION	OVEN				ULTRAVIOLET				FORCED DRAFT			
DAYS	SPEC #	WT in	LOAD lbs	STRESS psi	SPEC #	WT in	LOAD lbs	STRESS psi	SPEC #	WT in	LOAD lbs	STRESS psi
0 DAY	BO 10 BO 54 BO 49 AVG	2.537 2.568 2.552	1750.00 1681.25 1706.25	107.59 102.19 104.28 104.69								
1 DAY	BO 18 BO 60 BO 2 AVG	2.522 2.566 2.540	1931.25 1771.88 1962.50	119.44 107.70 120.51 115.88	BO 35 BO 52 BO 3 AVG	2.534 2.557 2.545	1712.50 1543.75 1718.75	105.41 94.17 105.33 101.64	BO 30 BO 8 BO 24 AVG	2.527 2.552 2.540	1925.00 1950.00 1975.00	118.81 119.19 121.27 119.75
7 DAYS	BO 31 BO 56 BO 26 AVG	2.516 2.548 2.545	1875.00 1812.50 1906.30	116.23 110.95 118.93 114.67	BO 21 BO 48 BO 33 AVG	2.516 2.554 2.531	1962.50 2100.00 1906.30	121.68 128.25 117.47 122.46	BO 58 BO 14 BO 40 AVG	2.509 2.515 2.528	2275.00 2250.00 2337.00	141.42 139.87 144.33 142.08
28 DAYS	BO 48 BO 59 BO 37 AVG	2.532 2.544 2.549	2500.00 2412.50 2512.50	154.00 147.91 153.74 151.88	BO 19 BO 53 BO 29 AVG	2.532 2.564 2.549	2500.00 2500.00 2212.50	154.00 152.08 135.38 147.15	BO 5 BO 47 BO 51 AVG	2.533 2.542 2.534	2625.00 2488.00 2562.00	161.64 152.66 157.69 157.33
90 DAYS	BO 45 BO 28 BO 41 AVG	2.528 2.536 2.544	3450.00 3200.00 3225.00	212.86 196.81 197.72 202.46	BO 55 BO 50 BO 34 AVG	2.539 2.532 2.505	3050.00 3137.00 3225.00	187.36 193.24 200.80 193.80	BO 8 BO 13 BO 27 AVG	2.518 2.550 2.532	3125.00 3250.00 3225.00	193.72 198.79 198.66 197.06

Table 8.1--continued

CHEVRON AC-20

DURATION	OVEN				ULTRAVIOLET			
DAYS	SPEC #	HT in	LOAD lbs	STRESS psi	SPEC #	HT in	LOAD lbs	STRESS psi
0 DAY	DI 1 DI 10 DI 25 AVG	2.523 2.538 2.553	2250.00 2050.00 1975.00	138.09 125.98 120.68 132.54				
1 DAY	DI 7 DI 2 DI 23 AVG	2.522 2.527 2.538	1987.50 1900.00 1750.00	122.92 117.27 107.63 120.09	DI 15 DI 16 DI 21 AVG	2.523 2.538 2.582	1937.50 1762.50 1737.50	119.78 108.31 105.78 114.04
7 DAYS	DI 13 DI 18 DI 26 AVG	2.527 2.537 2.547	2200.00 2137.50 2062.50	135.79 131.41 126.30 133.60	DI 17 DI 14 DI 9 AVG	2.531 2.535 2.556	2237.50 2062.50 2137.50	137.88 126.90 130.43 132.39
28 DAYS	DI 4 DI 8 DI 3 AVG	2.530 2.524 2.535	2625.00 2518.75 2737.50	161.83 155.65 169.43 158.74	DI 6 DI 22 DI 20 AVG	2.516 2.534 2.537	2693.75 2643.75 2718.75	166.99 162.73 167.15 164.88
50 DAYS	DI 12 DI 19 DI 27 AVG	2.508 2.538 2.539	3500.00 3325.00 3000.00	217.66 204.50 184.29 211.08	DI 11 DI 5 DI 24 AVG	2.500 2.516 2.560	3287.50 3250.00 3125.00	205.10 201.47 190.39 203.29

Table 8.1--continued

CHEVRON AC-20 MODIFIED

DURATION	OVEN				ULTRAVIOLET			
DAYS	SPEC #	HT in	LOAD lbs	STRESS psi	SPEC #	HT in	LOAD lbs	STRESS psi
0 DAY	DM 4 DM 17 DM 14 AVG	2.518 2.527 2.534	1787.50 1750.00 1725.00	110.72 108.01 106.18 108.30				
1 DAY	DM 16 DM 6 DM 12 AVG	2.517 2.512 2.536	1687.50 1625.00 1625.00	104.57 100.90 99.94 101.80	DM 15 DM 24 DM 23 AVG	2.514 2.537 2.520	1712.50 1525.00 1562.50	106.25 93.76 96.71 98.90
7 DAYS	DM 7 DM 21 DM 3 AVG	2.514 2.535 2.541	2050.00 1812.50 1887.50	127.18 111.52 115.66 118.19	DM 1 DM 19 DM 2 AVG	2.512 2.526 2.534	1962.50 2000.00 2100.00	121.65 123.49 129.26 124.87
26 DAYS	DM 25 DM 26 DM 9 AVG	2.505 2.534 2.563	2375.00 2237.50 2168.75	147.88 137.72 131.98 139.19	DM 8 DM 11 DM 5 AVG	2.505 2.526 2.529	2768.75 2481.25 2562.50	172.39 153.21 158.04 161.21
90 DAYS	DM 10 DM 13 DM 27 AVG	2.519 2.523 2.537	3125.00 2925.00 2912.50	193.49 180.82 179.06 184.46	DM 20 DM 18 DM 22 AVG	2.500 2.516 2.537	3000.00 3100.00 2875.00	187.17 192.17 176.75 185.36

Table 5.2 Results of Resilient Modulus Test

MARIANI AC-30

OVEN EXPOSURE										
			Deformation							
DURATION DAYS	SPEC #	HT in	IR(A) divn	IR(B) divn	TR(A) divn	TR(B) divn	TD(A) divn	TD(B) divn	RESILIENT MODULUS(IR) psi	RESILIENT MODULUS(TR) psi
NO EXP	MA 36	2.565	8.65	10.10	13.00	13.90	14.10	14.80	257829.76	179714.05
	MA 31	2.513	9.30	7.20	13.10	11.80	14.40	13.00	293051.00	199166.32
	MA 4	2.503	9.80	8.20	13.60	11.30	14.30	13.00	275225.29	198558.04
	AVG								277368.68	192279.47
7 DAYS	MA 58	2.524	8.10	8.10	11.40	12.50	12.00	13.00	303261.53	205558.02
	MA 20	2.517	8.50	8.90	11.90	13.00	12.40	13.50	283132.17	197851.40
	MA 47	2.539	8.10	8.40	12.80	12.80	13.20	13.50	295988.64	190773.93
									294127.45	198061.12
28 DAYS	MA 29	2.536	7.40	7.60	11.00	12.00	11.50	12.30	325972.66	212590.87
	MA 8	2.509	7.80	8.20	12.40	12.30	12.70	12.50	308888.00	200083.39
	MA 34	2.529	8.50	8.60	11.80	12.40	11.90	12.70	286732.38	202608.42
									307197.68	205096.23
90 DAYS	MA 26	2.508	7.20	8.40	9.90	10.40	9.90	10.40	316934.53	243555.60
	MA 40	2.540	7.90	7.70	10.00	11.10	10.20	11.40	314960.63	231369.18
	MA 53	2.530	6.50	6.90	8.50	10.80	8.90	10.90	365760.13	253947.45
									332551.76	242957.41

Note:
IR - Instantaneous Recoverable
TR - Total Recoverable
TD - Total Deformation
one divn = .00002 in

Table 9.2--continued

MARIANI AC-30

ULTRAVIOLET EXPOSURE										
			Deformation							
DURATION DAYS	SPEC #	HT in	IR(A) divn	IR(B) divn	TR(A) divn	TR(B) divn	TD(A) divn	TD(B) divn	RESILIENT MODULUS(IR) psi	RESILIENT MODULUS(TR) psi
NO EXP	MA 36	2.565	8.65	10.10	13.00	13.90	14.10	14.80	257829.76	179714.05
	MA 31	2.513	9.30	7.20	13.10	11.80	14.40	13.00	299051.00	190166.32
	MA 4	2.503	9.80	8.20	13.60	11.30	14.30	13.00	275225.29	190958.04
	AVG								277368.68	192279.47
7 DAYS	MA 54	2.514	8.60	7.60	13.90	11.90	14.30	12.30	304467.82	191177.47
	MA 43	2.517	8.80	8.10	13.10	12.80	13.30	13.50	291508.86	189480.76
	MA 16	2.537	8.40	7.80	13.30	11.20	13.70	11.60	307400.16	199496.43
	AVG								301125.62	193384.89
28 DAYS	MA 27	2.501	7.00	8.20	11.50	13.00	11.90	13.30	326185.32	202368.03
	MA 49	2.562	7.40	7.30	10.80	11.90	11.10	12.40	329249.58	213214.48
	MA 9	2.526	8.00	9.20	11.50	13.00	11.60	13.10	285403.59	200365.18
	AVG								313612.93	205315.90
90 DAYS	MA 3	2.513	7.90	6.60	11.70	10.10	11.80	10.20	340299.41	226345.94
	MA 45	2.558	7.90	5.90	11.90	9.00	12.00	9.80	351270.81	231939.58
	MA 39	2.539	7.50	5.80	10.10	9.10	10.40	9.20	367203.95	254365.24
	AVG								352924.72	237550.25

Note:
IR - Instantaneous Recoverable
TR - Total Recoverable
TD - Total Deformation
one divn - .00002 in

Table 8.2--continued

AMOCO AC-30

OVEN EXPOSURE										
DURATION DAYS	SPEC #	HT in	Deformation						RESILIENT MODULUS(IR) psi	RESILIENT MODULUS(TR) psi
			IR(A) divn	IR(B) divn	TR(A) divn	TR(B) divn	TD(A) divn	TD(B) divn		
NO EXP	AM 60	2.546	7.90	8.60	12.80	13.40	14.00	14.80	295174.84	185892.55
	AM 41	2.530	8.80	7.30	14.50	13.90	16.40	16.10	293484.18	172576.96
	AM 39	2.527	8.00	9.00	13.30	13.70	13.90	14.60	288547.31	181740.90
	AVG								292435.45	180070.14
7 DAYS	AM 5	2.505	9.00	7.50	13.60	12.20	14.40	12.90	300006.05	191864.33
	AM 36	2.539	8.50	8.60	13.40	13.10	14.30	13.80	285603.07	184294.81
	AM 26	2.532	8.20	7.40	13.30	11.90	13.60	12.50	313930.41	194337.87
									299846.51	190165.67
28 DAYS	AM 32	2.552	8.40	8.00	11.40	11.50	11.70	11.70	296276.47	212180.53
	AM 40	2.538	7.30	8.30	11.80	11.90	12.10	12.00	313189.26	206149.23
	AM 10	2.535	6.30	8.70	10.10	13.10	10.40	13.30	326101.25	210941.32
									311855.33	209723.70
90 DAYS	AM 45	2.532	7.00	7.00	9.30	9.30	10.00	9.50	349808.17	255068.46
	AM 18	2.529	7.70	7.80	12.00	11.30	12.10	11.40	316330.57	210434.50
	AM 22	2.551	7.70	7.20	10.50	10.10	10.50	10.20	326230.80	235363.05
									330789.84	233822.00

Note:
IR - Instantaneous Recoverable   TD - Total Deformation
TR - Total Recoverable   one divn = .00002 in

Table H.2--continued

AMOCO AC-30

DURATION DAYS	ULTRAVIOLET									
	SPEC #	HT in	Deformation						RESILIENT MODULUS(IR) psi	RESILIENT MODULUS(TR) psi
			IR(A) divn	IR(B) divn	TR(A) divn	TR(B) divn	TD(A) divn	TD(B) divn		
NO EXP	AM 60	2.546	7.90	8.60	12.80	13.40	14.00	14.80	295174.84	185892.55
	AM 41	2.530	8.80	7.90	14.50	13.90	15.40	16.10	293484.18	172576.96
	AM 39	2.527	8.00	9.00	13.30	13.70	13.90	14.60	288647.31	181740.90
	AVG								292435.45	180070.14
7 DAYS	AM 20	2.534	8.50	8.00	12.80	13.60	13.60	14.00	296572.67	185357.92
	AM 56	2.553	8.30	7.50	12.10	11.30	12.70	12.30	307407.02	207565.42
	AM 1	2.521	8.00	8.20	12.90	12.70	13.60	13.30	303622.41	192136.06
									302534.04	195019.80
28 DAYS	AM 14	2.526	8.70	7.20	11.60	10.70	12.00	11.20	309739.80	220132.15
	AM 21	2.572	7.40	8.90	12.00	12.90	12.60	13.20	295776.13	193620.52
	AM 42	2.538	7.40	6.40	10.20	8.70	10.40	9.20	354038.90	258504.59
									319517.94	224085.75
90 DAYS	AM 9	2.534	5.90	6.90	8.70	9.60	9.00	9.70	382300.71	267401.59
	AM 34	2.552	6.70	6.00	9.70	9.10	9.90	9.40	382593.24	258453.95
	AM 51	2.542	8.70	7.80	12.10	10.40	12.30	10.70	295639.32	216802.17
									353511.09	247552.57

Note:
IR - Instantaneous Recoverable
TR - Total Recoverable

TD - Total Deformation
one divn = .00002 in

Table E.2--continued

CHEVRON AC-20

OVEN EXPOSURE										
			Deformation							
DURATION DAYS	SPEC #	HT in	IR(A) divn	IR(B) divn	TR(A) divn	TR(B) divn	TD(A) divn	TD(B) divn	RESILIENT MODULUS(IR) psi	RESILIENT MODULUS(TR) psi
NO EXP	DI 1	2.523	7.50	9.10	11.10	13.30	11.10	14.20	296071.32	201425.57
	DI 10	2.538	9.60	9.80	14.50	14.20	15.40	15.70	251842.10	170234.73
	DI 25	2.553	8.00	8.10	13.80	12.50	14.60	13.70	301678.94	184677.98
	AVG								283197.48	185446.10
28 DAYS	DI 3	2.535	9.80	9.00	12.60	11.50	12.60	11.80	260187.17	202967.58
	DI 8	2.524	9.00	9.20	12.70	11.90	13.00	12.30	269936.09	199708.81
	DI 4	2.530	7.80	6.30	11.00	11.50	11.10	11.70	347601.83	217830.48
	AVG								292575.03	206835.62
90 DAYS	DI 12	2.508	7.30	7.60	9.90	10.70	10.10	10.70	331824.07	240008.67
	DI 27	2.539	7.20	8.70	10.80	9.50	11.00	9.60	351353.42	240581.90
	DI 19	2.538	7.70	7.90	10.70	10.30	10.90	10.30	313435.25	232837.61
	AVG								332204.25	237809.39

Note:
IR - Instantaneous Recoverable
TR - Total Recoverable
TD - Total Deflection
one divn = .00002 in

Table B.2--continued

CHEVRON AC-20

ULTRAVIOLET EXPOSURE										
			Deformation							
DURATION DAYS	SPEC #	HT in	IR(A) divn	IR(B) divn	TR(A) divn	TR(B) divn	TD(A) divn	TD(B) divn	RESILIENT MODULUS(IR) psi	RESILIENT MODULUS(TR) psi
NO EXP	DI 1 DI 10 DI 25 AVG	2.523 2.538 2.553	7.50 9.60 8.00	9.10 9.80 8.10	11.10 14.50 13.80	13.30 14.20 12.50	11.10 15.40 14.60	14.20 15.70 13.70	296071.32 251842.10 301678.94 283197.46	201425.57 170234.73 184677.98 185446.10
28 DAYS	DI 6 DI 22 DI 20 AVG	2.516 2.534 2.537	8.70 8.10 8.50	8.20 8.30 8.40	11.80 11.60 12.70	12.50 12.50 12.10	12.10 11.90 13.00	12.70 12.80 12.50	291624.73 298381.04 289210.80 293072.19	202817.20 201047.68 197083.17 200582.68
90 DAYS	DI 11 DI 5 DI 24 AVG	2.500 2.516 2.560	8.40 8.10 7.60	7.50 7.00 7.10	10.90 11.40 12.00	10.90 10.00 10.20	11.00 11.50 12.10	11.00 10.00 10.20	311949.69 326387.84 329506.80 322614.81	227522.94 230301.77 218185.94 225337.21

Note:
IR - Instantaneous Recoverable
TR - Total Recoverable
TD - Total Deformation
one divn = .00002 in

Table A.2--continued

CHEVRON AC-20 MODIFIED

OVEN EXPOSURE										
DURATION DAYS	SPEC #	HT in	Deformation						RESILIENT MODULUS(IR) psi	RESILIENT MODULUS(TR) psi
			IR(A) divn	IR(B) divn	TR(A) divn	TR(B) divn	TD(A) divn	TD(B) divn		
NO EXP	DM 17 DM 4 DM 14 AVG	2.527 2.518 2.534	10.00 9.70 8.10	9.85 9.10 9.20	16.70 15.90 14.70	16.30 14.50 15.70	17.70 16.50 15.80	17.80 15.70 16.60	247204.25 261943.79 282858.33 264002.12	148697.10 161991.56 160969.72 157219.13
28 DAYS	DM 25 DM 26 DM 9 AVG	2.505 2.534 2.563	8.40 8.70 9.20	9.70 9.00 8.80	12.20 13.40 13.20	13.90 14.40 14.40	12.50 13.70 13.50	14.30 14.80 14.70	273486.18 276466.05 268782.24 272911.49	189653.00 176023.35 175292.77 180323.04
90 DAYS	DM 10 DM 13 DM 27 AVG	2.519 2.523 2.537	7.80 7.30 8.00	8.50 8.20 7.70	10.60 10.00 11.70	11.40 11.70 10.70	10.70 10.00 11.70	11.40 11.60 10.80	301999.28 317082.84 311316.09 310132.74	223754.01 226487.74 218199.22 222813.66

Note:
IR - Instantaneous Recoverable
TR - Total Recoverable
TD - Total Deformation
one divn = .00002 in

Table B.2--continued

CHEVRON AC-20 MODIFIED

ULTRAVIOLET EXPOSURE										
			Deformation							
DURATION DAYS	SPEC #	HT in	IR(A) divn	IR(B) divn	TR(A) divn	TR(B) divn	TD(A) divn	TD(B) divn	RESILIENT MODULUS(IR) psi	RESILIENT MODULUS(TR) psi
NO EXP	IM 17	2.527	10.00	9.85	16.70	16.30	17.70	17.80	247204.25	148697.10
	IM 4	2.518	9.70	9.10	15.90	14.50	16.50	15.70	261943.79	161991.56
	IM 14	2.534	8.10	9.20	14.70	15.70	15.80	16.60	282858.33	160968.72
	AVG								264002.12	157219.13
28 DAYS	IM 8	2.505	7.30	8.00	10.70	11.90	10.90	12.10	323535.93	219030.96
	IM 11	2.526	8.00	8.10	14.40	12.20	14.70	12.40	304803.54	184546.88
	IM 5	2.529	8.80	8.50	11.90	12.00	12.20	12.30	283417.56	205151.62
	AVG								303952.34	202909.82
90 DAYS	IM 20	2.500	7.80	8.00	10.30	11.40	10.50	11.60	313924.05	228571.43
	IM 18	2.516	8.90	7.00	12.40	10.20	12.40	10.40	309965.90	218073.36
	IM 22	2.537	8.10	8.00	12.70	11.70	12.70	11.80	303581.53	200314.04
	AVG								309157.16	215652.94

Note:
IR - Instantaneous Recoverable
TR - Total Recoverable
TD - Total Deformation
one divn = .00002 in

Table 8.3 Computed Values of Fracture Energy

AMOCO AC-30 AND MARIANI AC-30

DURATION	NORMAL OVEN		ULTRAVIOLET		NORMAL OVEN		ULTRAVIOLET	
DAYS	SPEC #	ENERGY (pascals)	SPEC #	ENERGY (pascals)	SPEC #	ENERGY (pascals)	SPEC #	ENERGY (pascals)
0 DAY	AM 38 AM 60 AM 41 AVG	3269.65 2483.28 3097.20 2950.04			MA 4 MA 36 MA 31 AVG	3290.35 2800.59 2952.34 3014.43		
7 DAYS	AM 5 AM 36 AM 26 AVG	3145.49 3262.75 3221.37 3209.87	AM 20 AM 56 AM 1 AVG	2835.08 3017.29 3262.75 3038.37	MA 20 MA 47 MA 58 AVG	2966.14 2517.77 2952.34 2812.08	MA 54 MA 43 MA 16 AVG	3317.94 3166.19 2752.30 3078.81
28 DAYS	AM 10 AM 32 AM 40 AVG	3179.98 2978.84 3504.18 3221.37	AM 14 AM 21 AM 42 AVG	3235.16 3331.73 3324.84 3297.24	MA 29 MA 34 MA 8 AVG	3228.26 2752.30 3428.31 3136.29	MA 27 MA 49 MA 9 AVG	3366.22 2869.57 3359.33 3198.37
90 DAYS	AM 45 AM 18 AM 22 AVG	3676.63 4076.72 3814.59 3855.98	AM 9 AM 34 AM 51 AVG	3621.45 3842.19 4042.23 3835.29	MA 26 MA 48 MA 53 AVG	3655.94 3076.51 3076.51 3269.65	MA 3 MA 45 MA 39 AVG	3235.26 3317.94 3179.98 3244.36

Table 8.3--continued

CHEVRON AC-20 AND CHEVRON AC-20 MOD

DURATION	NORMAL OVEN		ULTRAVIOLET		NORMAL OVEN		ULTRAVIOLET	
DAYS	SPEC #	ENERGY (pascals)	SPEC #	ENERGY (pascals)	SPEC #	ENERGY (pascals)	SPEC #	ENERGY (pascals)
0 DAY	DI 1 DI 10 DI 25 AVG	2372.91 2428.10 2462.59 2421.20			DM 4 DM 17 DM 14 AVG	1917.64 1655.52 1558.95 1710.70		
28 DAYS	DI 4 DI 8 DI 3 AVG	2662.63 2835.08 2545.36 2681.02	DI 6 DI 22 DI 20 AVG	2545.36 2641.93 2676.42 2621.24	DM 25 DM 26 DM 5 AVG	2310.83 2428.10 1869.36 2202.76	DM 8 DM 11 DM 5 AVG	2462.69 2683.32 2372.91 2506.31
90 DAYS	DI 12 DI 19 DI 27 AVG	3269.65 2841.98 2697.12 2936.25	DI 11 DI 5 DI 24 AVG	2910.96 2697.12 2821.28 2809.79	DM 10 DM 13 DM 27 AVG	2773.00 2607.44 2752.30 2710.91	DM 20 DM 18 DM 22 AVG	2807.49 3021.32 2717.81 2848.87

APPENDIX C

RESULTS OF CONSISTENCY AND RHEOLOGY TESTS ON RECOVERED RESIDUES

Table C.1 Results of Absolute Viscosity Tests

ASPHALT	NO EXPR	ABSOLUTE VISCOSITY BY EXPOSURE											
		1 DAY			7 DAYS			28 DAYS			90 DAYS		
		Oven	UV	FD	Oven	UV	FD	Oven	UV	FD	Oven	UV	FD
CH	11322	9735	3825	11518	14395	14575	16120	20665	20610	24416	57250	119635	132900
BE	8905	10146	9819	10287	15239	14554	11475	19061	13248	20759	51853	32133	100829
AM	7334	9365	8419	10012	7861	9327	6996	14762	15817	24147	36623	41696	378433
MA	7096	8057	12702	11731	9744	12503	16132	15079	17413	12752	30462	43157	47693
TX	2345	2992	2857	3468	2569	2992	4153	4401	5102	5171	9051	10003	11465
TA	2392	2510	2491	2487	2937	2865	2802	3090	3998	4015	9192	7556	9928
BO	11315	10234	10434	9743	10247	12351	16260	15519	27126	22377	73475	86214	73359
SO	34021	28767	39125	17632	40872	48056	48176	61578	79891	93761	138952	142942	2.4+E6
DI	6645	7113	7949	*	8836	10221	*	14252	16794	*	34830	32337	*
DM	6343	6661	6514	*	14569	11040	*	16345	23090	*	50436	91463	*

Note: * Not tested at this condition

Table C.2 Results of Penetration and Rheometer Tests

CHEVRON AC-30

EXPOSURE (DAYS)	PARAMETER		NO EXPOSURE		
0	Pen		42		
	NJ (Pa.S)	25°C	1466730		
		15°C	15158200		
	C	25°C	0.7320		
		15°C	0.7949		
			OVEN	UV	FD
1	Pen		41	38	42
	NJ (Pa.S)	25°C	1199370	1172090	1385810
		15°C	18135000	18044900	16154100
	C	25°C	0.7009	0.7141	0.7079
		15°C	0.7112	0.7132	0.6193
7	Pen		37	38	35
	NJ (Pa.S)	25°C	2103860	1517970	2053030
		15°C	19888300	21124600	21559100
	C	25°C	0.6664	0.6831	0.5947
		15°C	0.6697	0.6858	0.6646
28	Pen		33	36	33
	NJ (Pa.S)	25°C	2666180	2290150	2933420
		15°C	30311500	34609800	30794400
	C	25°C	0.6292	0.6109	0.6293
		15°C	0.6193	0.5814	0.6739
90	Pen		27	16	21
	NJ (Pa.S)	25°C	5779800	7497670	8063270
		15°C	21693700	115243000	61587400
	C	25°C	0.5507	0.6627	0.6708
		15°C	0.7261	0.6349	0.7981

Table C.2--continued
BELCHER AC-30

EXPOSURE (DAYS)	PARAMETER		NO EXPOSURE		
0	Pen		41		
	Nj (Pa.S)	25°C	1019820		
		15°C	13221800		
	C	25°C	0.8176		
		15°C	0.7406		
			OVEN	UV	FD
1	Pen		41	38	37
	Nj (Pa.5)	25°C	1341180	1112790	1250690
		15°C	16157600	22878600	17485000
	C	25°C	0.7448	0.7621	0.7779
		15°C	0.7202	0.6810	0.7583
7	Pen		33	34	37
	Nj (Pa.5)	25°C	2049570	2559230	1142050
		15°C	24946400	21420500	29406300
	C	25°C	0.7742	0.7095	0.8073
		15°C	0.7917	0.7795	0.6432
28	Pen		29	35	29
	Nj (Pa.5)	25°C	2818320	2723700	4443710
		15°C	32538600	34475800	30701800
	C	25°C	0.7211	0.6409	0.6842
		15°C	0.6790	0.5506	0.6601
60	Pen		24	25	20
	Nj (Pa.S)	25°C	7666280	5219350	1236370
		15°C	43082000	32533900	96067700
	C	25°C	0.6673	0.6129	0.6025
		15°C	0.7421	0.7172	0.6019

Table C.2--continued

AMOCO AC-30

EXPOSURE (DAYS)	PARAMETER		NO EXPOSURE		
0	Pen		48		
	Nj (Pa.S)	25°C	414266		
		15°C	5679340		
	C	25°C	0.9073		
		15°C	0.8445		
			OVEN	UV	FO
1	PEN		42	45	42
	Nj (Pa.S)	25°C	551669	497371	496196
		15°C	12994400	7882370	10624800
	C	25°C	0.9918	0.8975	0.9866
		15°C	0.8750	0.9526	1.0320
7	Pen		43	48	45
	Nj (Pa.S)	25°C	553340	534001	502972
		15°C	12251500	12193300	12345100
	C	25°C	0.9672	0.8919	0.7981
		15°C	0.9197	0.7059	0.7366
28	Pen		33	35	28
	Nj (Pa.S)	25°C	926031	1273880	2238890
		15°C	17187100	23723300	25985400
	C	25°C	0.9103	0.8581	0.8501
		16°C	0.8959	0.7200	0.9418
90	Pen		25	23	15
	Nj (Pa.S)	25°C	2353160	4857170	78455200
		15°C	116341000	39172400	471825000
	C	25°C	0.9079	0.7776	0.8920
		15°C	0.5843	0.8810	0.4260

Table C.2--continued

MARIANI AC-30

EXPOSURE (DAYS)	PARAMETER		NO EXPOSURE		
0	Pen		40		
	Nj (Pa.S)	25°C	756375		
		15°C	8710030		
	C	25°C	0.9084		
		15°C	0.9171		
			OVEN	UV	FD
1	Pen		42	35	36
	Nj (Pa.S)	25°C	699315	1618680	1791950
		15°C	21288700	24215500	24130100
	C	25°C	0.8669	0.8425	0.8113
		15°C	0.7041	0.8378	0.9119
7	Pen		35	33	32
	Nj (Pa.S)	25°C	1204540	1947370	1626560
		15°C	18165500	26721200	26172300
	C	25°C	0.8553	0.7414	0.8261
		15°C	0.8342	0.7787	0.7823
28	Pen		31	28	32
	Nj (Pa.S)	25°C	1316360	1332730	1112130
		15°C	19967300	27609700	28510200
	C	25°C	0.9344	0.9313	0.9437
		15°C	0.9577	0.9202	0.7806
90	Pen		23	21	21
	Nj (Pa.S)	25°C	5657580	6468380	8625990
		15°C	49295200	47492700	41310300
	C	25°C	0.7873	0.7845	0.7219
		15°C	0.3581	0.3408	0.3616

Table C.2--continued

TEXACO 85-100

EXPOSURE (DAYS)	PARAMETER		NO EXPOSURE		
0	Pen		45		
	Nj (Pa.S)	25°C	1226920		
		15°C	15241000		
	C	25°C	0.8138		
		15°C	0.9701		
			OVEN	UV	FD
1	Pen		41	41	43
	Nj (Pa.S)	25°C	1300450	1626430	1966850
		15°C	24559500	24602900	19276700
	C	25°C	0.8421	0.7673	0.7828
		15°C	1.0250	0.8580	0.8364
7	Pen		45	40	32
	Nj (Pa.S)	25°C	1470870	1495110	2240400
		15°C	20648300	36348700	54599800
	C	25°C	0.7848	0.7675	0.8340
		15°C	0.7866	0.7742	0.8170
28	Pen		34	30	27
	Nj (Pa.S)	25°C	1660620	2252940	2448650
		15°C	49404000	39798500	47323000
	C	25°C	0.8072	0.8419	0.8094
		15°C	0.7035	0.9053	0.6682
90	Pen		23	20	20
	Nj (Pa.S)	25°C	4778830	5047860	7497510
		15°C	175008000	126867000	203351000
	C	25°C	0.8491	0.8705	0.8025
		15°C	0.5448	0.5741	0.5500

Table C.2--continued

TEXACO AIRBLOWN 85-100

EXPOSURE (DAYS)	PARAMETER		NO EXPOSURE		
0	Pen		42		
	Nj (Pa.S)	25°C 15°C	130317 1737820		
	C	25°C 15°C	0,9109 0.8651		
			OVEN	UV	FO
1	Pen		69	70	67
	Nj (Pa.S)	25°C 15°C	149471 2088880	155911 2153220	146110 2276590
	C	25°C 15°C	0,9222 0.8888	0,8873 0.8537	0.7892 0.7161
7	Pen		66	66	67
	Nj (Pa.S)	25°C 15°C	182791 2658610	188507 3702520	185506 3376700
	C	25°C 15°C	0,8765 0,8133	0,8486 0.7300	0,7857 0,6707
28	Pen		64	50	54
	Nj (Pa.S)	25°C 15°C	253776 4731520	291696 4310590	374098 5643860
	C	25°C 16°C	0,7743 0,6942	0,8036 0.7470	0,7601 0,6453
90	Pen		40	44	42
	Nj (Pa.S)	25°C 15°C	1667550 10024400	1459170 14661500	1550100 19519400
	C	25°C 15°C	0,6248 0,6598	0,5886 0.5762	0,5834 0.5372

Table C.2--continued

ESSO 25-35

EXPOSURE (DAYS)	PARAMETER		NO EXPOSURE		
0	Pen		22		
	Nj (Pa.S)	25°C	4653410		
		15°C	142813000		
	C	25°C	0.8594		
		15°C	0.5509		
			OVEN	UV	FD
1	Pen		23	22	22
	Nj (Pa.S)	25°C	6331160	11518100	3262550
		15°C	151677000	78346800	64347400
	C	25°C	0.7737	0.6412	0.6455
		15°C	0.5391	0.6425	0.5863
7	Pen		21	20	20
	Nj (Pa.S)	25°C	10514900	11285900	11954100
		15°C	145750000	161141000	100287000
	C	25°C	0.6510	0.7710	0.6347
		15°C	0.5400	0.6335	0.5900
28	Pen		20	18	13
	Nj (Pa.S)	25°C	16575800	12439300	12696200
		15°C	183096000	262314000	259193000
	C	25°C	0.7265	0.7017	0.0667
		15°C	0.5798	0.5797	0.5405
90	Pen		20	17	7
	Nj (Pa.S)	25°C	17988200	25127000	26794800
		15°C	102490000	139388000	391724000
	C	25°C	0.6625	0.6339	0.6967
		15°C	0.4809	0.5030	0.5604

Table C.2--continued

BOSCAN 85-100

EXPOSURE (DAYS)	PARAMETER		NO EXPOSURE		
0	Pen		49		
	Nj (Pa.S)	25°C	833639		
		15°C	8130710		
	C	25°C	0.7433		
		15°C	0.8446		
			OVEN	UV	FD
1	Pen		52	50	50
	Nj (Pa.S)	25°C	546937	758547	653943
		15°C	6465830	6455100	7222550
	C	25°C	0.8115	0.7904	0.7752
		15°C	0.8159	0.8945	0.7259
7	Pen		45	44	39
	Nj (Pa.S)	25°C	782024	778545	1067800
		15°C	6933830	9148710	10736100
	C	25°C	0.7062	0.7864	0.7561
		15°C	0.8344	0.7909	0.7823
28	Pen		42	33	34
	Nj (Pa.S)	25°C	1455600	1868930	1670540
		15°C	90908500	41372900	25548500
	C	25°C	0.6980	0.7280	0.7280
		15°C	0.8598	0.6358	0.7584
90	Pen		23	16	24
	Nj (Pa.S)	25°C	3602670	4587830	4227480
		15°C	74990000	85018300	77740000
	C	25°C	0.7992	0.7783	0.7465
		15°C	0.6826	0.6403	0.6822

Table C.2--continued

CHEVRON AC-20

EXPOSURE (DAYS)	PARAMETER		NO EXPOSURE	
0	Pen		44	
	Nj (Pa.S)	25°C	516251	
		15°C	16648900	
	C	25°C	0.8289	
		15°C	0.6362	
			OVEN	UV
1	Pen		42	43
	Nj (Pa.S)	25°C	609505	688666
		15°C	32626000	24066600
	C	25°C	0.8441	0.8304
		15°C	0.7204	0.7317
7	Pen		39	37
	Nj (Pa.S)	25°C	1074600	1825110
		15°C	28459500	23075200
	C	25°C	0.8229	0.6446
		15°C	0.6002	0.7026
28	Pen		34	4035
	Nj (Pa.S)	25°C	1466200	1808550
		15°C	13061500	18177100
	C	25°C	0.7491	0.7704
		15°C	0.7758	0.8069
90	Pen		24	26
	Nj (Pa.S)	25°C	4683940	4181300
		15°C	64749500	53960900
	C	25°C	0.6960	0.6391
		15°C	0.6879	0.5848

Table C.2--continued

CHEVRON AC-20 MOD

EXPOSURE (DAYS)	PARAMETER			NO EXPOSURE
0	Pen			61
	N_J (Pa.S)	25°C		199725
		15°C		4881450
	C	25°C		0.9470
		15°C		0.8067
			OVEN	UV
1	Pen		68	59
	N_J (Pa.S)	25°C	286097	246721
		15°C	3808680	3357900
	C	25°C	0.7632	0.8727
		15°C	0.8196	0.8623
7	Pen		55	51
	N_J (Pa.S)	25°C	691594	630321
		15°C	5594340	7209790
	C	25°C	0.6752	0.6382
		15°C	0.7748	0.6935
28	Pen		43	40
	N_J (Pa.S)	25°C	1395340	1385850
		15°C	7842700	10332800
	C	25°C	0.5817	0.5625
		15°C	0.5550	0.9530
90	Pen		33	28
	N_J (Pa.S)	25°C	6316080	7352100
		15°C	32135300	44807000
	C	25°C	0.5087	0.5046
		15°C	0.6050	0.6047

APPENDIX D

RESULTS OF IR SPECTRAL TESTS ON RECOVERED RESIDUES

Table D.1 Results of Spectral Tests

CHEVRON AC-30

EXPOSURE DURATION (DAYS)	EXPOSURE TYPE	ABSORBANCE @ WAVENUMBERS (1/CM) 1900	1700	1600	1375	ABSORBANCE wrt 1900 WAVENUMBERS (1/CM) 1700	1600	1375	CARBONYL RATIO CR1*	CR2*	KETONE FACTOR KF1*	KF2*
NO EXP	NO EXP	0.0157	0.1569	0.3315	0.6739	0.1412	0.3158	0.6582	0.4471	0.2145	1.0615	1.0840
1	OVEN	0.0190	0.1799	0.3800	0.7608	0.1609	0.3610	0.7418	0.4457	0.2169	1.0581	1.0960
	UV	0.0186	0.1798	0.3738	0.7026	0.1612	0.3552	0.684	0.4538	0.2356	1.0774	1.1908
	FD	0.0226	0.1898	0.3804	0.7229	0.1672	0.3578	0.7003	0.4673	0.2387	1.1094	1.2064
7	OVEN	0.0233	0.1925	0.3863	0.7423	0.1692	0.3630	0.7190	0.4681	0.2353	1.1066	1.1891
	UV	0.0265	0.2091	0.3968	0.7533	0.1826	0.3703	0.7268	0.4936	0.2515	1.1720	1.2709
	FD	0.0272	0.2015	0.3950	0.7665	0.1743	0.3678	0.7393	0.4738	0.2357	1.1251	1.1913
28	OVEN	0.0299	0.2302	0.4108	0.7160	0.2003	0.3609	0.6861	0.5258	0.2919	1.2464	1.4751
	UV	0.0329	0.2509	0.4246	0.7665	0.2180	0.3917	0.7336	0.5565	0.2971	1.3213	1.5015
	FD	0.0324	0.2460	0.4248	0.8003	0.2136	0.3924	0.7679	0.5443	0.2781	1.2923	1.4055
90	OVEN	0.0344	0.3087	0.4542	0.7921	0.2743	0.4198	0.7577	0.6534	0.3620	1.5512	1.8292
	UV	0.0372	0.3154	0.4633	0.7583	0.2762	0.4261	0.7611	0.6526	0.3655	1.5500	1.8470
	FD	0.0354	0.3182	0.4460	0.7441	0.2626	0.4106	0.7087	0.6887	0.3950	1.6352	2.0163

*Note:
CR1 = Relative Absorbance @1700 / Relative Absorbance @1600
CR2 = Relative Absorbance @1700 / Relative Absorbance @1375
KF1 = CR1 for sample / CR1 for original asphalt
KF2 = CR2 for sample / CR2 for original asphalt
CR1 original asphalt =0.4212
CR2 original asphalt =0.1979

Table D.1--continued

BELCHER AC-30

EXPOSURE DURATION (DAYS)	EXPOSURE TYPE	ABSORBANCE @ WAVENUMBERS (1/CM) 1900	1700	1600	1375	ABSORBANCE wrt 1900 WAVENUMBERS (1/CM) 1700	1600	1375	CARBONYL RATIO CR1*	CR2*	KETONE FACTOR KF1*	KF2*
NO EXP	NO EXP	0.0191	0.1821	0.4058	0.6191	0.1630	0.3867	0.6	0.4215	0.2037	1.3802	1.6260
1	OVEN	0.0230	0.1846	0.4151	0.6356	0.1617	0.3920	0.6125	0.4126	0.1990	1.3510	1.5889
	UV	0.0328	0.1977	0.4207	0.7797	0.1649	0.3879	0.7469	0.4251	0.2207	1.3919	1.7620
	FD	0.0314	0.1904	0.4071	0.6227	0.159	0.3757	0.7913	0.4232	0.2009	1.3857	1.6034
7	OVEN	0.0235	0.2017	0.4166	0.9036	0.1782	0.3931	0.8801	0.4533	0.2024	1.4843	1.6159
	UV	0.0322	0.2031	0.4212	0.7947	0.1709	0.389	0.7625	0.4393	0.2241	1.4385	1.7887
	FD	0.0347	0.2071	0.4177	0.8142	0.1724	0.383	0.7795	0.4501	0.2211	1.4739	1.7651
28	OVEN	0.0248	0.2290	0.4231	0.8149	0.2042	0.3963	0.7901	0.5126	0.2584	1.6787	2.0626
	UV	0.0329	0.2465	0.4446	0.7824	0.2136	0.4119	0.7495	0.5185	0.2849	1.6980	2.2744
	FD	0.0348	0.2520	0.4401	0.8288	0.2172	0.4053	0.794	0.5358	0.2735	1.7547	2.1831
90	OVEN	0.0299	0.2974	0.4661	0.8697	0.2675	0.4362	0.8396	0.6132	0.3165	2.0080	2.5421
	UV	0.0426	0.6471	0.9901	1.5851	0.6045	0.9475	1.5425	0.6379	0.3918	2.0890	3.1276
	FD	0.0368	0.3378	0.4766	0.8534	0.301	0.4398	0.8166	0.6844	0.3686	2.2410	2.9417

*Note:
CR1 = Relative Absorbance @1700 / Relative Absorbance @1600
CR2 = Relative Absorbance @1700 / Relative Absorbance @1375
KF1 = CR1 for sample / CR1 for original asphalt
KF2 = CR2 for sample / CR2 for original asphalt
CR1 original asphalt =0.3054
CR2 original asphalt =0.1253

Table 6.1--continued

AMOCO AC-30

EXPOSURE DURATION (DAYS)	EXPOSURE TYPE	ABSORBANCE @ WAVENUMBERS (1/CM) 1900	1700	1600	1375	ABSORBANCE wrt 1900 WAVENUMBERS (1/CM) 1700	1600	1375	CARBONYL RATIO CR1*	CR2*	KETONE FACTOR KF1*	KF2*
NO EXP	NO EXP	0.0497	0.2059	0.4160	0.9567	0.1562	0.3663	0.9070	0.4264	0.1722	1.2520	1.3309
1	OVEN UV FD	0.0457 0.0503 0.0553	0.2096 0.2156 0.2284	0.4241 0.4283 0.4476	0.9439 0.9421 0.9642	0.1639 0.1653 0.1731	0.3784 0.3780 0.3923	0.8982 0.8918 0.9089	0.4331 0.4373 0.4412	0.1825 0.1854 0.1904	1.2717 1.2839 1.2955	1.4102 1.4324 1.4718
7	OVEN UV FD	0.0527 0.0570 0.0588	0.2185 0.2342 0.2381	0.4198 0.4296 0.4344	0.9776 0.9835 0.9895	0.1658 0.1772 0.1793	0.3671 0.3726 0.3756	0.9249 0.9265 0.9307	0.4516 0.4756 0.4771	0.1793 0.1913 0.1927	1.3260 1.3963 1.4008	1.3853 1.4780 1.4888
28	OVEN UV FD	0.0600 0.0600 0.0628	0.2559 0.2720 0.2765	0.4519 0.4614 0.4638	1.0292 1.0359 1.0271	0.1959 0.2120 0.2137	0.3919 0.4014 0.4010	0.9692 0.9759 0.9643	0.4999 0.5282 0.5329	0.2021 0.2172 0.2216	1.4676 1.5507 1.5646	1.5620 1.6788 1.7126
90	OVEN UV FD	0.0679 0.0702 0.0773	0.3240 0.3371 0.4290	0.4975 0.5142 0.5771	1.0518 1.0611 1.0472	0.2561 0.2669 0.3517	0.4296 0.4440 0.4998	0.9839 0.9909 0.9699	0.5961 0.6011 0.7037	0.2603 0.2694 0.3626	1.7503 1.7649 2.0660	2.0115 2.0815 2.8023

*Note:
CR1 = Relative Absorbance @1700 / Relative Absorbance @1600
CR2 = Relative Absorbance @1700 / Relative Absorbance @1375
KF1 = CR1 for sample / CR1 for original asphalt
KF2 = CR2 for sample / CR2 for original asphalt
CR1 original asphalt =0.3406
CR2 original asphalt =0.1294

Table D.1--continued

MARIANI AC-30

EXPOSURE DURATION (DAYS)	EXPOSURE TYPE	ABSORBANCE @ WAVENUMBERS (1/CM) 1900	1700	1600	1375	RELATIVE ABSORBANCE WAVENUMBERS (1/CM) 1700	1600	1375	CARBONYL RATIO CR1*	CR2*	KETONE FACTOR KF1*	KF2*
NO EXP	NO EXP	0.0047	0.1440	0.3405	0.8316	0.1393	0.3358	0.8269	0.4148	0.1684	1.3790	1.3798
1	OVEN UV FD	0.0324 0.0380 0.0475	0.1804 0.2017 0.2152	0.3728 0.3898 0.3979	0.7924 0.8367 0.9186	0.1480 0.1837 0.1677	0.3402 0.3518 0.3504	0.7600 0.7987 0.8711	0.4350 0.4653 0.4788	0.1947 0.2050 0.1925	1.4463 1.5469 1.5911	1.5949 1.6788 1.5787
7	OVEN UV FD	0.0528 0.0610 0.0668	0.2053 0.2279 0.2454	0.4034 0.4031 0.4200	0.8595 0.8597 0.8546	0.1525 0.1669 0.1788	0.3506 0.3421 0.3534	0.8067 0.7987 0.7880	0.4350 0.4879 0.5059	0.1890 0.2090 0.2269	1.4460 1.6219 1.6820	1.5483 1.7114 1.8583
28	OVEN UV FD	0.0700 0.0709 0.2028	0.2574 0.2708 0.4153	0.4371 0.4433 0.6017	0.8234 0.8792 1.0196	0.1874 0.1999 0.2125	0.3871 0.3724 0.3989	0.7534 0.8083 0.8168	0.5105 0.5368 0.5327	0.2487 0.2473 0.2602	1.6971 1.7845 1.7710	2.0372 2.0255 2.1307
90	OVEN UV FD	0.0785 0.0762 0.0401	0.3192 0.3479 0.3399	0.4540 0.4650 0.4525	0.8901 0.9008 0.7539	0.2407 0.2717 0.2998	0.3755 0.3868 0.4124	0.8116 0.8246 0.7138	0.6410 0.6988 0.7270	0.2966 0.3295 0.4200	2.1310 2.3232 2.4168	2.4289 2.6986 3.4398

*Note:
CR1 = Relative Absorbance @1700 / Relative Absorbance @1600
CR2 = Relative Absorbance @1700 / Relative Absorbance @1375
KF1 = CR1 for sample / CR1 for original asphalt
KF2 = CR2 for sample / CR2 for original asphalt
CR1 original asphalt =0.3008
CR2 original asphalt =0.1221

Table D.1--continued

TEXACO 85-100

EXPOSURE DURATION (DAYS)	EXPOSURE TYPE	ABSORBANCE @ WAVENUMBERS (1/CM) 1900	1700	1600	1375	RELATIVE ABSORBANCE WAVENUMBERS (1/CM) 1700	1600	1375	CARBONYL RATIO CR1*	CR2*	KETONE FACTOR KF1*	KF2*
NO EXP	NO EXP	0.0554	0.2247	0.4487	0.8753	0.1693	0.3933	0.8199	0.4304	0.2064	1.5984	1.3989
1	OVEN UV FD	0.0539 0.0544 0.0558	0.2353 0.2088 0.2224	0.4658 0.4372 0.4489	0.9652 0.9071 0.9784	0.1814 0.1544 0.1666	0.4119 0.3828 0.3931	0.9113 0.8527 0.9226	0.4403 0.4033 0.4238	0.1990 0.1810 0.1805	1.6353 1.4977 1.5737	1.3486 1.2267 1.2234
7	OVEN UV FD	0.0570 0.0640 0.0673	0.2416 0.2389 0.2449	0.4590 0.4557 0.4550	0.8336 0.9042 0.8481	0.1846 0.1749 0.1776	0.4020 0.3917 0.3877	0.7766 0.8402 0.7808	0.4592 0.4465 0.4580	0.2377 0.2081 0.2274	1.7051 1.6580 1.7010	1.6104 1.4103 1.5410
28	OVEN UV FD	0.0718 0.0718 0.0728	0.3031 0.2938 0.2825	0.5047 0.4952 0.4767	0.8761 0.8678 0.8724	0.2313 0.2220 0.2097	0.4329 0.4134 0.4039	0.8043 0.7980 0.7996	0.5343 0.5370 0.5191	0.2875 0.2788 0.2622	1.9840 1.9940 1.9279	1.9483 1.8895 1.7768
90	OVEN UV FD	0.0768 0.0833 0.0839	0.3577 0.3753 0.3919	0.5098 0.5313 0.5435	0.8212 0.8742 0.9218	0.2809 0.2920 0.3080	0.4330 0.4480 0.4596	0.7444 0.7909 0.8379	0.6487 0.6517 0.6701	0.3773 0.3691 0.3675	2.4089 2.4202 2.4884	2.5565 2.5013 2.4904

*Note: CR1 = Relative Absorbance @1700 / Relative Absorbance @1600
CR2 = Relative Absorbance @1700 / Relative Absorbance @1375
KF1 = CR1 for sample / CR1 for original asphalt
KF1 = CR2 for sample / CR2 for original asphalt
CR1 original asphalt =0.2693
CR2 original asphalt =0.1476

Table D.1--continued

TEXACO AIRBLOWN 95-100

EXPOSURE DURATION (DAYS)	EXPOSURE TYPE	ABSORBANCE @ WAVENUMBERS (1/CM) 1900	1700	1600	1375	RELATIVE ABSORBANCE WAVENUMBERS (1/CM) 1700	1600	1375	CARBONYL RATIO CR1*	CR2*	KETONE FACTOR KF1*	KF2*
NO EXP	NO EXP	-0.0364	0.3127	0.3675	0.7876	0.3491	0.4039	0.8240	0.8643	0.4237	1.1346	1.0608
1	OVEN UV FD	-0.0393 -0.0384 -0.0315	0.3275 0.3049 0.3299	0.3824 0.3765 0.3975	0.8349 0.8432 0.7597	0.3658 0.3433 0.3614	0.4207 0.4149 0.4290	0.8732 0.8816 0.7912	0.8695 0.8274 0.8424	0.4189 0.3894 0.4568	1.1414 1.0861 1.1058	1.0489 0.9750 1.1437
7	OVEN UV FD	-0.0254 -0.0152 -0.0134	0.3374 0.3734 0.3540	0.3985 0.4445 0.4361	0.7884 0.8511 0.8804	0.3629 0.3896 0.3674	0.4239 0.4597 0.4495	0.8138 0.8663 0.8938	0.8559 0.8453 0.8174	0.4458 0.4486 0.4111	1.1235 1.1097 1.0729	1.1162 1.1231 1.0292
28	OVEN UV FD	0.0110 0.0111 0.0082	0.4175 0.4186 0.4019	0.4341 0.4418 0.4296	0.7791 0.8135 0.9170	0.4065 0.4075 0.3937	0.4231 0.4307 0.4214	0.7681 0.8024 0.9088	0.9608 0.9461 0.9343	0.5292 0.5079 0.4332	1.2612 1.2420 1.2264	1.3251 1.2715 1.0846
90	OVEN UV FD	0.0140 0.0191 0.0179	0.4640 0.4996 0.4855	0.4927 0.4943 0.5157	1.1593 0.9850 1.1349	0.4500 0.4805 0.4676	0.4787 0.4752 0.4979	1.1453 0.9659 1.1169	0.9400 1.0112 0.9393	0.3929 0.4975 0.4197	1.2340 1.3273 1.2330	0.9838 1.2455 1.0482

*Note:
CR1 = Relative Absorbance @1700 / Relative Absorbance @1600
CR2 = Relative Absorbance @1700 / Relative Absorbance @1375
KF1 = CR1 for sample / CR1 for original asphalt
KF2 = CR2 for sample / CR2 for original asphalt
CR1 original asphalt = 0.7619
CR2 original asphalt = 0.3994

Table 0.1--continued

ESSO 25-35

EXPOSURE DURATION (DAYS)	EXPOSURE TYPE	ABSORBANCE @ WAVENUMBERS (1/CM) 1900	1700	1600	1375	RELATIVE ABSORBANCE WAVENUMBERS (1/CM) 1700	1600	1375	CARBONYL RATIO CR1*	CR2*	KETONE FACTOR KF1*	KF2*
NO EXP	NO EXP	0.0302	0.2121	0.4439	0.8799	0.1819	0.4137	0.8497	0.4396	0.2140	1.2777	1.1749
1	OVEN	0.0321	0.2171	0.4468	0.8672	0.185	0.4147	0.8351	0.4461	0.2215	1.2964	1.2158
	UV	0.2109	0.4096	0.6408	1.1046	0.1987	0.4299	0.8937	0.4622	0.2223	1.3432	1.2202
	FD	0.0226	0.2216	0.4423	0.7941	0.199	0.4197	0.7715	0.4741	0.2579	1.3779	1.4156
7	OVEN	0.2152	0.4208	0.6439	1.0173	0.2056	0.4287	0.8021	0.4795	0.2563	1.3937	1.4068
	UV	0.2316	0.4460	0.6744	1.0982	0.2144	0.4428	0.8666	0.4841	0.2474	1.4071	1.3578
	FD	0.2171	0.4339	0.6463	1.0812	0.2168	0.4292	0.8641	0.5051	0.2508	1.4679	1.3770
28	OVEN	0.2188	0.4664	0.6522	1.0468	0.2476	0.4334	0.8280	0.5712	0.2990	1.6602	1.6412
	UV	0.2197	0.4682	0.6592	1.1370	0.2485	0.4395	0.9173	0.5654	0.2709	1.6431	1.4869
	FD	0.3943	0.6420	0.8370	1.2633	0.2477	0.4427	0.8690	0.5595	0.2850	1.6260	1.5644
90	OVEN	0.0228	0.3424	0.4863	0.8191	0.3196	0.4635	0.7963	0.6895	0.4013	2.0038	2.2028
	UV	0.0138	0.3529	0.5233	0.8495	0.3391	0.5095	0.8357	0.6655	0.4057	1.9341	2.2270
	FD	0.4024	0.7642	0.8920	1.2766	0.3618	0.4896	0.8742	0.7389	0.4138	2.1475	2.2714

*Note:
CR1 = Relative Absorbance @1700 / Relative Absorbance @1600
CR2 = Relative Absorbance @1700 / Relative Absorbance @1375
KF1 = CR1 for sample / CR1 for original asphalt
KF2 = CR2 for sample / CR2 for original asphalt
CR1 original asphalt =0.3441
CR1 original asphalt =0.1822

Table D.1--continued

BOSCAN 85-100

EXPOSURE DURATION (DAYS)	EXPOSURE TYPE	ABSORBANCE @ WAVENUMBERS (1/CM)				RELATIVE ABSORBANCE WAVENUMBERS (1/CM)			CARBONYL RATIO		KETONE FACTOR	
		1900	1700	1600	1375	1700	1600	1375	CR1*	CR2*	KF1*	KF2*
NO EXP	NO EXP	0.0290	0.2023	0.4203	1.0800	0.1733	0.3913	1.0510	0.4428	0.1648	1.1590	0.8646
1	OVEN UV FD	0.0338 0.0388 0.0407	0.2087 0.208 0.2251	0.4127 0.4156 0.4406	0.9266 0.9834 0.9970	0.1759 0.1692 0.1844	0.3789 0.3768 0.4001	0.6928 0.9446 0.9563	0.4642 0.4490 0.4608	0.1970 0.1791 0.1928	1.2149 1.1752 1.2061	1.0331 0.9392 1.0111
7	OVEN UV FD	0.0533 0.0611 0.0683	0.2316 0.2453 0.2443	0.4258 0.4447 0.4189	0.9622 0.9648 0.9307	0.1783 0.1842 0.1760	0.3725 0.3836 0.3506	0.9089 0.9037 0.8624	0.4786 0.4801 0.5019	0.1961 0.2038 0.2040	1.2527 1.2567 1.3137	1.0286 1.0688 1.0701
28	OVEN UV FD	0.0742 0.0788 0.0822	0.2878 0.2972 0.2920	0.4642 0.4705 0.4783	0.9696 1.0472 1.0495	0.2136 0.2184 0.2098	0.3900 0.3917 0.3941	0.8954 0.9684 0.9673	0.5476 0.5575 0.5323	0.2385 0.2255 0.2168	1.4333 1.4592 1.3932	1.2509 1.1826 1.1373
90	OVEN UV FD	0.0821 0.0821 0.0763	0.3586 0.3779 0.3617	0.4949 0.5180 0.5008	0.5475 0.9977 0.9938	0.2765 0.2958 0.2854	0.4128 0.4359 0.4245	0.8654 0.9156 0.9175	0.6698 0.6785 0.6723	0.3195 0.3230 0.3110	1.7529 1.7759 1.7595	1.6754 1.6941 1.6311

*Note: CR1 = Relative Absorbance @1700 / Relative Absorbance @1600
CR2 = Relative Absorbance @1700 / Relative Absorbance @1375
KF1 = CR1 for sample / CR1 for original asphalt
KF2 = CR2 for sample / CR2 for original asphalt
CR1 original asphalt =0.3821
CR2 original asphalt =0.1907

Table D.1--continued

CHEVRON AC-20

EXPOSURE DURATION (DAYS)	EXPOSURE TYPE	ABSORBANCE @ WAVENUMBERS (1/CM)				ABSORBANCE wrt 1900 WAVENUMBERS (1/CM)			CARBONYL RATIO		KETONE FACTOR	
		1900	1700	1600	1375	1700	1600	1375	CR1*	CR2*	KF1*	KF2*
NO EXP	NO EXP	0.0141	0.1754	0.3922	0.7962	0.1613	0.3781	0.7821	0.4266	0.2062	1.5581	1.6863
1	OVEN	0.0153	0.1874	0.3937	0.7924	0.1721	0.3784	0.7771	0.4548	0.2215	1.6611	1.8108
	UV	0.0169	0.1980	0.4059	0.7991	0.1811	0.3890	0.7822	0.4656	0.2315	1.7003	1.8931
7	OVEN	0.0201	0.2106	0.4166	0.7997	0.1905	0.3965	0.7796	0.4805	0.2444	1.7548	1.9980
	UV	0.0231	0.2232	0.4221	0.7974	0.2001	0.3990	0.7743	0.5015	0.2584	1.8316	2.1131
28	OVEN	0.0306	0.2595	0.4422	0.8300	0.2287	0.4114	0.7992	0.5559	0.2862	2.0303	2.3398
	UV	0.0255	0.2569	0.4369	0.7942	0.2314	0.4114	0.7687	0.5625	0.3010	2.0543	2.4614
90	OVEN	0.0313	0.3203	0.4736	0.8284	0.2890	0.4423	0.7971	0.6534	0.3626	2.3864	2.9645
	UV	0.0347	0.3311	0.4786	0.8308	0.2964	0.4439	0.7961	0.6677	0.3723	2.4387	3.0443

*Note:
CR1 = Relative Absorbance @1700 / Relative Absorbance @1600
CR2 = Relative Absorbance @1700 / Relative Absorbance @1375
KF1 = CR1 for sample / CR1 for original asphalt
KF2 = CR2 for sample / CR1 for original asphalt
CR1 original asphalt =0.2738
CR2 original asphalt =0.1223

Table D.1--continued

CHEVRON AC-20 (MOD)

EXPOSURE DURATION (DAYS)	EXPOSURE TYPE	ABSORBANCE @ WAVENUMBERS (1/CM) 1900	1700	1600	1375	ABSORBANCE wrt 1900 WAVENUMBERS (1/CM) 1700	1600	1375	CARBONYL RATIO CR1*	CR2*	KETONE FACTOR KF1*	KF2*
NO EXP	NO EXP	0.2281	0.3651	0.5931	1.0192	0.1570	0.3650	0.7911	0.4301	0.1985	1.3649	1.5713
1	OVEN	0.2431	0.4062	0.6155	1.0760	0.1651	0.3724	0.6329	0.4433	0.1962	1.4274	1.5695
	UV	0.2398	0.4026	0.6169	1.0304	0.1626	0.3771	0.7906	0.4317	0.2059	1.3899	1.6304
7	OVEN	0.2409	0.4171	0.6208	1.0506	0.1762	0.3799	0.8097	0.4638	0.2176	1.4933	1.7230
	UV	0.2412	0.4245	0.6307	1.0419	0.1833	0.3895	0.6007	0.4706	0.2269	1.5151	1.8125
28	OVEN	0.2491	0.5270	0.6809	1.1423	0.2779	0.4318	0.6932	0.6436	0.3111	2.0721	2.4634
	UV	0.2503	0.4760	0.6629	1.1336	0.2257	0.4126	0.8833	0.5470	0.2555	1.7612	2.0231
90	OVEN	0.2478	0.4526	0.6381	1.0313	0.2048	0.3903	0.7835	0.5247	0.2614	1.6894	2.0696
	UV	0.2468	0.5360	0.6679	1.1147	0.2892	0.4211	0.8679	0.6868	0.3332	2.2111	2.6383

*Note: CR1 = Relative Absorbance @1700 / Relative Absorbance @1600
CR2 = Relative Absorbance @1700 / Relative Absorbance @1375
KF1 = CR1 for sample / CR1 for original asphalt
KF2 = CR2 for sample / CR2 for original asphalt
CR1 original asphalt =0.3106
CR2 original asphalt =0.1263

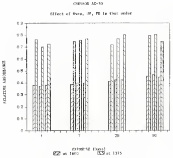

Figure D.2 Relation Between Relative Absorbance and Exposure

BELCHER AC-30

Effect of Oven, UV, FO in that order

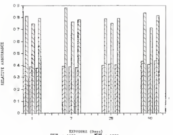

Figure D.2--continued

AMOCO AC-30

Effect of Oven, UV, PO in that order

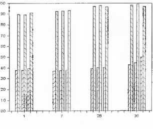

Figure D.2--continued

MARIANI AC-30

Effect of Oven, UV, FD in that order

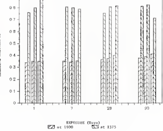

Figure D.2--continued

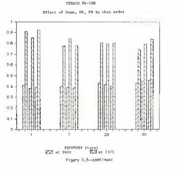

Figure D.2--continued

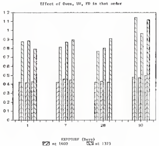

Figure D.2--continued

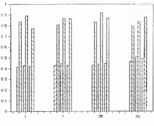
ESSO 23-35

Effect of Oven, UV, FD in that order

Figure D.2—continued

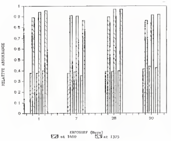
BOMCAN 85-100

Effect of Oven, UV, FD in that order

Figure D.2--continued

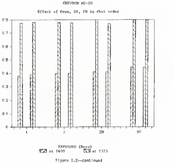

Figure D.2--continued

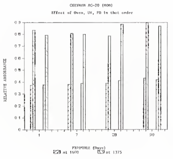

Figure 0.2--continued

APPENDIX E

RATIOS USED FOR MULTIPLE REGRESSION ANALYSIS

ASPHALT	KF	AVR	LPR	CPVR
ma ov 0	1.379	2.392	.355	1.0
ma ov 1	1.446	2.716	.323	2.444
ma ov 7	1.446	3.284	.435	2.086
ma ov 28	1.697	5.082	.50	2.292
ma ov 90	2.131	10.267	.629	56.596
ma uv 1	1.547	4.281	.435	2.780
ma uv 7	1.622	4.214	.468	3.068
ma uv 28	1.785	5.869	.548	3.170
ma uv 90	2.323	14.546	.661	54.526
ma fd 1	1.591	3.954	.419	2.77
ma fd 7	1.682	4.298	.484	3.005
ma fd 28	1.771	5.43	.484	3.273
ma fd 90	2.417	16.142	.661	47.428
am ov 0	1.252	2.222	.342	1.054
am ov 1	1.272	2.837	.425	2.411
am ov 7	1.326	3.196	.411	2.273
am ov 28	1.468	4.472	.548	3.189
am ov 90	1.750	11.155	.658	21.587
am uv 1	1.284	2.55	.384	1.463
am uv 7	1.396	3.056	.342	2.261
am uv 28	1.551	4.792	.521	4.402
am uv 90	1.765	12.631	.685	7.268
am fd 1	1.296	3.033	.425	1.971
am fd 7	1.401	3.081	.384	2.291
am fd 28	1.565	7.315	.616	4.822
am fd 90	2.066	113.43	.795	87.547
be ov 0	1.380	3.235	.388	2.015
be ov 1	1.351	3.685	.388	2.015
be ov 7	1.484	5.535	.507	2.768
be ov 28	1.679	6.924	.567	3.611
be ov 90	2.008	18.835	.642	4.781
be uv 1	1.392	3.567	.433	2.539
be uv 7	1.439	5.287	.493	2.377
be uv 28	1.698	4.812	.478	3.826
be uv 90	2.089	11.672	.612	3.610
be fd 1	1.386	3.737	.448	1.94
be fd 7	1.474	4.168	.448	3.263
be fd 28	1.755	7.541	.567	3.407
be fd 90	2.241	36.625	.701	10.661
ch ov 0	1.062	3.652	.382	1.172
ch ov 1	1.058	3.140	.397	1.402
ch ov 7	1.107	4.644	.456	1.538
ch ov 28	1.249	6.667	.515	2.344
ch ov 90	1.551	18.468	.603	1.677
ch uv 1	1.078	4.46	.441	1.395
ch uv 7	1.172	4.702	.441	1.633
ch uv 28	1.321	6.648	.471	2.676
ch uv 90	1.550	38.592	.765	8.910

ch	fd	7	1.125	5.2	.485	1.667
ch	fd	28	1.292	7.876	.515	2.381
ch	fd	90	1.635	42.871	.691	4.762
tx	ov	0	1.598	2.204	.489	1.589
tx	ov	1	1.635	2.812	.534	2.56
tx	ov	7	1.705	2.414	.489	2.152
tx	ov	28	1.984	4.136	.614	5.15
tx	ov	90	2.409	8.507	.739	18.242
tx	uv	1	1.498	2.685	.534	2.565
tx	uv	7	1.658	2.812	.545	3.789
tx	uv	28	1.994	4.795	.659	4.149
tx	uv	90	2.420	9.401	.773	13.224
tx	fd	1	1.574	3.259	.511	3.052
tx	fd	7	1.701	3.903	.636	5.691
tx	fd	28	1.928	4.86	.693	4.933
tx	fd	90	2.489	10.776	.773	21.197
bo	ov	0	1.159	2.970	.355	2.543
bo	ov	1	1.215	2.686	.316	2.022
bo	ov	7	1.253	2.69	.368	2.169
bo	ov	28	1.433	4.073	.447	2.843
bo	ov	90	1.753	19.285	.697	23.455
bo	uv	1	1.175	2.739	.342	2.019
bo	uv	7	1.257	3.242	.421	2.861
bo	uv	28	1.459	7.12	.566	12.94
bo	uv	90	1.776	25.253	.789	26.591
bo	fd	1	1.206	2.557	.342	2.259
bo	fd	7	1.314	4.268	.487	3.358
bo	fd	28	1.393	5.873	.553	8.116
bo	fd	90	1.760	19.254	.684	24.315
ts	ov	0	1.135	1.239	.122	1.082
ts	ov	1	1.141	1.300	.159	1.30
ts	ov	7	1.124	1.521	.195	1.656
ts	ov	28	1.261	1.6	.22	2.947
ts	ov	90	1.234	4.76	.512	6.243
ts	uv	1	1.086	1.29	.146	1.341
ts	uv	7	1.110	1.484	.195	2.306
ts	uv	28	1.242	2.07	.39	2.684
ts	uv	90	1.327	3.913	.463	9.13
ts	fd	1	1.106	1.288	.183	1.418
ts	fd	7	1.073	1.451	.183	2.103
ts	fd	28	1.226	2.079	.341	3.515
ts	fd	90	1.233	4.624	.488	12.156
so	ov	0	1.278	1.902	.185	1.215
so	ov	1	1.296	1.608	.148	1.29
so	ov	7	1.394	2.285	.222	1.24
so	ov	28	1.660	3.449	.259	1.558
so	ov	90	2.004	7.657	.259	1.0
so	uv	1	1.343	2.188	.185	1.0
so	uv	7	1.407	2.687	.259	1.371
so	uv	28	1.643	4.456	.333	2.232
so	uv	90	1.934	7.992	.37	1.186

```
so fd 7  1.468  2.694  .259  1.0
so fd 28 1.626  5.242  .519  2.205
so fd 90 2.148  134.19 .741  3.333
```

REFERENCES

1. Ruth, B. E., Class Notes for ECI-6426, Bituminous Materials, Department of Civil Engineering, University of Florida, Fall 1986.

2. Button, J. W., J. A. Epps, D. H. Little, and B. M. Gallaway, "Asphalt Temperature Susceptibility and Its Effects on Pavements," TRB, Transportation Research Record 843, 1982, pp. 118-126.

3. Puzinauskas, V. P., "Properties of Asphalt Cements," Proceedings AAPT, Vol. 48, 1979, pp. 646-710.

4. Anderson, D. A., and E. L. Dukatz, "Asphalt Properties and Composition: 1950-1980," Proceedings AAPT, Vol. 49, 1980, pp. 1-20.

5. Burati, J. L., S. N. Kalidindi, H. W. Busching, and W. C. Bridges, "Variability in Asphalt Cement Properties Based on Source and Time," Engineering Report, Department of Civil Engineering, Clemson University, 1986, 61 pages.

6. Wright, J. R., and P. G. Campbell, "Determination of Oxidation Rates of Air-Blown Asphalts by Infrared Spectroscopy," Journal of Applied Chemistry, Vol. 12, 1962, pp. 256-266.

7. Kumar, A., and W. H. Goetz, "Asphalt Hardening as Affected by Film Thickness, Voids and Permeability in Asphaltic Mixtures," Proceedings AAPT, Vol. 46, 1977, pp. 571-605.

8. Coons, R. F., and P. H. Wright, "An Investigation of the Hardening of Asphalt Recovered from Pavements of Various Ages," Proceedings AAPT, Vol. 37, 1968, pp. 510-528.

9. Gietz, R. H., and D. R. Lamb, "Age Hardening of Asphalt Cement and Its Relationship to Lateral Cracking of Asphaltic Concrete," Proceedings AAPT, Vol. 37, 1968, pp. 141-158.

10. Goode, J. F., and L. A. Lufsey, "Voids, Permeability, Film Thickness vs Asphalt Hardening," Proceedings AAPT, Vol. 34, 1965, pp. 430-463.

11. Page, G. C., K. H. Murphy, B. E. Ruth, Reynaldo Roque, "Asphalt Binder Hardening," Proceedings AAPT, Vol. 54, 1985, pp. 140-167.

12. Skog, J., "Setting and Durability Studies on Paving Grade Asphalts," Proceedings AAPT, Vol. 36, 1967, pp. 387-420.

13. Dickinson, E. J., "The Hardening of Middle East Petroleum Asphalts in Pavement Surfacings," Proceedings AAPT, Vol. 49, 1980, pp. 30-63.

14. Corbett, L. W., and H. E. Schweyer, "Composition and Rheology Considerations in Age-Hardening of Bitumen," Proceedings AAPT, Vol. 50, 1981, pp. 571-604.

15. Culley, R. W., "Relationships Between Hardening of Asphalt Cements and Transverse Cracking of Pavements in Saskatchewan," Proceedings AAPT, Vol. 38, 1969, pp. 629-659.

16. Green, E. L., W. J. Tolonen, and R. J. Peters, "Predictability Techniques for Asphalt Durability," TRB, Transportation Research Record 595, 1976, pp. 1-8.

17. Kemp, G. R., and N. H. Predoehl, "A Comparison of Field and Laboratory Environments on Asphalt Durability," Proceedings AAPT, Vol. 50, 1981, pp. 492-534.

18. Santucci, L. E., J. E. Goodrich, and J. E. Sundberg, "The Effect of Crude Source and Additives on the Long Term Oven Aging of Paving Asphalts," Proceedings AAPT, Vol. 50, 1981, pp. 560-570.

19. Peters, O. J., J. M. Hayes and G. M. Hieftje, Chemical Separations and Measurements, Saunders Golden Series, W. B. Saunders and Company, Philadelphia, 1974.

20. Petersen, J. C., "Quantitative Functional Group Analysis of Asphalts Using Differential Infrared Spectrometry and Selective Chemical Reactions - Theory and Application," Proceedings of the 65th Annual Meeting of the Transportation Research Board, Wahington D. C., 1986, in press.

21. Beitchman, B. D., "Infrared Spectra of Asphalts," Journal of Research, National Bureau of Standards, Vol. 63A, No. 2, 1959, pp. 189-192.

22. Smith, C. D., C. C. Schuetz, and R. S. Hodgson, "Relationship Between Chemical Structures and Weatherability of Coating Asphalts as Shown by Infrared Spectroscopy," I&EC Product Research and Development, Vol. 5, June 1966, pp. 153-161.

23. Petersen, J. C., "Chemical Composition of Asphalt as Related to Asphalt Durability - State of the Art," Transportation Research Record 999, 1985, pp. 13-30.

24. Halstead, W. J., "Relation of Asphalt Chemistry to Physical Properties and Specifications," Proceedings AAPT, Vol. 54, 1985, pp. 91-116.

25. Dorrence, S. M., F. A. Barbour, and J. C. Petersen, "Direct Evidence of Ketones in Oxidized Asphalts," Analytical Chemistry, Vol. 46, 1974, pp. 2242-2244.

26. Martin, C. L., and R. H. Bowering, "The Durability of Various Asphalts in Pavement Seals in South Eastern Australia," Proceeding AAPT, Vol. 50, 1981, pp. 417-441.

27. Kennedy, T. W., L. O. Cummings, and T. O. White, "Changing Asphalt Through Creation of Metal Complexes," Proceedings AAPT, Vol. 50, 1981, pp. 442-456.

28. Petersen, J. C., F. A. Barbour, S. M. Dorrence, "Identification of Dicarboxylic Anhydrides in Oxidized Asphalts," Analytical Chemistry, Vol. 47, 1975, pp. 107-111.

29. Petersen J. C., H. Plancher, and G. Miyake, "Chemical Reactivity and Flow Properties of Asphalts Modified by Metal Complex-Induced Reaction with Atmospheric Oxygen," Proceedings AAPT, Vol. 52, 1983, pp. 32-60.

30. Grossman, G. W., "Correlations of Laboratory to Natural Weathering," Journal of Coatings Technology, Oct. 1977, Vol. 49, No. 633, pp. 45-54.

31. Logan, R. W., "Ultraviolet Light Takes on CPI Role," Chemical Engineering, Vol. 41, Jan. 1982, pp. 95-96.

32. ASTM G 53-84, "Standard Practice for Operating Light and Water-Exposure Apparatus (Fluorescent UV-Condensation Type) for Exposure of Non-metallic Materials," American Society for Testing Materials, Philadelphia, Pennsylvania, 1987.

33 Ferraro, J. R. and L. J. Basile, Fourier Transform Infrared Spectroscopy, Vol. 1, Academic Press, New York, 1978.

34. Schmidt, R. J., "A Practical Method for Measuring the Resilient Modulus of Asphalt-Treated Mixes," Highway Research Board, Record No. 404, 1972, pp. 22-32.

35. Timoshenko, S., and J. N. Goodier, Theory of Elasticity, 2nd Edition, McGraw-Hill, New York, 1951.

36. Tia, M. "Characterization of Cold-Recycled Asphalt Mixtures," Joint Highway Research Project FWHA/IN/JHRP-82/5, Purdue University, 1982, 228 pages.

37. Frocht, M. M., Photoelasticity, Vol. 2, John Wiley and Sons, New York, 1967.

38. Hondros, G., "The Evaluation of Poisson's Ratio and the Modulus of Materials of a Low Tensile Resistance by the Brazilian Test with Partial Reference to Concrete," Australian Journal of Applied Science, Vol. 10, No. 3, pp. 32-38.

39. Hadley, W. O., W. R. Hudson and T. W. Kennedy, "An Evaluation of Factors Affecting the Tensile Properties of Asphalt-Treated Materials," Research Report 98-2, Project 3-8-66-98, The University of Texas at Austin, March 1969, 113 pages.

40. Manlouk, M. S., "Characterization of Cold Mixed Asphalt Emulsion Treated Bases," Joint Highway Research Project IN/JHRP-79-19, Purdue University, Oct. 1979, 173 pages.

41. Maupin, G. W., "Results of Indirect Tensile Tests Related to Asphalt Fatigue," Highway Research Board, Record No. 404, 1972, pp. 1-7.

42. Hadley, W. O., "A Method of Estimating Tensile Properties of Materials Tested in Indirect Tension," Research Report 98-7, Center for Highway Research, The University of Texas at Austin, July 1970.

43. Tia, M., and Ruth, B. E., "Basic Rheology and Rheological Concepts Established by H. E. Schweyer," Asphalt Rheology: Relationships to Mixtures, ASTM STP 941, O.E. Briscoe, Ed., American Society for Testing and Materials, Philadelphia, Pennsylvania, 1987, pp. 118-145.

44. Bikales, N. M., Characterization of Polymers, Encyclopedia Reprints, Wiley-Interscience, New York, 1967.

45. Randall, H. M., R. G. Fowler, N. Fuson, and J. R. Dangl, Infrared Determination of Organic Structures, D. Van Nostrand Company, London, 1949.

46. Tia, M., B. E. Ruth, L. I. Josephson, and C. T. Chari, 'Preliminary Investigation of Original and In-Service Asphalt Properties for the Development of Improved Specifications,' Final Report, Project 245-D53, Department of Civil Engineering, University of Florida, Feb. 1987, 237 pages.

47. Edler, A. C., M. M. Hattingh, V. P. Servas, and C. P. Marais, "Use of Aging Test to Determine the Efficiency of Hydrated Lime Additions to Asphalt in Retarding its Oxidative Hardening,' Proceedings AAPT, Vol. 54, 1985, pp. 118-139.

48. Frantz, H. W., and Hoyd E. Malm, Laboratory Studies in General Chemistry, W. H. Freeman and Company, San Francisco, 1970.

49. Ruth, B. E., R. Reque, and E. Puyana, "Low Temperature Pavement Response and Cracking Models,' Final Report, Project 245-U70, Department of Civil Engineering, University of Florida, Sept. 1983, 207 pages.

50. Manzione, C. W., "Evaluation and Response of Aged Flexible Airfield Pavements at Ambient Temperatures Using the Falling Weight Deflectometer,' Ph.D, Thesis, University of Florida, April 1988.

51. Conway, J. M., K. Norris, and C. E. Bodwell, "A New Approach for the Estimation of Body Composition Infrared Interactance," American Journal of Clinical Nutrition, Vol. 40, Dec. 1984, pp. 1123-1130.

BIOGRAPHICAL SKETCH

Commander T. Chari was born in Poona, India, on September 7, 1942. He received his early education at St. Bede's Anglo-Indian High School, San Thome, Madras, India. After completing his high school examinations, he entered St. Ignatius Loyola College, Madras, in 1957. A year later, he was selected for a three year training program at the National Defence Academy, Poona, an inter-service training establishment which provides all-round instruction to cadets planning careers in uniform. In 1961, he graduated into the Indian Military Academy, Dehra Dun, as an Army cadet in the technical stream. He was commissioned into the elite Madras Sappers and Miners of the Indian Corps of Engineers in 1962.

While in service, he completed his Bachelor of Science in Civil Engineering at the College of Military Engineering, Poona in 1967. Later, in 1972, he obtained his master's degree from Thomason Engineering College, University of Roorkee, the premier institution for civil engineering in India, with specialization in transportation engineering.

He has handled a wide variety of civil engineering projects in executive, design, planning and quality control assignments. He has also served as an associate professor, soils and pavements at the College of Military Engineering for a period of three years.

Chari represents the Corps on a number of Committees of the Indian Roads Congress and the Indian Standards Institution. He returns to

India in April 1988 as Director of Designs at the Office of the Engineer-in-Chief, New Delhi. He will assume the appointment in the rank of Colonel.

Chari is married to Mythily, who will also be completing a graduate program in special education at the University of Florida, in April 1988. They have two boys, Ranjan and Satyan. The whole family is actively interested in conservation of wild life in India.

I certify that I have read this study and that in my opinion it conforms to acceptable standards of scholarly presentation and is fully adequate, in scope and quality, as a dissertation for the degree of Doctor of Philosophy.

Byron E. Ruth

Byron E. Ruth, Chairman
Professor of Civil Engineering

I certify that I have read this study and that in my opinion it conforms to acceptable standards of scholarly presentation and is fully adequate, in scope and quality, as a dissertation for the degree of Doctor of Philosophy.

Mang Tia

Mang Tia, Cochairman
Associate Professor of Civil
Engineering

I certify that I have read this study and that in my opinion it conforms to acceptable standards of scholarly presentation and is fully adequate, in scope and quality, as a dissertation for the degree of Doctor of Philosophy.

Jerry W. Williams

J. W. Williams
Assistant Professor of Materials
Science and Engineering

I certify that I have read this study and that in my opinion it conforms to acceptable standards of scholarly presentation and is fully adequate, in scope and quality, as a dissertation for the degree of Doctor of Philosophy.

G. C. Page
Bituminous Materials and Research
Engineer
Florida Department of Transportation

I certify that I have read this study and that in my opinion it conforms to acceptable standards of scholarly presentation and is fully adequate, in scope and quality, as a dissertation for the degree of Doctor of Philosophy.

P V Rao

P. V. Rao
Professor of Statistics

This dissertation was submitted to the Graduate Faculty of the College of Engineering and to the Graduate School and was accepted as partial fulfillment of the requirements for the degree of Doctor of Philosophy.

April 1988

Dean, College of Engineering

Dean, Graduate School